OTTE, ELMAR FRANCOIS

CORROSION CHARACTERISTICS OF FATTY ACIDS IN WATER SOLUTIONS

MIng UP 1994

CORROSION CHARACTERISTICS OF FATTY ACIDS IN WATER SOLUTIONS

by

ELMAR FRANCOIS OTTE

Submitted in partial fulfilment of the requirements
for the degree
MASTER OF ENGINEERING
DEPARTMENT OF CHEMICAL ENGINEERING
FACULTY OF ENGINEERING

UNIVERSITY OF PRETORIA

MARCH 1994

INDEX

LIST OF SYMBOLS

SYMBOL	MEANING	UNITS
CHEMICALS		
C_2	Acetic acid.	
C_3	Propionic acid.	
C_4	Butyric acid.	
C_5	Valeric acid.	
C_6	Hexanoic acid.	
C_8	Octanoic acid.	
C_9	Pelargonic acid.	
C_{10}	Decanoic acid.	
C_{12}	Lauric acid.	
C_{14}	Myristic acid.	
C_{16}	Palmitic acid.	
C_{18}	Stearic acid.	
GREEK LETTERS		
α	Transfer coefficient	
ß	Tafel-slope	mV/decade
δ	Diffusion layer thickness	cm
ρ	Density	g/cm^3
η	Overpotential	mV
ϕ	Reduction half-cell potential	mV
μ	Viscosity	cP
ν	Kinematic viscosity	g/cm.s

GENERAL

a	Constant	
as	Specie activity	
b,d,f,h	Constants	
AN	Acid number	mg KOH/g solution
A	Exposed area	m^2
C	Concentration	$mole/dm^3$
CR	Corrosion rate	μmpy
d	Characteristic length	m
D	Diffusion constant	
Di	Inner pipe diameter	m
Electrochem A	Electrochemical results adapted	μmpy
Electrochem N	Raw electrochemical results	μmpy
e	Electron	
E	Oxidation half-cell potential	mV
F	Faraday's constant	C/kgeq
ΔG	Gibbs-free energy	J/mole
i	Current density	A/cm^2
I	Current	A
k	Electrochemical equivalent	kg/C
L	Pipe length	m
m	Mass	g
M	Mass	kg
MM	Mole mass	kg/kmole
n	Electrons involved in reaction	
p	Partial pressure	kPaa
p'	Transport number of all ions involved in the electrode process	
pH	-log(hydrogen ion activity)	
Q	Activity coefficient	
R	Gas constant	J/gmole.K
Re	Reynold's number	

KEY-WORDS

Corrosion.
Organic acids.

ACKNOWLEDGEMENTS

All thanks and praises to God.

The loyal support of my mother, family members and Reinette Kruger is appreciated.

Thanks to Prof. Skinner for his patience also to the Chemical Engineering Department at the University of Pretoria for granting me the use of their facilities.

SASOL's financial support is greatly appreciated.

Advice was gratefully received from: Prof. Böhmer, Prof. de Vaal, Johan Gericke, Wessel van Wyk, Wessel Bonnet, Wessel Nienaber and Barend Gildenhuis.

" Whoever loves discipline loves knowledge, but he who hates correction is stupid. " Prov. 12:1

SYNOPSIS

The main investigation consisted of determining corrosion rates of mild steel (AISI 1020) exposed to de-aerated stagnant solutions of fatty acids in water at different acid numbers and temperatures, with the aid of mass loss tests.

The temperature range investigated varied from 25°C to 250°C. Results showed that corrosion rates initially increased with temperature and at certain elevated temperatures thick multi-laminated corrosion product films formed on the specimen surfaces which led to decreases in corrosion rates with further increases in temperature. Corrosion product films influenced the control mechanism of the corrosion process and it was seen that the characteristics of these films were dependent on the temperature as well as fatty acid type. The acid number range investigated was from 0 to 25 mg KOH/g solution. Corrosion rates increased with an increase in acid number irrespective of the control mechanism. Results indicated that the corrosivity of acid solutions decreased with an increase in chain length of the organic acid molecule, when no corrosion product films were present. The presence of corrosion product films rendered complex relationships.

Electrochemical tests were done on specific fatty acid systems at 25°C. Corrosion rates evaluated from electrochemical observations correlated well with mass loss results and it was concluded that the corrosion mechanism was electrochemical.

Supplementary investigations were conducted on specific fatty acid systems and included the following:

Turbulence did not influence the corrosion process. This is typical for an activation-controlled system where no corrosion product films are present on the specimen surfaces.

Mixing of acids showed a corrosion rate of approximately an average of the two individual corrosion rates of the pure systems.

Monitoring studies showed that results obtained with the Corrator correlated better with mass loss and electrochemical corrosion rates than Corrosometer results.

Corrosion rates increased with an increase in dissolved oxygen content level of the solution and with additions of chloride, but sulphur additions rendered lower corrosion rates.

A water phase process stream received from SASOL showed that the corrosion rate increased with temperature and levelled out towards 200°C The corrosion characteristics of the received stream can be simulated by acetic acid with the same acid number.

SINOPSIS

Die hoofondersoek het bestaan uit die bepaling van korrosietempo's van laekoolstofstaal (AISI 1020) wat blootgestel word aan ontlugte stagnante oplossings van organiese sure in water by verskillende temperature en suurgetalle. Die korrosietempo's is bepaal deur gebruik te maak van massaverliestoetse.

Die temperatuurgebied wat ondersoek is, was van 25°C tot 250°C. Dit is waargeneem dat die korrosietempo aanvanklik toeneem met 'n toename in temperatuur en daarna is 'n afname in die korrosietempo waargeneem. Die afname word toegeskryf aan 'n dik multi-laminêre-korrosieprodukfilm wat op die monsteroppervlak gevorm het. Hier is waargeneem dat die beheermeganisme beïnvloed word deur die teenwoordigheid van korrosieprodukfilms terwyl eienskappe van die films afhanklik was van die tipe suur, asook die temperatuur waarby eksperimente gedoen is. Die suurgetalgebied wat ondersoek is, was vanaf 0 tot 25 mg KOH/g oplossing. Korrosietempo's het toegeneem met 'n toename in suurgetal ongeag die beheermeganisme wat bestaan het. Die korrosiwiteit van die suuroplossings het afgeneem met 'n toename in organiese molekuullengte, waar geen korrosieprodukfilm teenwoordig was nie. Die teenwoordigheid van korrosieprodukfilms het komplekse korrosietempo-tipe suur verhoudings by konstante temperature opgelewer.

Elektrochemiese toetse is gedoen op sekere sisteme by 'n temperatuur van 25°C. Korrosietempo's verkry deur gebruik te maak van elektrochemiese toetsmetodes vergelyk baie gunstig met massaverliestoetsresultate. Die gevolgtrekking wat dus gemaak is, was dat 'n elektrochemiese korrosiemeganisme bestaan.

Newe-ondersoeke is gedoen op sekere organiese suursisteme en het die volgende ingesluit:

Turbulensie het geen effek op die korrosieproses gehad nie. Dit is tipies wat verwag word van 'n aktiveringsbeheerde sisteem waar geen korrosieprodukfilms teenwoordig is op die monsteroppervlak nie.

Mengsels van die sure het getoon dat die korrosietempo's 'n gemiddelde waarde van die individuele korrosietempo's van die suiwer suursisteme oplewer.

In die moniteringstudies het die Corrator resultate beter gekorreleer met massaverlies en elektrochemiese toetsresultate as Corrosometer resultate.

Die korrosietempo het verhoog met 'n toename in opgeloste suurstofinhoud van die oplossing asook met die byvoeging van chloriede, terwyl 'n afname in korrosietempo waargeneem is met die byvoeging van swael.

'n SASOL waterfase produkstroom het getoon dat die korrosietempo toeneem soos die temperatuur toeneem tot ongeveer 200°C waarna 'n afplatting in korrosietempo waargeneem is. Die korrosiekarakteristiek van die SASOL waterfase produkstroom word redelik goed verteenwoordig deur 'n asynsuur sisteem met dieselfde suurgetal.

Refer	C_2 system at an acid number of 25	
R)	Electrical resistance	Ω.cm
R_p	Polarisation resistance	$mV.cm^2/\mu A$
Sc	Schmidt's number	
Sh	Sherwood's number	
t	Exposure time	days or h
T	Temperature	K
v	Velocity	m/s

SUPERSCRIPTS

a	Activation
b,c,d,f,h	Constants
o	Standard
I	Polarised

SUBSCRIPTS

A	Anodic
B,D,F,H,X,Y,Z	Constants
C	Cathodic
CORR	Corrosion
c	Concentration
f	Film
EX	Experimental
L	Limiting
o	Equilibrium
R	Resistance
soln	Solution
solv	Solvated

1 INTRODUCTION

An objective of engineering is to make a profit. While corrosion is associated with a negative profit, corrosion of plant materials should be minimised to realise maximum profit. Poor material specifications and inadequate corrosion restrictions cost South Africa R 10 000x10^6 in 1990.

Synthol reactors are responsible for production of petroleum products as well as organic acids and water. Organic acids and water have been blamed for corrosion of pipelines, especially mild steel pipelines. To prove or refute this theory it was necessary to conduct certain experiments. After establishing the prevailing conditions in pipelines it was realised that the investigation had to be divided into two sections, the organic phase as well as the water phase of the stream. The investigation considered in this paper involves the water phase. A literature study showed that little data were available for the system; thus intensive laboratory tests had to be done. The project embraced a study of the corrosion characteristics of mild steel exposed to de-aerated solutions of fatty acids in water as a solvent.

The investigation consisted of a main investigation and supplementary investigations.

Objectives of the main investigation.

1. Mass loss tests were conducted to obtain corrosion rates of mild steel in various de-aerated, diluted and stagnant organic acid solutions. Parameters investigated were the following :

   * Different acids $C_2;C_3;C_4;C_5;C_6;C_8;C_{10};C_{12};C_{14};C_{16};C_{18}$
   * Acid numbers 0 ; 5 ; 12.5 ; 25 [mg KOH/g solution]
   * Temperatures 25°C;60°C;90°C;130°C;170°C;210°C;250°C

2. Electrochemical tests were conducted to study corrosion mechanisms. Parameters investigated were the following:

   * Different acids $C_2;C_3;C_4;C_5$
   * Acid numbers 0 ; 5 ; 12.5 ; 25 [mg KOH/g solution]
   * Temperature 25°C

   During electrochemical tests the following were examined in the unsteady and steady states:

   * Unsteady state - changes in the corrosion potential and polarisation resistance as a function of time. Overpotentials of ± 30 mV were used.
   * Steady state - corrosion potentials, Tafel-slopes and corrosion rates. Overpotentials of ± 200 mV were used and the Greene and Gandhi Betacrunch program[1] was used to determine corrosion rates of the systems.

Objectives of the supplementary investigations.

1. Turbulence is an important parameter in the design of processing equipment and pipelines. The influence of turbulence on corrosion properties depends on both the construction material and medium present[2]. In acivation controlled systems without any corrosion product films present on the metal, turbulence will not normally influence the corrosion process. In diffusion controlled systems, increased turbulence will promote corrosion. In passivation systems, increased turbulence may either reduce corrosion by promoting passivation or increase corrosion by erosion of passivation films. A degree of turbulence is necessary to reduce pit corrosion problems of stainless steel in the presence of chloride contaminated solutions[3]. Turbulence tests were done on cylindrical mild steel specimens and consisted of

electrochemical and mass loss tests. The systems investigated were specific systems at a temperature of 25°C.

2. Impurities are often present in streams found in chemical plants. It was thus necessary to recognise the main contaminants present and investigate their contribution to the corrosion characteristics of an acetic acid solution, at an acid number of 25 mg KOH/g solution and at temperatures ranging from 25°C to 250°C. Impurities added to the investigated system were Cl^-, S^{2-} and dissolved oxygen.

3. Corrosion monitoring has become an important means by which continuous information on the plant condition can be obtained. Effective monitoring of corrosion can aid the replacement process of corroded equipment, thus insuring minimum hazard for humans due to unexpected corrosion failures. The effectiveness of the Corrator and Corrosometer as monitoring equipment was tested to establish their applicabilities for an acetic acid solution with an acid number of 25 mg KOH/g solution at a temperature of 25°C.

4. Mixtures of acids were investigated to determine whether synergistical effects were present. The system investigated was a mixture of acetic acid and decanoic acid to produce an acid number of 25 mg KOH/g solution. The system was tested at temperatures ranging from 25°C to 250°C at stagnant conditions.

5. A process stream as received from SASOL was used to produce a test solution which was investigated. Results were compared with results obtained from the main investigations.

2 THEORY

2.1 DEFINITION OF CORROSION

The two major definitions of corrosion are the following:

1. According to *Corrosion Science*, corrosion is the reaction of a solid with its environment.[4]
2. According to *Corrosion Engineering*, corrosion is the reaction of an engineering constructional metal (material) with its environment with a consequent deterioration in properties of the metal (material).[4]

2.2 AN APPROACH TO THE CORROSION PHENOMENA

A fundamental approach to the phenomena of corrosion involves consideration of the structural features of the metal, the nature of the environment and reactions that may occur at the metal/environment interface. Factors involved can be summarised as follows:

1. Metal - composition, detailed atomic structure, microscopic and macroscopic heterogeneities and stress.
2. Environment - chemical nature, concentration of the reactive species and deleterious impurities, pressure, temperature, velocity and impingement.
3. Metal/environment interface - kinetics of metal oxidation and dissolution, kinetics of reduction of species in solution, nature and location of corrosion products, film growth and film dissolution.

2.3 CORROSION MECHANISMS IN AQUEOUS SOLUTIONS

The corrosion mechanism will be discussed concerning electrochemistry, thermodynamics, kinetics and the role environmental factors play in the corrosion process.

2.3.1 ELECTROCHEMISTRY

Consider two electrodes in an electrolyte with a potential difference between the two electrodes. For an electrical current to flow between the two electrodes, migration of charges is necessary, with an oxidation reaction taking place at the one electrode and a reduction reaction at the other electrode. The electrode undergoing oxidation is called an anode, while the one undergoing reduction is called the cathode. The oxidation reaction produces electrons, which migrate to the cathode by means of an external conductor. Migration of charges through the medium occurs through migration of ions. Reagents and soluble electrode products move to and away from electrodes by means of convection, diffusion and migration[5].

At the electrode medium interlayer, a charge rearrangement takes place in both phases; thus causing the electrode to be polarised and the interlayer becomes charged, forming an electrical double layer. Helmholtz proposed the first model describing the electrical double layer. According to this model, the electrical double layer can be simulated by a capacitor and a resistor connected in parallel. The charge on the electrode influences the adsorption of species on electrode surfaces. If the charge on an electrode surface is neutral, it is called zero charge. At potentials more electropositive then zero potential, anions will be adsorbed on the electrode surface and vice versa[6].

2.3.2 THERMODYNAMICS

Thermodynamics provides a means of predicting the equilibrium state of a system of specified components, but provides no information on the detailed course of the reaction, nor of the rate at which systems proceed to equilibrium. More information concerning the above mentioned will be given when kinetics of reactions is discussed..

Thermodynamics of a system determines the inclination of the reaction to take place. Reactions take place if the Gibbs-free energy of a system can be

lowered to form a more stable system. Changes in the Gibbs-free energy can be calculated with the Van't Hoff-equation.

For a general reaction

bB + dD → fF + hH the equation is

$$\Delta G = \Delta G^o + RT \ln Q \qquad (1)$$

with $$Q = \frac{as_F^f as_H^h}{as_B^b as_D^d} \qquad (2)$$

If the reaction is electrochemical, it is usually divided into two half-cell reactions. The anodic zones undergo oxidation with anodic half-cell reactions taking place on the anode, while the cathodic zones undergo reduction and cathodic half-cell reactions take place on the cathode. Electrons migrate from anodic zones through the metal to cathodic zones, while ions migrate through the medium to produce electrical neutrality in the system. The electrode potential of the half-cell reaction is given by the Nernst equation

$$\phi = \phi^o - \frac{R\,T \ln Q}{n\,F} \qquad (3)$$

In order for an electrochemical corrosion reaction to be spontaneous ϕ_C must be more electropositive than ϕ_A. The driving potential of the corrosion reaction can be evaluated with the aid of Eqn(4), if the individual anodic and cathodic-half-cell-reduction potentials are known

$$\Delta\phi = \phi_C - \phi_A \qquad (4)$$

It is standard to express the thermodynamical inclination as the corrosion cell potential difference ($\Delta\phi$) with the relationship between corrosion cell potential difference and the Gibbs free energy as

$$\Delta G = -n\,F\,\Delta\phi \qquad (5)$$

It is possible to determine whether corrosion reactions are thermodynamically possible with the aid of the potential differences of half-cell reactions.

The following are typical half-cell reactions involved in corrosion reactions in aqueous corrosion systems.

A. Anodic half-cell reactions of a metal vary with different conditions of the solution[7].

1. **At low pH values** (acidic solutions)

$$M \rightharpoonup M^{z+} + ze^-$$

Corrosion products are soluble and diffuse away from the metal surface. Corrosion products can be oxidised in the medium and products can precipitate on the surface to form weak adhesive films. Corrosion protection qualities of films are minimal and can cause secondary corrosion problems, like the formation of differential aeration corrosion cells.

2. **At intermediate pH values** (neutral solutions)

$$M + ZH_2O \rightharpoonup M(OH)_z + ZH^+ + Ze^-$$
$$M + ZH_2O \rightharpoonup MO_z + 2ZH^+ + 2Ze^-$$
$$M + Z(OH)^- \rightharpoonup M(OH)_z + Ze^-$$

Corrosion product films form on metal surfaces that reduce corrosion rates. The efficiency of the corrosion product films is determined by the adhesiveness, porosity, solubility, electrical conductivity of the film and the amount of stress the film can resist.[8]

3. **High pH values** (alkaline solutions)

$$M + ZH_2O \rightharpoonup MO_z^{x-} + 2ZH^+ + (2z - x)e^-$$

Corrosion products are relatively soluble and diffuse away from metal surfaces. Corrosion products can be oxidised in the medium and they can precipitate on the surface to form weak adhesive films. Corrosion protection qualities of the films are minimal and can cause secondary corrosion problems like the formation of differential aeration corrosion cells.

B. Possible cathodic half-cell reactions are:

1. The cathodic hydrogen reaction

   $2H^+ + 2e^- \rightharpoonup H_2$

   occurs at low pH values and at normal temperature and pressure (NTP) the Nernst equation reduces to

   $$\phi = -0.0591\ pH - 0.03\ \log(p_{H_2}) \qquad (6)$$

2. The cathodic oxygen reaction

   $\frac{1}{2}\ O_2 + H_2O + 2e^- \rightharpoonup 2OH^-$

   is common in aerated solutions and at normal temperature and pressure (NTP) the Nernst equation reduces to

   $$\phi = 1.23 - 0.0591\ pH + 0.015\ \log(p_{O_2}) \qquad (7)$$

3. Reduction of foreign metal cations present in the solution.

   The cations are reduced and plated on the surface of corroding metal and the bi-metal effect can be enhanced. The reaction takes place in conjunction with reactions as described above in (B1) and (B2).

2.3.2.1 POURBAIX DIAGRAMS

In practice an important application of thermodynamics of corroding systems is the composition of potential-pH-equilibrium diagrams, also known as Pourbaix-diagrams. Pourbaix and co-workers[9] plotted thermodynamical

equilibrium equations for different M-H_2O-systems at 25°C in diagram form.

The general electrode reaction is

$$fF + mH^+ + ne^- \rightleftharpoons bB + cH_2O$$

while the Nernst equation can be written as

$$\phi = \phi^\circ - \frac{0.0591\, m}{n} pH - \frac{0.0591}{n} \log Q$$

$$\phi = \phi^\circ - \frac{0.0591}{n} [m.pH - \log Q] \qquad (8)$$

with $$Q = \frac{as_B^b}{as_F^f} \qquad (9)$$

In elementary Pourbaix diagrams corrosion is associated with the activity of a soluble corrosion product $\geq 10^{-6}$; thus reducing the Pourbiax diagram to single lines, making it possible to divide the diagram into different zones of immunity, corrosion and passivation. Zones for different systems can be determined experimentally, but have the following limitations:

* A restriction on the use of Pourbaix diagrams applies when species form complexes during the reaction because corrosion zones increase when complexes form.
* Corrosion zones cannot be quantified in zones of specific corrosion rates.
* Passivation zones do not necessarily ensure effective passivation.
* The presence of impurities can cause the corrosion zone to be drastically shifted on the diagram.

Some systems are extended to a M-H_2O-X-system, at 25°C, where X represents anions of a certain concentration.

A typical Pourbaix-diagram is represented in figure 2.1., with some slopes presented by the following equations :

1. Where H^+ and e^- are involved in the reaction

slope $= -0.0591 \frac{m}{Z}$

2. Where no e^- are involved in the reaction

   slope $= \infty$

3. Where no H^+ are involved in the reaction

   slope $= 0$

FIGURE 2.1 *A simple Fe/H_2O Pourbaix-diagram at NTP conditions*[9]

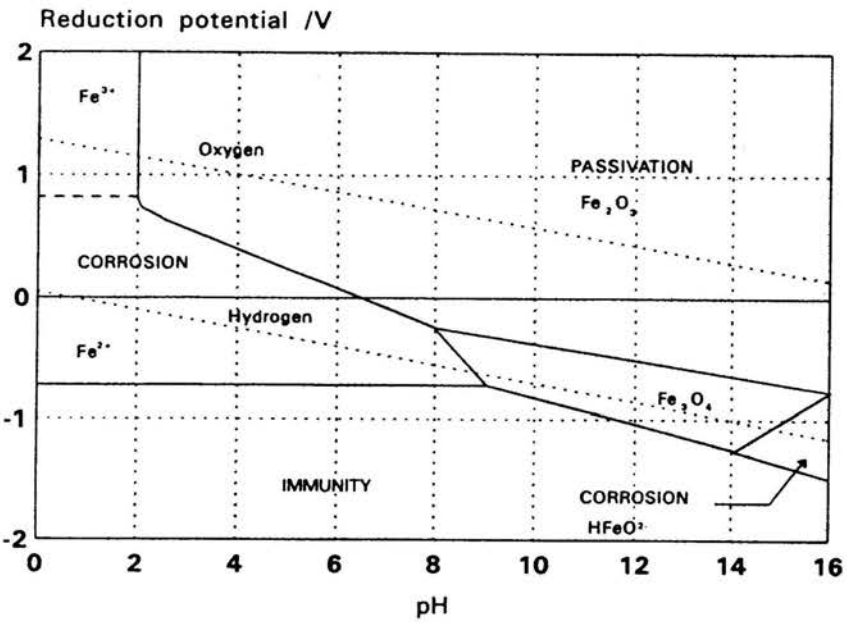

2.3.3 KINETICS

The rate and type of corrosion reaction will be affected by a variety of factors associated with the metal, metal surface and the environment. Before considering the essential factors that control the rate of corrosion of a single metal, it will be helpful to examine the charge transfer process that occurs at the two separate electrodes of a well-defined electrochemical cell.

An electrochemical cell is a device by means of which the enthalpy of a spontaneous chemical reaction is converted into electrical energy; conversely, an electrolytic cell is a device in which electrical energy is used to bring about a chemical change. The enthalpy of such a system will then increase and both types of cells are characterised by the fact that, during their operation, charge transfer takes place at one electrode in a direction that leads to the oxidation of either the electrode or of the species in solution, while the converse process of reduction takes place at the other electrode[3,10].

Electrode equilibrium is a dynamic state with metal ions continually leaving the metal crystal and entering the solution and while metal ions from the solution enter the metal crystal. No nett half-cell reaction takes place, but the current that flows during this process, is called the exchange current density (i_o). The current i_o depends on the type and surface of the electrode, species-activities and the temperature of the solution[11].

If it is thermodynamically possible for two half cells to lead to a reaction and they are electrochemically coupled, the one with the more positive reduction potential will act cathodically, while the one with the more negative reduction potential will act anodically. A nett half-cell current starts flowing and electrode potentials polarise away from the equilibrium potential values of the individual half cells. If the electrochemical resistance is negligible, which is the case when the half cells are dispersed on the electrode surfaces, individual half-cell potentials will be polarised to a single value known as the corrosion potential (ϕ_{CORR}). The current that flows at the corrosion potential is known as the corrosion current (I_{CORR}) and is shown on the diagram in figure 2.2.

FIGURE 2.2 *Polarisation diagram to show the corrosion potential*

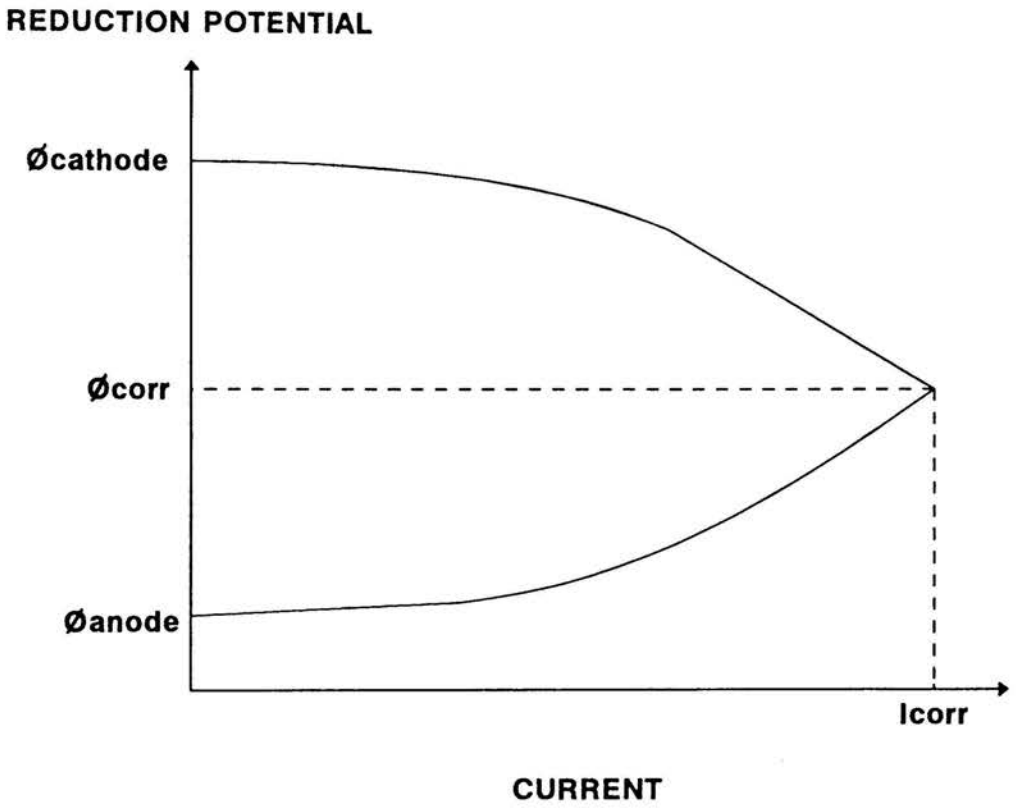

When IR-losses are present, a part of the driving potential is absorbed as resistance polarisation and the corrosion potential does not reduce to a single value. This happens when anodic and cathodic zones are separated from one another.

The corrosion rate can be determined with the aid of Faraday's law

$$m = kI_{CORR}t \qquad (10)$$

with $$k = \frac{atomic\ mass}{n\,F} \qquad (11)$$

Potential differences between polarised potentials and the equilibrium potential are known as overpotentials. Different kinds of overpotentials are identified and will be discussed as activation overpotential, concentration overpotential and resistance overpotential.

2.3.3.1 ACTIVATION OVERPOTENTIAL

Any electrode reaction takes place spontaneously, if the free energy of the system can be lowered, which can be achieved if the activation energy barrier is overcome. For any given electrode process under specific conditions, charge transfer at a finite rate will involve an activation overpotential (η^a), which provides the activation energy required for reactants to surmount the energy barrier that exists between the energy states of reactants and products.

The relationship between the activation overpotential and the rate of charge transfer per unit area of the electrode surface, can be quantified by the Tafel-equation. The equation originated from experimental work done by Tafel on investigation of the cathodic hydrogen reaction on different metals and he presented it as follows[3]

$$\eta^a = a + \beta \log i \qquad (12)$$

For a nett cathodic half reaction η^a and β are negative and for a nett anodic half reaction η^a and β are positive. The constant a always has an opposite sign as the Tafel slope. Cathodic Tafel slopes are noted as positive quantities and it must be remembered that a negative sign must be incorporated in the equation. The Tafel equation was derived from basic electrochemical principles[3]. For anodic reactions the following applies

$$a = \frac{-2.303\ R\ T \log i_o}{\alpha_A\ n\ F} \qquad (13)$$

$$\beta = \frac{2.303RT}{\alpha_A nF} \qquad (14)$$

and for cathodic reactions

$$a = \frac{2.303\ R\ T \log i_o}{\alpha_C\ n\ F} \qquad (15)$$

$$\beta = \frac{-2.303RT}{\alpha_C nF} \qquad (16)$$

A combination of the experimental and theoretical Tafel-relationships gives the following equation:

$$\eta = \pm \beta \log \frac{i}{i_o} \qquad (17)$$

i, in Eqn(17) is the nett half-cell current and at large positive overpotentials, $i = i_A$, while at large negative overpotentials a nett cathodic current flows with $i = i_C$.

2.3.3.2 TRANSPORT (DIFFUSION OR CONCENTRATION) POLARISATION

Previous considerations have been confined to the kinetics of charge transfer, but the rate of an electrode reaction will also depend on mass transfer,i.e. the rate at which reactants are transported to the electrode surface and the rate at which products are transported away from the electrode. Transport through the solution to and from the metal surface occurs by diffusion, ionic migration and convection. Diffusion through the thin static layer (diffusion layer δ) of the solution adjacent to the metal surface, is usually the rate-limiting step. The limiting current density, the maximum rate per unit area under the conditions prevailing, for a cathodic process is given by[3]

$$i_L = \frac{DnF\Delta C}{\delta(1-p')} \qquad (18)$$

The relation between transport overpotential and current density for pure concentration polarisation is given by[3]

$$\eta_c = \frac{\pm 2.303\, R\, T \log\left[1 - \frac{i}{i_L}\right]}{nF} \qquad (19)$$

with the positive sign associated with the nett cathodic reaction and the negative sign associated with the nett anodic reaction. Unlike activation overpotential, transport overpotential is not controlled by the kinetics of charge transfer, the magnitude of η_c will be the same for any cation (providing n, D and C remain constant) and any metal surface. The rate-

controlling parameter in transport overpotential is thus, i_L, and it will be seen that factors in Eqn(18) causing i_L to change, will result in a different corrosion rate, providing the latter is solely determined by the kinetics of the cathodic process.

2.3.3.3 RESISTANCE OVERPOTENTIAL

The resistance to charge transfer in the metal is negligible. Resistance overpotentials, η_R, are thus determined by factors associated with the solution or with the metal surface. Resistance overpotential is defined[3] as

$$\eta_R = I(R_{soln} + R_f) \qquad (20)$$

where R_{soln} is the electrical resistance depending on the electrical resistivity (Ω.cm) of the solution and the geometry of the corroding system, while R_f is the resistance produced by films or coatings on the surface.

2.3.3.4 SIMULTANEOUS REACTIONS

If more then one anodic and/or cathodic reaction takes place simultaneously at the electrode surface, the nett overpotential current relationship will be given by the summation of the relevant reaction currents at certain overpotentials.

$$i_{C,T} = \sum_{j=1}^{n} i_{C,j} \text{ and } i_{A,T} = \sum_{j=1}^{n} i_{A,j} \qquad (21)$$

2.3.3.5 POLARISATION DIAGRAMS

Polarisation diagrams are graphical presentations of potential-current relationships and present one of the most important applications of the kinetics of corroding systems. The potential axis can either be the overpotential or potential (relative to a reference electrode) and can be presented on a linear scale on the vertical axis. The current axis can either be current density or total current and can be presented on a logarithmic scale on the horizontal axis, in order for pure activation controlled reactions

to be presented as straight lines on diagrams. If anodic and cathodic reaction areas are dispersed, current may be presented on a current density scale. When anodic and cathodic reaction areas are separate, the current may be presented on a total current scale, where $I_{CORR,A} = I_{CORR,C}$ but $i_{CORR,A} \neq i_{CORR,C}$.

Important information concerning corrosion characteristics of a system can be obtained from polarisation diagrams, such as : corrosion potentials; corrosion currents; Tafel-slopes; passivation potentials; critical current densities; passivation potentials; break-down potentials and types of corrosion control mechanisms present for specific systems. Anodic, cathodic and mixed control systems can be distinguished when the system is activation controlled. Systems can also be identified as resistance controlled, cathodic diffusion controlled and passivation controlled[4].

2.3.4 ENVIRONMENTAL CHARACTERISTICS

Environmental characteristics will be discussed by considering the influence, which temperature, turbulence and some impurities have on the corrosion process.

2.3.4.1 TEMPERATURE

The influence of temperature on the corrosion process is illustrated with the aid of a polarisation diagram as shown in figure 2.3. An increase in temperature causes the value of i_o to increase, while the Tafel-slopes decrease.

FIGURE 2.3 *The influence of temperature on a corrosion half-cell reaction*

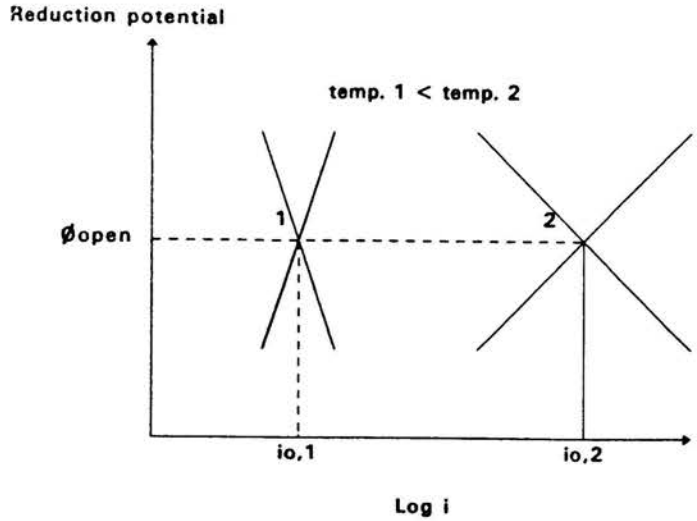

A new theory has been developed for high temperature aqueous corrosion of mild steel in a de-aerated medium[12]. The theory is known as the Potter-Mann duplex film theory.

When mild steel corrodes in high temperature (>200°C) de-oxygenated water, a Fe_3O_4 film is formed on the surface of the steel. In acid solutions, a thick multi-laminated film grows according to a linear time law, while in neutral and alkaline solutions it is found that duplex films grow according to a parabolic time law. Below ± 100°C, iron becomes covered with a thin film, which rarely exceeds 50 Å in thickness[8].The duplex 'Potter-Mann' films are of most concern here, as they are the prototypes of protective films that form on structural steels in most high temperature plants.

Duplex films consist of an inner layer of fine-grained oxide and an outer layer of loosely packed, larger grains, which appear to have precipitated from the solution[13]. The boundary between the layers is found to lie at the position

of the original metal surface, which indicates that the inner layer grows at the metal-oxide interface, while the outer layer grows at the oxide-solution interface.

A number of models of the duplex layer growth process have been developed. Castle and Masterson[14] recognised that the key problem in successfully modelling the corrosion mechanism was the diffusion of O^{2-} ions through the oxide lattice, which is much too slow to account for the inner layer growth. Finding that the oxide was porous, they therefore proposed that the pores provide access of the oxidant (water) to the oxide-metal interface. They then proposed that iron needed to form the outer layer, dissolves at pore bases, while diffusion of dissolved iron is the rate-limiting step. This theory was called the solution-pores model of corrosion.

On reexamination of the solution-pores model of aqueous corrosion it was found deficient in three respects[15].

* Firstly: it does not account for the fact that there is similarity between the corrosion rates in steam and neutral water.
* Secondly: it predicts a temperature dependence of the rate, which is of an order of magnitude too weak.
* Thirdly: direct measurements of the permeability of the oxide suggest that effective pore sizes are too small to account for the observed corrosion rates.

A 'grain-boundaries pores' model of aqueous corrosion was therefore proposed analogous to gaseous oxidation[16]. The model describes the situation when a coherent inner layer has developed. Micropores are taken to exist across the oxide-metal interface. The water oxidises roughly half the metal *in situ* to form the inner layer. The remaining metal, which cannot be accommodated in the vacant spaces of the metal, diffuses as ions along oxide grain boundaries to form new oxide at the external surface by reacting with the solution. Diffusion occurs under conditions of local equilibrium and charge neutrality, as in Wagner's theory of thick film oxidation.

The model therefore unites, in a common framework, the description of duplex oxide growth in liquid and gaseous environments. However problems remain with pore models, such as to how pores initiate, and why they do not block up, which are common to both cases and which are not accounted for here. Effertz[17] and Tomlinson[18] have previously proposed models for high temperature aqueous corrosion involving solid state diffusion across the oxide, but both models were deficient in occupying oxygen transport by O^{2-} ions. The idea that the aqueous corrosion of very corrosion-resistant alloys like Inconel or Stellite might be limited by solid state diffusion, is not a new idea. However, it was generally believed that solution transport, limited aqueous corrosion of the less passive steels, like mild steel. It is shown in detail[15] how solid state diffusion limits high temperature corrosion of the majority of steels and related alloys.

In conclusion the model shows how corrosion rates are limited by the outward diffusion of metal ions along grain boundaries in the oxide. The theory accounts for temperature dependence, pH dependence and parabolic corrosion rate of the corrosion process as a function of temperature.

2.3.4.2 TURBULENCE

When a system is activation-controlled without any corrosion products present on the metal, turbulence will normally not influence the corrosion process[3]. However, some exceptions to the rule are that at high turbulence special types of erosion-corrosion such as cavitation and impact corrosion, can lead to high corrosion rates[19,20].

Lacking corrosion product films on the surface of the metal and with the cathodic process being diffusion controlled, an increase in turbulence leads to the reduction of the boundary layer thickness, which in turn leads to a higher limiting current, causing higher corrosion rates, as represented in figure 2.4.

FIGURE 2.4 *The influence of turbulence on the corrosion process for a diffusion controlled system*

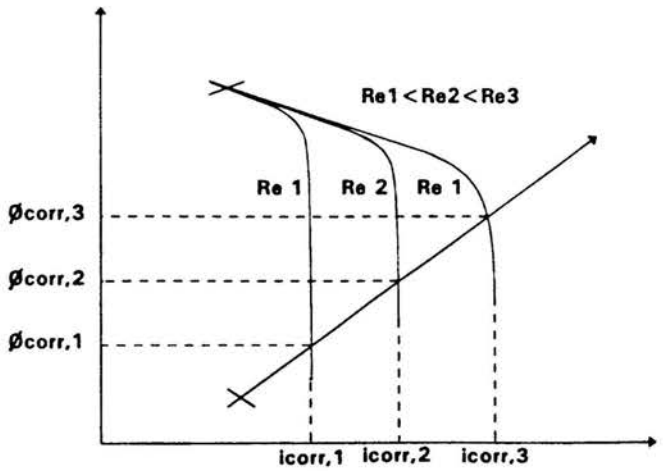

The mass-transport at a liquid-solid interface is described by the Sherwood Eqn(22)[21]

$$Sh = a\,Re^{b}Sc^{c} \qquad (22)$$

The Sherwood number with the aid of Faraday's law, can be used to determine the corrosion rate[3,22]. Values of the constants are functions of the flow region as well as geometry of equipment, for example :

* Laminar flow (Re < 2300), rotating disc[23]

$$i_L = 0.62\,n F \delta a' Re^{0.5} Sc^{0.333} \qquad (23)$$

* Laminar flow (2000 < Re < 5000), pipes[24]

$$i_L = 1.64\,n F D a' \left(\frac{Re\,Sc\,Di}{L} \right)^{0.333} \qquad (24)$$

* Turbulent flow (Re > 2300), pipes[25]

$$Sh = 0.023\, Re^{0.8}\, Sc^{0.333} \quad (25)$$

* Turbulent flow (Re > 2300), rotating cylinders[26]

$$Sh = 0.0791\, Re^{0.7}\, Sc^{0.356} \quad (26)$$

$$Sh = 0.0096\, Re^{0.913}\, Sc^{0.316} \quad (27)$$

If the viscosity, density and concentration of the controlling diffusion species and the cylinder diameter are kept constant, the corrosion rate is proportional to the relative velocity, and it follows that

$$CR \; \alpha \; v^{b} \quad (28)$$

When corrosion products form, the influence of turbulence on the corrosion process is more complex[2]. A high turbulence can cause the limiting current to exceed the critical passivation current and cause the system to be stable and passivated; thus reducing the corrosion rate. At high turbulence the system may also become transpassive, causing the corrosion rate to increase. Corrosion product films can be destroyed at high turbulence, exposing fresh metal to the solution, causing the corrosion rate to increase.

Research[27,28,29] has shown that erosion-corrosion of the corrosion product films do not normally take place in natural water with velocities of < 3 m/s in iron- and copper-alloys.

Foroulis[30] investigated the influence of turbulence and concentration of dissolved oxygen on the corrosion characteristics of iron. It was found that at constant oxygen levels, turbulence did not effect the corrosion rates, but the tests were done after only 15 minutes of exposure to the aggressive medium.

2.3.4.3 IMPURITIES

The concentration of dissolved substances may have a substantial effect on the corrosivity of the medium and it is a complex relationship. As an illustration, consider the influence of the hydrogen ion concentration on the corrosivity of iron in an aerated water medium.

At a $pH > 12$ an increase in the hydrogen ion concentration reduces the corrosivity of the medium, which is due to more effective passivation of the metal. At a $10 < pH < 12$, an increase in the hydrogen ion concentration gives an increase in corrosivity of the medium, due to weaker passivation of the metal. At a $10 < pH < 4$ the hydrogen concentration does not effect the corrosivity of the medium that much, because the system is cathodic diffusion controlled with regard to the oxygen reaction. At $pH < 4$ the corrosivity increases with an increase in the hydrogen ion concentration, because $\Delta\phi$ increases while the system is activation controlled.

The effects of oxidisers on the corrosion rate can be represented in figure 2.5[19].

FIGURE 2.5 *Effect of oxidisers and aeration on the corrosion rate*[19]

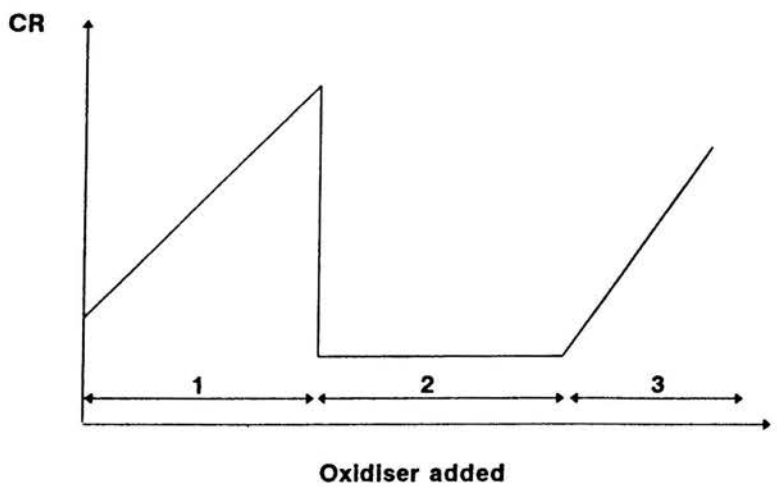

Note that this figure is divided into three different sections. The behaviour corresponding to section 1 is characteristic of normal metals and also of active-passive metals when they exist only in the active state. For metals, which demonstrate active-passive transition, passivity is achieved only if a sufficient quantity of oxidiser or a sufficiently powerful oxidiser is added to the medium. Increasing corrosion rate with increasing oxidiser concentrations as shown in section 1, is characteristic of monel and copper in acid solutions containing oxygen. Both of these materials do not passivate. Although iron can be made to passivate in water, the solubility of oxygen is limited and in the most cases it is insufficient to produce a passive state[31].

If an active-passive metal is initially passive in a corrosion medium, the addition of further oxidising agents has only a negligible effect on corrosion rate. This condition frequently occurs when active-passive metal is immersed in an oxidising medium such as nitric acid or ferric chloride. The behaviour represented by sections 2 and 3 results when a metal, initially in the passive state, is exposed to very powerful oxidisers and makes a transition into the transpassive region. This kind of behaviour is frequently observed with stainless steel when very powerful oxidising agents such as chromates are added to the corrosive medium. In hot nitrating mixtures containing concentrated sulphuric and nitric acids, the entire active-passive-transpassive transition can be observed with the increased ratios of nitric to sulphuric acid.

It is readily seen that the effect of oxidiser additions or the presence of oxygen on corrosion rate depends on both the medium and the metals involved. The corrosion rate may be increased by the addition of oxidisers, it may have no effect on the corrosion rate or a complex behaviour may be observed.

By knowing the basic characteristics of a metal or alloy and the environment to which it is exposed, it is often possible to predict the effect of oxidiser

additions [19].

The contamination of a solution with chlorides produces a decrease in corrosion resistance of most metals, which possesses protective properties due to corrosion product films that form on the metal surface. An exception is silver, where silver chloride forms effective passivation films. Chlorides promote crevice corrosion, pit-corrosion and stress corrosion cracking mechanisms[3].

Sulphur is corrosive to ferrous materials at elevated temperatures (> 250° C) by a straight forward sulphination reaction. Sulphur corrosion is controlled by the concentration of sulphur and by temperature. As the temperature and concentration of sulphur increase, the corrosion rate will also increase[32].

2.4 CORROSION WITH ORGANIC SUBSTANCES

2.4.1 NATURE OF THE SOLUTION

Organic acids, also called carboxylic acids, belong to the broad family of organic compounds, which contain the organic acid radical or carboxyl group (COOH). The shape of the carboxyl group in carboxylic acids (RCO_2H) influences the tendency of R to ionize or form hydrogen bonds, which influence the corrosiveness of the acid[32]. Corrosion investigations showed that the corrosiveness of mono-carboxylic acids decreases with an increase in the chain length[33]. It has been attributed to an increase in steric hindrance and a decrease in protic character as the chain length increases. The protic character of an organic compound refers to the availability of acidic hydrogen, which may split as a proton and leads to corrosion of metals. The protic character and therefore corrosiveness, is determined by the structure of organic compounds. Acidic behaviour of acids is reflected by dissociation constants.

Corrosion rates increase with an increase in the dissolved oxygen level, present in solutions as described in paragraph 2.3.4.3.

Alkane carboxylic acids are also termed fatty acids. Fatty acids, which contain one to seven carbon atoms in the chain are known as lower fatty acids, those containing 8 to 12 carbon atoms are known as medium fatty acids, while those containing more than 12 carbon atoms are known as higher fatty acids.

Up to pelargonic acid (C_9), organic acids are liquids at NTP conditions and possess foul odours. The solubility of fatty acids in water decreases with an increase in carbon numbers. Up to butyric acid (C_4), the acids are soluble in water at all concentrations, whereas valeric acid (C_5) and the higher acids are only sparingly soluble in water at NTP conditions.

Heitz[34] classifies corrosion reactions in organic solvents as follows :

1. Electrochemical reactions, which follow a similar mechanism to those in aqueous solutions.
2. Chemical reactions, which involve direct charge transfer between the neutral atom, in the lattice of the metal, and the oxidising species.

2.4.2 ELECTROCHEMICAL REACTIONS

Two reactions are involved namely, an anodic oxidation reaction of the metal (material) and a cathodic reduction reaction of the environment (active medium). The two reactions are both half-cell reactions, which are similar to reactions where water is the solvent.

The anodic reaction results in the formation of a solvated metal cation M^{z+}_{solv}, a charged or uncharged metal complex $MX^{\cdot}$ or a solid compound MX_z, where X is a halogen ion or an organic acid anion.

Cathodic reactions involved can be the following:

1. Reduction of a solvated proton to H_2 gas

   $2H^+_{solv} + 2e^- \rightarrow H_2$

2. Reduction of acidic hydrogen of a proton donor

   $HA + e^- \rightarrow \frac{1}{2}H_2 + A^-$ where A^- is a carboxyl acid anion or alcoholate ion.

3. Reduction of a dissolved oxidising gas Y

   $Y_z + Zme^- \rightarrow ZY^{m-}$ where Y can be O_2,Cl_2,F2, Br_2, O_3 or N_2O_4.

4. Reduction of oxidising ions such as Fe^{3+}, Cu^{2+}, MnO_4^- or ClO_3^-.

2.4.3 CHEMICAL REACTIONS

A general chemical reaction is: $M + 2C_xH_yX_z \rightarrow MX_2 + C_{2x}H_{2y}X_{2z-2}$ where X is a halogen and M is a divalent metal. The Grignard reaction is an example of the general reaction $Mg + CH_3Cl \rightarrow CH_3MgCl$

When organic sulphur compounds react at high-temperature (> 250°C) with a metal, the reaction is as follows: $2M + 2RSH \rightarrow 2MS + H_2 + R_2$

Heitz[34] quoted a number of case studies of the corrosion of metals in organic solvents and concluded that the phenomenology indicated no specific differences from that experienced in aqueous corrosion.

Corrosion control in organic solvents is based on the same principle as those used for corrosion control in aqueous solutions, although there are minor differences. Cathodic and anodic protection is seriously limited by the resistance of the solvent.

It must be realised that paint coatings deteriorate rapidly in contact with organic solvent, which can lead to high corrosion rates.

2.5 CORROSION TESTS

Corrosion tests provide the basis for control of corrosion. Corrosion tests may be classified conveniently as follows:[35,36]

1. Laboratory tests, in which conditions can be precisely defined and controlled, but are usually remote from those that prevail in practice. Laboratory tests are usually accelerated tests.
2. Field tests, in which a number of replicates of different types of specimens are subjected to the environment experienced in service under the same conditions of environmental exposure.
3. Service tests, in which the specimens or protective treatments are incorporated in the actual plant or structure under consideration, with a consequent lower degree of control than that obtained in field tests.

Laboratory tests are useful in:

1. Studying the chemistry and mechanism of corrosion.
2. Indicating the environment in which a particular metal or alloy may be used satisfactorily.
3. Determining the possible effects of metals and alloys on the characteristics of an environment to which they may be exposed.
4. Serving as a control test during the manufacture of homogeneous, corrosion-resisting metals or alloys.
5. Determining the value of changes in composition or treatment in developing corrosion-resisting alloys.
6. Determining whether a metal, an alloy, or a protective coating conforms to a specification requiring a certain performance in a specified corrosion test.

Plant, field and service corrosion tests are most suitable for:

1. Selection of the most suitable material to withstand a particular environment and estimation of its probable durability in that environment.
2. Assessing the effectiveness of methods of preventing corrosion.

Standardised test procedures existed for most of the corrosion types to be investigated[4,36,37].

2.5.1 MASS LOSS TESTS

Mass loss tests embrace the evaluation of corrosion rates of species exposed to corrosive environments. The object of the tests is to determine corrosion rates of specimens with knowledge about mass loss during experiments, exposed area of specimens and exposure time of the specimen to the corrosive environment.

2.5.2 ELECTROCHEMICAL TESTS

Electrochemical test methods involve the determination of specific properties of the electrical double layer formed, when a metal is placed in contact with a solution and can be summarised as:

1. *The potential difference across the electric double layer.*

   It cannot be determined in absolute terms, but must be defined with reference to another charged surface, the reference electrode. In the case of a corroding metal, the potential is the corrosion potential, which arises from the mutual polarisation of the anodic and cathodic reactions, constituting the overall corrosion reaction.

2. *The reaction rate per unit area (i).*

For a corroding metal the anodic and cathodic current densities cannot be determined directly by means of an ammeter, unless the anodic and cathodic areas can physically be separated. If the metal is polarised, a nett current, i_C for cathodic polarisation and i_A for anodic polarisation, will be obtained and can be measured by means of an ammeter.

3. *The capacitance.*

The electrical double layer may be regarded as a resistor and capacitor in parallel[38], and measurements of the electrical impedance by the imposition of an alternating potential of known frequency can provide information on the nature of a surface.

Tests can be subdivided as follows:

* Zero current tests.

  No external current is superponated on the working electrode and the corrosion potential is measured relative to a reference electrode. Pourbaix-diagrams are used for the interpretation of the results. Tests are used to investigate the corrosion resistance and cathodic protection possibilities of underground structures.

* Potentiostatic tests.

  Determination of the potential-current relationship during polarisation, at a constant potential, with the current being the variable. Tests are used for investigations of the applicability of metals for electroplating and electrochemical etching.

* Galvanostatic tests.

  Determination of the potential-current relationship during polarisation, at constant current densities, with the potential being the variable. Tests are used for investigations of the applicability of metals for electroplating and electrochemical etching.

* Impedance tests.

  Periodically and at a preset frequency, the working electrode potential is varied and the impedance characteristics of the working electrode, is noted. Tests are used for investigations of corrosion protection mechanisms of surface coverings. Sathyharayana[39] described a method using faradaic rectification to determine the instantaneous corrosion rates, in which no reference electrode is required. The electrodes consist of the metal under investigation and a counter electrode of the same metal.

* Potentiodynamic tests.

  The working electrode potential is varied at a preset rate and the superponated current is noted as a function of the potential.

* Galvanodynamic tests.

  The superponated current is varied at a fixed rate and the working electrode potential is noted as a function of the current.

Potentiodynamic and galvanodynamic tests often form the basis of laboratory tests. They are important as corrosion rates, Tafel-slopes, critical current densities, passivation ability, break-down potentials and protection potentials of systems can be determined.

Electrochemical tests cannot detect chemical corrosion, but are suitable for corrosion mechanism determinations.

If electrochemical test results and mass loss test results compare favourably, it means an electrochemical mechanism is present. If mass loss test results are higher than electrochemical test results, a mixture between a chemical and an electrochemical mechanism exists. If no corrosion rate can be detected with electrochemical tests, but a corrosion rate is detected with mass loss tests, the mechanism is chemical.

Some passivation characteristics, such as passivation current, can only be detected by potentiodynamical tests and not by galvanodynamical tests,

making potentiodynamical tests more suitable for laboratory corrosion tests.

The relationship between theoretical and experimental polarisation curves for pure activation-controlled half-cell reactions is illustrated in figure 2.6. $M_1 \rightleftharpoons M_1^+ + e^-$ and $M_2 \rightleftharpoons M_2^+ + e^-$ with M_1 reacting cathodically and M_2 reacting anodically, in the representation.

FIGURE 2.6. *Experimental curves obtained with potentiodynamical tests compared to theoretical curves*

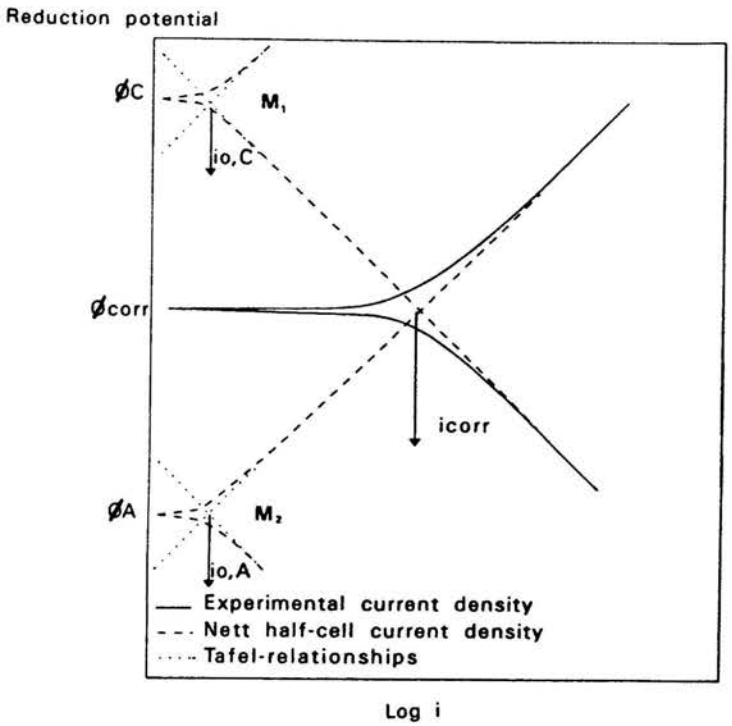

Experimental results can be substituted in modified Tafel equations to produce corrosion rates for corroding systems. The potential-current relationship at (ϕ_{CORR},i_{CORR}) is similar to the relationship at (ϕ_E,i_o) and the Tafel equation can be presented as

$$\eta = \pm\beta \log \frac{i}{i_{CORR}} \qquad (29)$$

To obtain the actual polarisation relationship and corrosion current from experimental curves, a trial and error method is used. Anodic scanning is based on the fact that $i = i_A - i_C$, while for cathodic scanning $i = i_C - i_A$.

Evans and Hoar[40] were of the first people to conduct electrochemical tests. The first potentiostat was designed by Hickling[41] in 1942. Improvements on the potentiostat have led to programmable potentiostats being commercially available today.

A potentiostat is an electronic device, which can control the potential on the working electrode at a specific potential, relative to a reference electrode. A schematic representation of a potentiostat for the conduction of electrochemical tests, is given in figure 2.7.

FIGURE 2.7 *Schematic electrochemical test set-up*

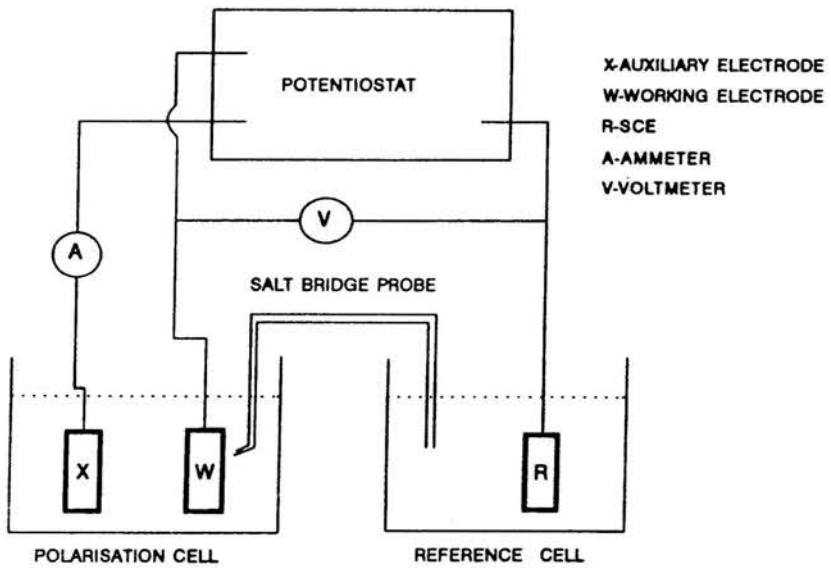

When the potentiostat is unconnected, the working electrode will corrode according to the prevailing corrosion conditions of the system. The voltmeter reading ($\Delta\phi$) will be

$$\Delta\phi = \phi_{RE} - \phi_{WE} \qquad (30)$$

with $\phi_{WE} = \phi_{CORR}$

When the potentiostat is connected, the potential difference $\Delta\phi$, is compared with the set voltage (SV) on the potentiostat. If $\Delta\phi$ = SV, the potentiostat will take no action. If $\Delta\phi \neq$ SV the potentiostat will generate a

current between the working electrode and the counter electrode and an electrochemical half-cell reaction will be superponated on the working electrode. The working electrode potential will be changed to become equal to the set voltage. The generated current is measured with an ammeter. Potential-current relationships experimentally determined are plotted on diagrams and are known as polarisation diagrams.

Since the fifties the use of potentiodynamic corrosion test methods has increased, but problems have arisen with the correlation of electrochemical results and mass loss results differing from 10% to 100%[42]. The interpretation of polarisation relationships is complex when there is a transition of one control type to another or when there are side reactions involved, that has minimal effect at (ϕ_{CORR},i_{CORR}) but become significant, even predominant, at large overpotentials. Results obtained from such polarisation characteristics can have large deviations. Deviations can also be incorporated when the specific electrical resistance between the working electrode and reference electrode is large.

Corrosion product films on the working electrode surface can cause interpretation problems. Films can cathodically be reduced; thus introducing non-relevant side reactions and conductivity of films which also influence results. Resistance polarisation and the electrical double layer effect can also play an important role[43]. The film can react as a membrane; thus reducing the medium pH on the electrode surface and introducing the cathodic hydrogen reaction, which would not have been present without a film[44]. Concentration polarisation commences at large overpotentials producing intermediate ß-values, which do not correspond with Tafel-values of diffusion or activation controlled systems[43].

2.5.2.1 POLARISATION RESISTANCE TESTS

Another format of potentiodynamical corrosion tests has been developed since 1951, known as polarisation resistance tests. The corrosion potential provides no information about the corrosion rate, and it is evident for a corroding metal where the anodic and cathodic sites are inseparable, that it is not possible to determine i_{CORR} by means of an ammeter.

It was found in studies on the corrosion of steel and cast iron in natural water that a linear relationship existed between potential and applied anodic and cathodic current densities in small overpotential regions[45]. The recognition of the importance of this observation was due to the work done by Stern[45] and his co-workers who used the term, linear polarisation, to describe the linearity of the $\eta - i$ curve in the region of ϕ_{CORR}. The slope of the linear curve, $\Delta\phi - \Delta I$ or $\Delta\phi - \Delta i$ is termed the polarisation resistance, R_p, since it has dimensions of ohms[46].

$$R_p = \text{polarisation resistance} = \frac{\Delta\eta}{\Delta i_{applied}} \qquad (31)$$

Assumptions involved in the Stern-Geary technique are:

1. Both reactions are charge-transfer controlled (transport overpotential is negligible).
2. IR drop involved in determining the potential is negligible.

The relationship between corrosion currents, Tafel-slopes and polarisation resistance will be presented as derived by Stern[45] et.al.

$$\eta_A = \beta_A \log\left(\frac{i_A}{i_{CORR}}\right)$$

and $$\eta_C = -\beta_C \log\left(\frac{i_C}{i_{CORR}}\right)$$

$$i_A = i_{CORR} \exp\left(\frac{-2.3 \times \eta}{\beta_A}\right)$$

and $$i_C = i_{CORR} \exp\left(\frac{-2.3 \times \eta}{\beta_C}\right)$$

$$i_{applied} = i_A - i_C = i_{CORR}\left(\exp\left(\frac{2.3 \times \eta}{\beta_A}\right) - \exp\left(\frac{-2.3 \times \eta}{\beta_C}\right)\right)$$

$$\frac{di_{applied}}{d\eta} = i_{CORR}\left[\frac{2.3}{\beta_A}\exp\left(\frac{2.3 \times \eta}{\beta_A}\right) + \frac{2.3}{\beta_C}\exp\left(\frac{-2.3 \times \eta}{\beta_C}\right)\right]$$

$$\eta = \phi - \phi_{CORR} = d\eta = d\phi$$

$$\frac{di_{applied}}{d\phi}\Big|_{\phi_{CORR}} = 2.3 \times i_{CORR}\left(\frac{1}{\beta_A} + \frac{1}{\beta_C}\right) = \frac{1}{R_p}$$

$$i_{CORR} = \frac{\beta_A \times \beta_C}{2.3 \times R_p \times (\beta_A + \beta_C)} \qquad (32)$$

$$B = \frac{\beta_A \times \beta_C}{2.303(\beta_A + \beta_C)} \qquad (33)$$

$$\therefore i_{CORR} = \frac{B}{R_p} \qquad (34)$$

Although ß$_A$ and ß$_C$ can vary over a large range, B does not vary that much. Stern and Weisert[47] have shown, for most practical situations where one ß-value varies from 0.6 to 0.12 V/decade and the other ß-value varies between 0.6 and ∞ V/decade, that B will only vary between 0.01305 and 0.0522 V/decade. It is clear that estimated ß-values can produce relatively accurate corrosion rates.

Analyses are fast and the system will not be disturbed as much as the case would be for complete corrosion rate-time investigations. If B-values are not available, corrosion rates are presented qualitatively and are compared as

polarisation conductance values. $K_p = [1/R_p]$

2.5.2.2 DATA PROCESSING

Methods have been developed which use point values to determine corrosion rates and Tafel-slopes. Examples are the three point method of Barnartt[48,49] and the four point method of Jankowski and Juchniewicz[50]. Analyses in the region of (ϕ_{CORR},i_{CORR}) has the advantage that influences from side reactions are less. It is important to ensure accurate experimental observations, because the methods are very sensitive and may easily lead to the square root of a negative number[51].

A trial-and-error method to determine corrosion characteristics from experimental results can easily be done with the aid of a computer. Programs available are CORFIT[52], POLCURR[53], BETACRUNCH[1] and LOOPFIT[54] and are based on basic electrochemical equations.

The BETACRUNCH program needs data points in the format of (ϕ,I_{EX}) or (η,I_{EX}) and in multiples of three, with a minimum of three data point sets. Results obtained are $ß_A$, $ß_C$, I_{CORR} and corrosion rate. For most accurate results the biggest potential region without side reactions present, should be chosen.

For a process with a diffusion controlled cathodic reaction and activation controlled anodic reaction a similar linear relationship applies

$$\frac{1}{R_p} = \left[\frac{\Delta i}{\Delta \phi}\right]_{\phi_{CORR}} = \frac{2.3\, i_L}{\beta_A} = \frac{2.3\, i_{CORR}}{\beta_A} \qquad (35)$$

where i_L is the limiting current density of the cathodic reaction and it is assumed that $i_L = i_{CORR}$.

2.5.3 CORROSION MONITORING

Corrosion monitoring has become important in plants, because some plants are now expected to operate continuously for periods of up to three years without shutdown times. For such operating conditions it is essential to have some idea of the corrosion rates of metals used in the chemical plants. With known corrosion rates of the metals, no unscheduled shutdown would be necessary and a safe environment for operating personnel would prevail.

Variables that affect the rate and type of corrosion are : temperature, pressure, trace compounds, velocity, presence of insoluble materials (abrasives or deposits), crevices, stress (magnitude and type are important), interface effects, phase changes of the medium, chemical composition of the metal, metallurgical condition of the metal and galvanic effects[55]. Unfortunately a single method of corrosion inspection cannot accommodate all the variables and it is extremely dangerous to rely on data provided by one corrosion monitoring method. A study is required of all methods available and usually two or three methods are chosen which are necessary to serve as a suitable corrosion monitoring system for a plant.

The selection of inspection points is of paramount importance and factors to be considered was outlined by Abramchuk[56] as follows:

1. Changes in direction of flow such as elbows, tees, return bends and changes in pipe size that create turbulence or changes in velocity.
2. Presence of "dead-ends", loops, crevices, obstructions or other conditions, which may produce turbulent flow causing erosion or stagnant flow, which will allow debris or corrosive media to accumulate and set up corrosion cells.
3. Junctions of dissimilar metal that promote galvanic action.
4. Stressed areas such as those at welds, rivets, treads or areas that undergo cyclic temperature or pressure changes.

Selection of inspection points should be based on a thorough knowledge of process conditions, materials of construction, geometry of the system, external factors and historical records.

2.5.3.1 TESTING METHODS AVAILABLE

2.5.3.1.1 Visual inspection

Visual inspection is regarded by Abramchuk[56] as so fundamental that it should be a logical prelude to most other inspection methods. A proper visual inspection accomplishes the following:

1. Aids the analyses of causes of failure.
2. Indicates the need for further exploration.
3. Helps to define the search area, if further exploration is warranted.
4. Aids in suggesting techniques for further exploration.
5. Aids in determining the measures needed to prevent the recurrence of damage to equipment.
6. Reduces the possibility of installing faulty fabrications by ensuring that the right materials and procedures are used and that workmanship is of the proper quality.

Signs of possible damage can include rust staining, bulging, cracked or distorted insulation and hot spots that suggest possible corrosion damage. A disadvantage is that inspection can only be carried out when plants are shut down, but it provides information that can be used in the future.

2.5.3.1.2 "Tell-tale" holes

The method comprises of the drilling of 6.5 mm holes into vessels or pipe walls to a depth which equals the design pressure wall thickness[57]. The depth of the wall remaining is equal to the corrosion allowance. When this thickness has been consumed a small leak develops. The method has been

used by the oil industry, but even a controlled leak of highly inflammable liquid can be regarded as hazardous.

2.5.3.1.3 Coupons

Cylindrical rods or strips are mounted in suitable racks. The coupons are electrically insulated from each other and the rack material with teflon, or other suitable insulating material. The different kinds of racks are described by Dillon, et al[55]. A disadvantage of coupon techniques is that the response to severe corroding conditions that may occur for short periods of time is not detected, but only an average over the period of exposure time can be detected. Coupons can be withdrawn at different intervals in time to investigate the effect exposure time has had on the corrosion process.

2.5.3.1.4 Electrical resistance probes

Resistance probes such as the Corrosometer is a well-proven method for the detection and measurement of corrosion[58]. A wire element, made of the metal to be tested, is mounted in a suitable casing and exposed to the corrosive medium, either liquid or gas. The wire decreases in cross-sectional area due to the corrosion of the wire, caused by the corrosiveness of the environment. Most corrosion products have greater electrical resistance than the metal from which it was formed; thus an accurate measurement of the increase in resistance can be equated to metal loss and corrosion rates.

A variety of elements in different geometric forms e.g. wire, tube, strip and a 'flush' strip are available and find their application depending on the temperature and pressure of the system. Data obtained from electrical resistance probes and of test coupons are similar in giving average corrosion rates, but the former has the advantage that data are obtained continuously, while the plant is in operation. The probe reading is plotted against time and the slope will indicate the corrosion rate at any particular time.

The instrument cannot discriminate between localised and general corrosion attack, but pitting can be expected if the slope of the plotted graph suddenly increases without any change in the plant process conditions that would normally increase the general corrosion rate.

2.5.3.1.5 Polarisation resistance probes

Polarisation resistance instruments (Corrators) are capable of monitoring corrosion rate, produce an alarm signal and also provide information regarding the type of corrosion. Polarisation resistance instruments are capable of measuring the instantaneous corrosion rate of metals in conductive liquids. A drawing of a three-electrode probe with lead wires and instrument is shown in figure 2.8. The electrode can be made from any machinable metal. The voltmeter measures the potential between the reference and test electrodes. A current source, I, will supply the power necessary to polarise the test electrode in either the cathodic or anodic direction from the null point. The output of the polarisation resistance corrosion monitor can be either a current or voltage signal that is proportional to the corrosion rate of the metal[59].

FIGURE 2.8 *Polarisation resistance corrosion monitor*

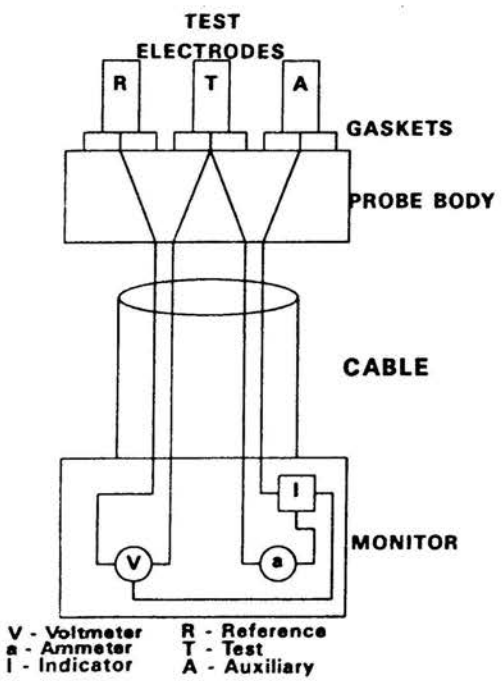

With this technique it is possible to measure the general corrosion rate as well as localised corrosion with reference to the pitting index. The pitting index is obtained by a difference of reading between two identical electrodes. Probes are available in both two and three electrode forms. Three electrode probes can be used in higher resistive solutions, while two electrode probes are usually suitable for industrial application. A variety of probe designs are available on the market, which can be retracted or have screw-in fittings.

The units can be combined with the measurement of pH and total dissolved solids content. Automatic control of addition of corrosion inhibitors and acids is possible because of the signal produced by the Corrator.

2.5.3.1.6 Ultrasonics

Ultrasonics involves the transmission of very high frequency sound waves through the metal by which thickness is monitored[60]. Two methods that are commonly used are the pulse-echo method and resonance method.

With the pulse-echo method a short burst of energy is transmitted via a transducer probe, into the metal. The time taken for the sound to transverse the thickness of the metal and return to the probe provides the thickness of the metal. This is displayed on an oscilloscope and with the aid of modern instruments it provides a digital readout of the wall thickness.

With the resonance method the frequency varies from ultrasound to a value that equals twice the thickness of the test material. A condition of resonance then occurs resulting in standing waves in the metal causing a resonance at a greater amplitude that will be recorded by the transmitting probe. Metal thickness can be determined from its sound velocity properties after a number of resonant frequencies are determined.

A problem associated with plant inspection is the coupling of the probe to

the metal under examination, because the metals are usually covered with rust. This results in spurious and inaccurate results. The disadvantage of this method is that often the probe is moved by operators to an area where adequate coupling is obtained, circumventing the real objective of the measurement[61] and often it is impossible to obtain any coupling on severely corroded steel surfaces.

A common problem to both the methods is that temperature can destroy the piezoelectric properties of the probes. Pitting causes problems as it is impossible to obtain resonance in some circumstances and the measurement on the pitted surface will be the average of the pit depth and the wall thickness. It must also be realised that sound travels about twice as fast in steel as in paint, which may give the wrong impression of the wall thickness and a wrong corrosion rate will be observed.

2.5.3.1.7 Other methods used for corrosion monitoring.

Eddy current methods are used for *in situ* inspection of condensed tubes by mounting eddy-current coils in probes which can be inserted in condenser tubes. The principle of operation has been described by Britton[62].

Infra-red radiation has been explored by the CEGB (Central Electricity Generating Board) for assessing corrosion in boiler tubes at power-stations. An external heat source is placed onto the outside of the boiler tubes while cold water is circulated inside the tubes. Hot spots due to poor heat conductivity caused by excessive corrosion products indicate areas of high corrosion. The tests can only be done during shutdown times.

Radiography is used in detecting welding defects and cracks and can successfully reveal corrosion in the plant; Berk and McGregor[63] have discussed various investigation techniques. An advantage is that lagging need not be removed. Disadvantages are radiation hazards, the time required to complete exposure and the fact that access is required to both sides of

the item.

Another form of monitoring can be to fit testing equipment to side-stream units in the plants for corrosion measurements and while the plant is operational, experiments can be done on this equipment.

3 EXPERIMENTAL

3.1 APPARATUSES

Groups of apparatuses used in the investigations involved: acid number determination, medium preparation, sample preparation, mass loss tests, electrochemical tests, turbulence tests and corrosion monitoring.

3.1.1 ACID NUMBER DETERMINATION

The following apparatuses were used during acid number determination experiments:

* 600 ml conical flasks.
* 100 ml measuring cylinder, grade A.
* Microburette grade A, 10 ml capacity.
* Burette grade A, 50 ml capacity.
* Auto-titrator with 20 ml burette. (A metrohm piston burette should be used instead of glass burette.)

3.1.2 MEDIUM PREPARATIONS

The following apparatuses were used during medium preparations :

* De-aeration cascade.
* Dissolved oxygen meter Hanna instruments HI 8043.
* Nitrogen gas.
* Water saturater.

3.1.3 SAMPLE PREPARATION

The following apparatuses were used in sample preparations :

* Turning tables with fixed sandpaper.
* Magnet.
* P220 sandpaper.
* P600 sandpaper.
* Samples used for different corrosion tests are shown in picture 1.
  1. Samples used in electrochemical tests with an exposed area of 1 cm^2.
  2. Samples used in turbulence tests with an exposed area of 6.28 cm^2.
  3. Samples used in mass loss tests with an exposed area 4 cm^2.
* All samples used were made of AISI 1020 mild steel.

PICTURE 1 *Samples used to conduct the different corrosion tests*

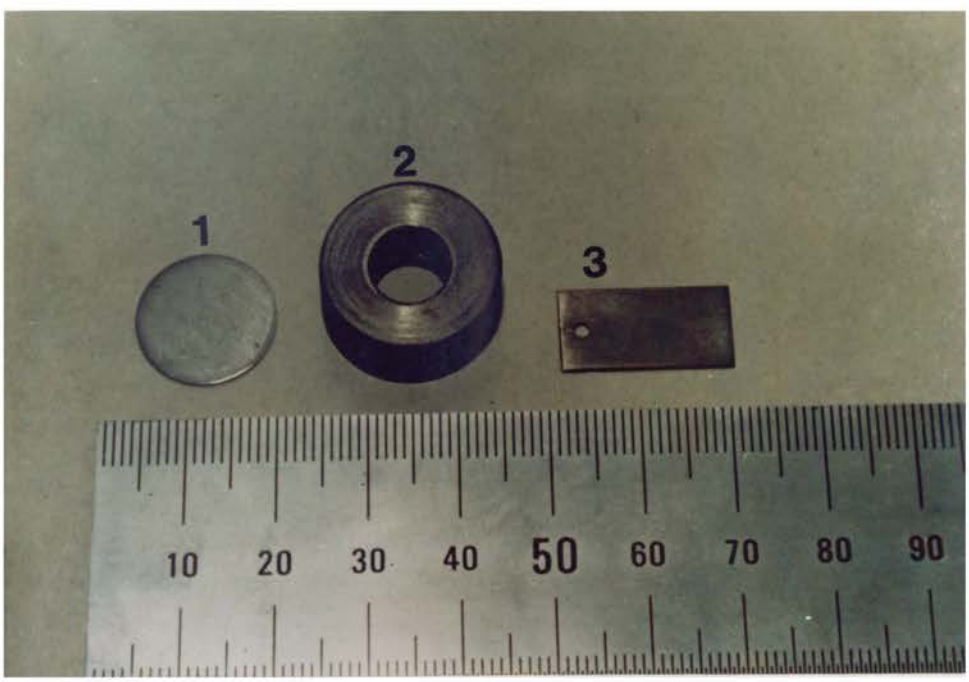

3.1.4 MASS LOSS TESTS

Two different experimental set-ups were used in the conduction of mass loss tests, the first consisted of the lower temperature range from 25°C to 90°C, while the second consisted of the higher temperature range from 130°C to 250°C.

A. Low temperature range.

For the lower temperature range, tests were conducted in water-baths in glass bottles at 25°C, 60°C and 90°C. Apparatuses used are shown in picture 2 and consisted of the following :

1. Water-bath.
2. Temperature controller.
3. Medicine glass bottle with a screw cap.

PICTURE 2 *Lower range mass loss tests*

B. **High temperature range.**

Apparatuses used for the higher temperature range are shown in picture 3 and consisted of the following :

6. Special glass containers were made to fit precisely into the Parr autoclaves.
7. Teflon tape was used to mount the specimens.
8. Teflon seals were used to seal the autoclave and protect the test solution from evaporating (not shown).
9. Temperature controller[64].
10. Parr autoclave.
11. Thermocouple used to measure the temperature inside the autoclave.
12. Pressure release valve.
13. Heat jacket.
14. Pressure gauge.

PICTURE 3 *High temperature range mass loss tests (autoclave)*

3.1.5 ELECTROCHEMICAL TESTS

Apparatuses used for conducting electrochemical tests are shown in pictures 4,5 and 6 and consisted of the following :

1. A Princeton model 362 Scanning Potentiostat.
2. A Soar model 73 Voltmeter.
3. A model Metrix ITT instrument MX112 Ammeter.
4. Water-bath with the temperature controlled within ± 1°C from the set-point, as shown in picture 2 no 1.
5. Electrochemical cell.
6. Luggin capillary, as shown in picture 5 no 5, was used for the reduction of IR-losses.

PICTURE 4 *Electrochemical test set-up*

Apparatuses used in the electrochemical cell are shown in pictures 5 and 6 and consist of the following :

1. A 1.5 l glass beaker.
2. A teflon top, with drilled holes, to hold the different electrodes and a de-aerator in position.
3. Two inert platina counter electrodes were used to ensure homogeneous distribution of current on the working electrode surface.
4. The reference electrode was a calomel electrode.
5. A luggin capillary was brought into electrical contact, with the solution and reference electrode, to reduce IR losses. The luggin tube was filled with a 3% agar solution (A) and with a saturated KCl solution (S). Feitler[65] alleged that IR-losses would take an effect if the specific conductance of the test solution < 0.1 mS/m, while Mansfield[66] has shown that IR-losses become less significant at higher specific conductance values.
6. The working electrode is represented in picture 6 and will be discussed in more detail.
7. A tygon tube (not shown) was used to ensure a positive nitrogen gas pressure level inside the electrochemical cell by blowing water saturated N_2 gas at a rate of 0.5 l/min above the liquid level in the container. The dissolved oxygen meter showed that the dissolved oxygen level did not increase, while the experiments were being conducted. Nitrogen gas was saturated with water before entering the electrochemical cell, ensuring minimal evaporation of test solutions.
8. Specimen to be tested.
9. Rubber ring.
10. Teflon working electrode covers.

PICTURE 5 *Close-up of the electrochemical cell components*

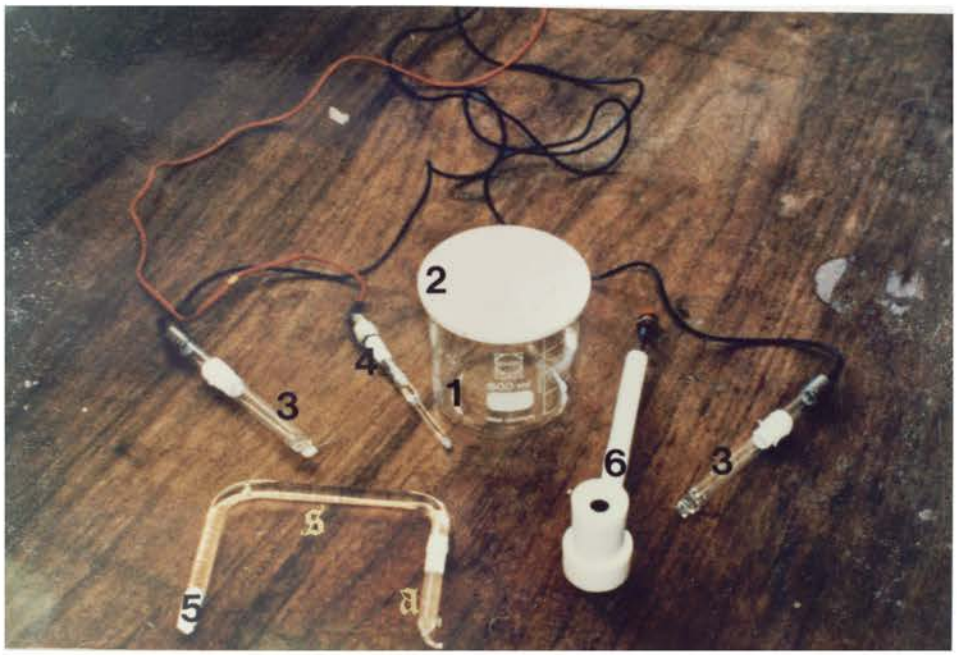

PICTURE 6 *The working electrode in detail*

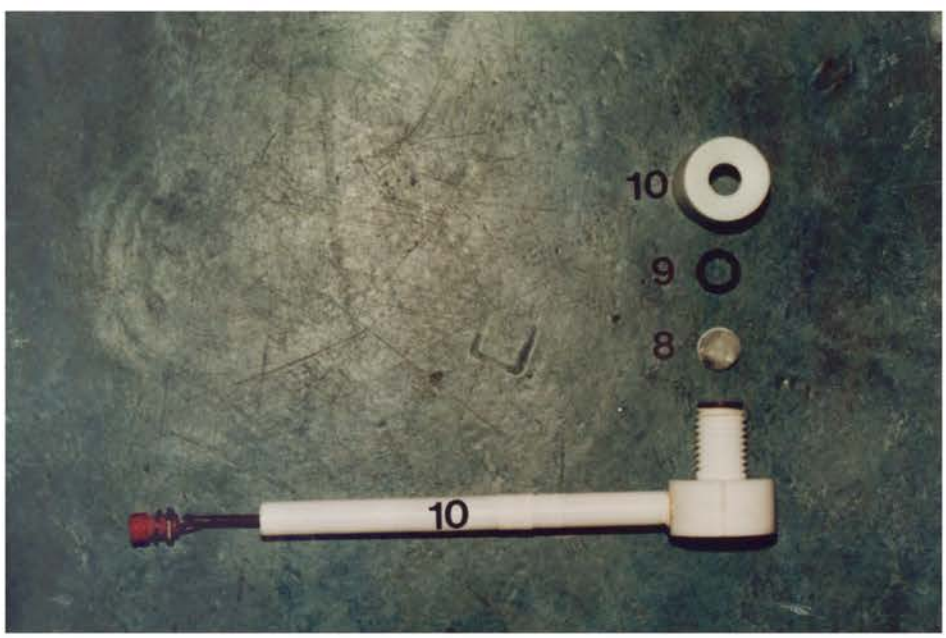

3.1.6 TURBULENCE TESTS

Turbulence tests involved mass loss tests and electrochemical tests.

3.1.6.1 MASS LOSS TURBULENCE TESTS

Apparatuses used in mass loss turbulence tests are shown in pictures 7 and 8 and consisted of the following :

1. The specimen was a rotating cylinder with the curved surface area exposed to the medium. See picture 1 no 2.
2. A Heidolph RGL 500 stirrer was used to produce rotation of the working electrode. The degree of turbulence was determined by the speed by which the motor turned, which could be controlled and was indicated on the gauge. The tachometer was calibrated with a stroboscope.

PICTURE 7 *Apparatuses used for mass loss turbulence tests*

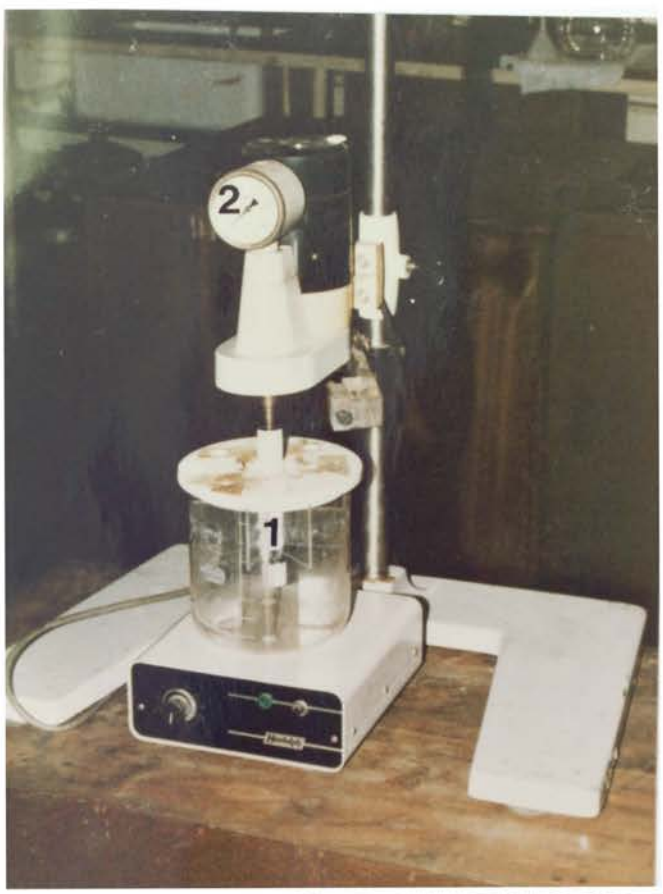

3. The holder and lid were designed to prevent the vortex effect and are shown in picture 8.

PICTURE 8 *A close-up of the beaker specially designed to prevent the vortex effect*

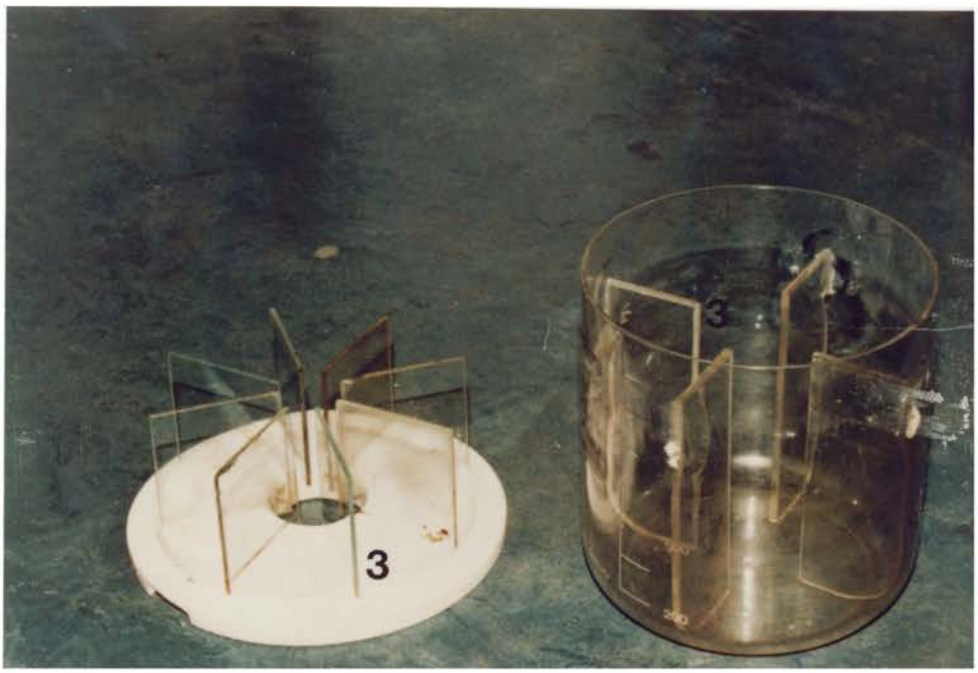

3.1.6.2 ELECTROCHEMICAL TURBULENCE TESTS

A combination of apparatuses as shown in pictures 4,7 and 8 were used for electrochemical turbulence tests.

3.1.7 MONITORING

The apparatuses used in this section are shown in pictures 9 and 10 and consisted of the electrical resistance probe apparatus (Corrosometer) and polarisation resistance probe apparatus (Corrator).

1. Monitoring was done with the aid of an electrical resistance probe apparatus, a model CK-3 Portable Corrosometer# as shown in picture 9, and with a polarisation resistance probe apparatus, the Model 9030 Corrator* Instrument (no 4), as shown in picture 10.
2. Probe.

3. Electrode.
4. Discussed in no 1.
5. Probe.
6. Recorder.
7. Electrodes.
8. Recording paper.

Rohrback Corporation.
• Rohrback Cosasio Systems

PICTURE 9 *The portable Corrosometer*

PICTURE 10 *The model 9030 Corrator*

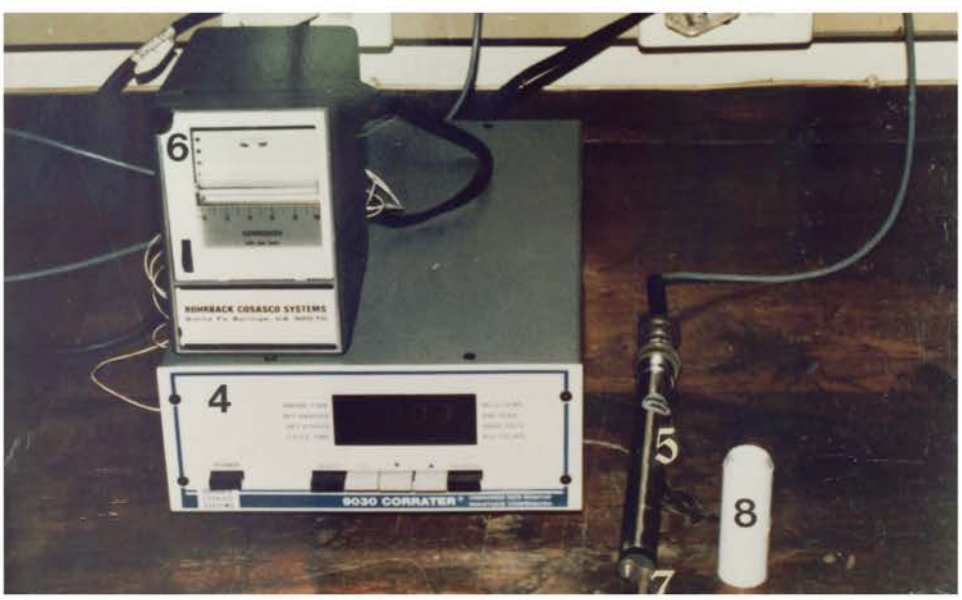

3.2 PROCEDURES

In the procedures the following will be discussed: standardisation, cleaning procedures, acid number determination, medium preparation, sample preparation, mass loss tests, electrochemical tests, corrosion monitoring and preparation of a stabilised-Synthol-light-oil-water phase.

3.2.1 STANDARDISATION

ASTM standardisation procedures used were[67]:

ASTM G1-81 Preparing, cleaning and evaluating corrosion test specimen.

ASTM G3-74 Conventions applicable to electrochemical measurements in corrosion testing.

ASTM G5-82 Standard reference method for making potentiostatic and potentiodynamic anodic polarisation measurements.

ASTM G31-72 Laboratory immersion corrosion testing of metals.

Standardisation of the dissolved oxygen meter (HI 8043), model CK-3 portable Corrosometer and model 9030 Corrator were done according to the procedures prescribed by the manufacturers.

Exposure time for mass loss tests was kept to 72 hours as far as possible, which is according to recommended exposure times proposed in ASTM standards[37].

A method was developed to determine exposure times necessary for potentiodynamical tests. Polarisation resistance tests at different times were done and $1/R_p$ were plotted as a function of time. As soon as $1/R_p$ did not vary with time, the system was stable and potentiodynamical tests were done on the system.

3.2.2 CLEANING PROCEDURES

1. Care was taken to ensure that glass containers were thoroughly cleaned before use.
2. Glassware was washed with a mixture of H_2SO_4 and HNO_3.
3. After this, glassware was washed with soap and thoroughly rinsed with water and acetone.

3.2.3 ACID NUMBER DETERMINATION

The method that was used for acid number determination was based on the ASTM standard test method for neutralisation number by colour-indicator titration[68]. The total acid number is the quantity of base, expressed in milligrams of potassium hydroxide, that is required to neutralise the total acidic constituents present in one gram of sample at 25°C. To determine the total acid number, the sample is titrated at room temperature with KOH to the end point indicated by the colour change to pink caused by the addition of the phenolphthalein indicator (pH value of 9.5).

3.2.3.1 REAGENTS REQUIRED

Chemically pure reagents were used for all the experiments.

3.2.3.1.1 KOH solutions : 0.025 N and 1.0 N

Standardised 0.025 N and 1.0 N KOH solutions were prepared.

3.2.3.1.2 Phenolphthalein indicator, 1.0 % solution in ethanol

1.0 ± 0.01 g of phenolphthalein crystals were dissolved in 100 ml ethanol and 0.025 N alkali was added, until the first permanent pink colour appeared.

3.2.3.2 EXPERIMENTAL PROCEDURE

1. 100 ml of distilled water was measured into a 600 ml conical beaker.
2. 5 drops of phenolphthalein indicator were added to the solution and neutralised with 0.025 N KOH solution, until the first perceptible pink colour appeared.
3. 200 ± 0.1 g of the sample (M) was measured in a conical beaker.
4. The solution was titrated with 1.0 N KOH solution, until the first perceptible pink colour appeared, and the volume (V) was noted accurately.
5. The following theoretically derived formula was used to determine the acid number of the samples:

$$AN = \frac{V\ N\ MM \times 10^3}{M} \qquad (36)$$

6. Duplicate results obtained by the same analyst were considered suspect if they differed more than 1 mg KOH/g solution.

3.2.4 MEDIUM PREPARATION

The following procedures were followed in the medium preparation section:

1. Specific quantities of organic acids were added to distilled water, to obtain the required acid numbers.
2. Test solution volumes for lower temperature ranges were 250 ml, while 400 ml samples were tested for the higher temperature ranges.
3. The medium was then de-aerated with water saturated nitrogen gas for one hour to reduce the dissolved oxygen content of the medium to less than 1.0 ppm. Nitrogen gas had to be saturated with water to reduce evaporation of the test solution.
4. The oxygen contamination was constantly checked with the dissolved oxygen meter, model HI 8043, to ensure that the required level was maintained.
5. Care was taken to ensure that no further oxygen contamination occurred

during the conduction of experiments.

6. Separate solutions were also prepared which incorporated impurities.
7. A solution was made which had a concentration of 20 ppm Cl^- that was obtained by dissolving 0.03314 g NaCl in 1000 g acetic acid with an acid number of 25 mg KOH/g solution.
8. A solution was made which had a concentration of 1000 ppm S^{2-} which was obtained by dissolving 2.438 g Na_2S in 1000 g acetic acid with an acid number of 25 mg KOH/g solution.
9. A concentration of 7.86 ppm O^{2-} was obtained by saturation of the solution with medically clean air for one hour.

3.2.5 SAMPLE PREPARATION

Specimens used were AISI 1020 mild steel.

1. Specimens were sanded with waterproof silicon carbide paper P220 in the presence of water until a shining surface appeared.
2. Specimens were polished with P600 waterproof silicon carbide sandpaper.
3. Al_2O_3 was used to remove organic material from the specimen surfaces.
4. Specimens were rinsed with running water to remove the Al_2O_3 and then rinsed with acetone and dried with hot air.
5. The masses of the specimens were determined accurately to ± 0.0001 g and were then ready for conduction of the tests.

3.2.6 MASS LOSS TESTS

The procedure followed to conduct mass loss tests were the following :

1. The medium was prepared as noted above.
2. Specimen preparation was done as stated above.
3. The masses of specimens were determined and accurately noted to ± 0.0001 g.

4a. For the lower temperature range from 25°C to 90°C corrosion tests were conducted in glass bottles placed in water-baths.

b. Specimens were mounted in solutions with the aid of cotton thread and sealed with the cap which had nitrile rubber installed inside the cap. Cotton thread was tied through a hole drilled in the specimen as shown in picture 1 no 3 and the loose end of the cotton thread, was kept in place by closing the cap. Nitrile rubber seals were used to avoid oxygen contamination from the atmosphere, because the test medium needed to be de-aerated. Nitrile rubber is immune to the attack of organic acids; thus the danger of test solution contamination with oxygen and rubber was eliminated.

5a. For the higher temperature range from 130°C to 250°C, corrosion tests were done in autoclaves.

b. Special glass containers were made to fit precisely into the autoclaves to avoid contact between the test solution and metal from the autoclave; thus ensuring minimal contamination of the tests solution by the autoclave body. Also avoiding electrical and electrochemical contact between the specimen and autoclave body. The specimens were mounted in the solution with the aid of teflon tape rolled into a thin thread and tied through the hole drilled in the specimen.(See in picture 1 no 3). The loose end was tied to the glass rod in the upper section of the glass container. Teflon tape was used to be able to withstand the high temperatures inside the autoclaves.

6. Turbulence tests were only conducted at 25°C.
7. After completion of tests corrosion products were removed from the

specimen surface with the aid of a copper-brush.

8. Specimens were then washed with acetone and dried in hot air.
9. Masses of the specimens were determined accurately to ± 0.0001 g.
10. Corrosion rates were determined with the aid of the following formula:

$$CR = \frac{\Delta m \times 10^6}{A\, t\, 27.4\, \rho}\ \mu\text{mpy} \qquad (37)$$

11. Duplicate results were considered suspect if they differed more than 10 % from each other for tests done in the same corrosive medium and further tests were performed until the deviation in results was less than 10%.

3.2.7 ELECTROCHEMICAL TESTS

Electrochemical tests were divided into polarisation resistance tests, done when systems were unsteady, and potentiodynamical tests, done when systems reached a steady state.

3.2.7.1 POLARISATION RESISTANCE TESTS

1. The tests were done according to ASTM G59-78.
2. The scanning rate was 10 mV/min.
3. Scanning was done from η = 0 mV to η = -30 mV and then from η = 0 mV to η = +30 mV. The polarisation resistance (R_p) was determined at the point ($\eta = 0$, $I_{EX} = 0$), and tests were done at 1,2,4,8,12,24,48,72,96,120 and 144 hours after first exposure to the corrosive solution.
4. The inverses of polarisation resistances were plotted at the corresponding times when tests were conducted, to determine when the system reached stability.

3.2.7.2 POTENTIODYNAMICAL TESTS

1. After stability was reached, potentiodynamical tests were conducted.
2. Scanning rate was 10 mV/min.
3. The potential region of $\eta = \pm$ 200 mV was examined. Polarisation curves were plotted and Tafel-slopes, corrosion currents (I_{CORR}) and corrosion rates were obtained.

3.2.8 CORROSION MONITORING

The two electrical appliances used for conducting corrosion monitoring were the Corrator and Corrosometer which were both standardised and used according to procedures provided and described by the manufacturers.

3.2.9 PREPARATION OF A STABILISED-SYNTHOL-LIGHT-OIL-WATER PHASE

1. The test solution was prepared by mixing 1 part distilled water and 10 parts of stabilised-Synthol-light-oil received from SASOL, in a beaker. The ratio of 1:10 is according to ASTM standards[69].
2. The mixture was mechanically stirred for two hours and then left to separate in two phases.
3. The acid number of the water phase was determined and mass loss corrosion tests were done on this system, which will be called system A.
4. An addition of pure acetic acid was made to system A to produce system B with an acid number of 25 mg KOH/g solution.

3.3 ANALYSIS METHODS

Analysis methods will be discussed considering mass loss tests, electrochemical tests and corrosion monitoring.

3.3.1 MASS LOSS TESTS

Evaluation of mass loss corrosion rates were done with the aid of Eqn(37), according to ASTM G1-81.

3.3.2 ELECTROCHEMICAL TESTS

Electrochemical tests included polarisation resistance tests and potentiodynamical tests.

3.3.2.1 POLARISATION RESISTANCE TESTS

Polarisation resistance evaluations were done in accordance with ASTM standards[37].

3.3.2.2 POTENTIODYNAMICAL TESTS

Evaluation of corrosion rates, determined with the aid of potentiodynamical tests were done according to ASTM G5-82.

i_{CORR} can be determined graphically or with the aid of computer programs. The corrosion rate was determined with the aid of the Betacrunch program[1]. The following procedures were followed:

1. Polarisation characteristics were plotted on a semi-logarithmic graph paper in the region from $\eta = 0$ mV to $\eta = \pm$ 200 mV.
2. With visual inspections, regions were identified where non-relevant side reactions occurred, usually at high overpotentials.
3. Data from side reactions were ignored when the Betacrunch program was used. At large overpotential regions nine data point pairs consisting of overpotentials and currents (η,i) were used to obtain corrosion rates, Tafel-slopes and corrosion currents from the Betacrunch program.

3.3.3 CORROSION MONITORING

3.3.3.1 CORRATOR

The corrosion rate was directly indicated on the display of the Corrator.

3.3.3.2 CORROSOMETER

1. Results were obtained over a period of time. Data were plotted against time and the slope of the graph represented indirectly the corrosion rate.
2. Instantaneous corrosion rates were obtained when slopes were determined at specific times. The corrosion rate was obtained with the aid the following equation:

$$CR = \frac{\Delta reading}{\Delta time\,[days]}\,0.365\,s \qquad (38)$$

s = probe span

4 RESULTS

All the results noted were at least done in duplicate. If problems with repetition occurred, tests were repeated up to six times. A deviation of 10% was allowed to accommodate experimental errors.

4.1 PRELIMINARY INVESTIGATIONS

Preliminary investigations include results associated with acid number determinations and de-aeration of the medium.

4.1.1 ACID NUMBER DETERMINATION

Acid number was one of the variables to be investigated. In order to facilitate the make up of solutions with different predetermined acid numbers, correlations between acid concentrations and acid numbers were established. Acid numbers for the lower fatty acids were determined according to the method described in paragraph 3.2.3.2. Numerical data are tabulated in Appendix(A.1.1) and a graphical representation with concentration as mass percentage is given in figure 4.1.

In figure 4.2 concentration is expressed as mole percentage. Numerical data are tabulated in Appendix(A.1.2). The correlation is a linear relationship between mole percentage and acid number which is independent of the type of fatty acid. Use was made of this correlation in preparing acid solutions of desired acid numbers for all the fatty acids.

The solubilities of fatty acids in water decrease with chain length of molecules[38]. No data could be found on the solubilities of the higher fatty acids in water at higher temperatures and pressures. All solutions were prepared as if the acids were soluble at the relevant conditions. Systems where solutions became saturated at relatively low acid numbers could be

detected from results as shown in paragraph 4.2.1 and discussed in chapter five.

FIGURE 4.1 *Acid number as a function of mass % at 25°C*

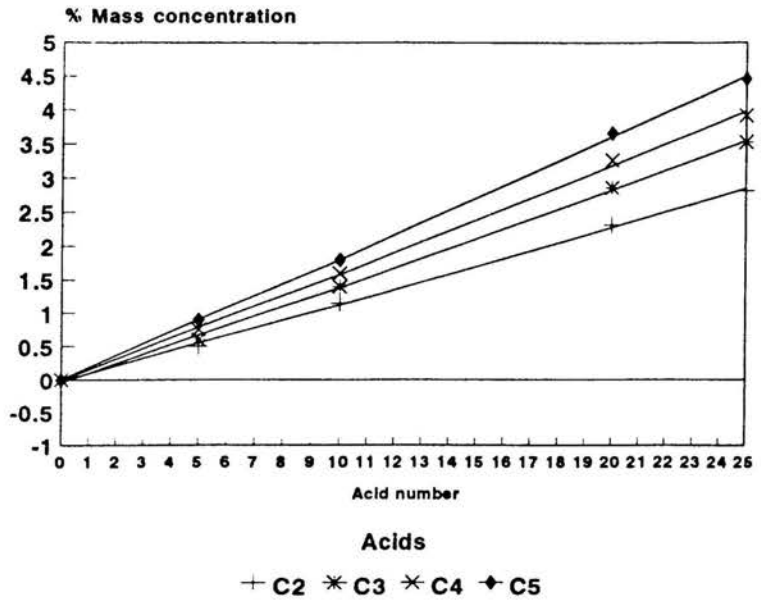

FIGURE 4.2 *Acid number as a function of mole % at 25°C*

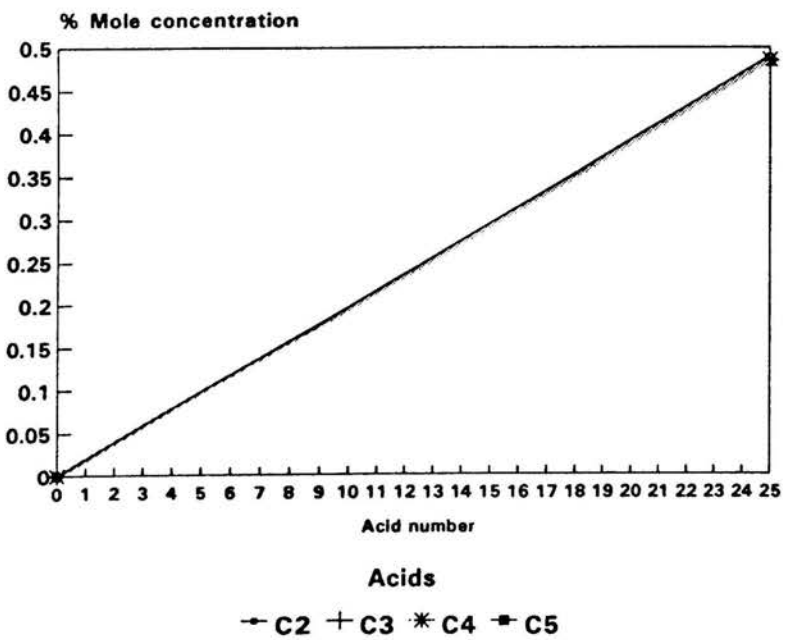

4.1.2 DE-AERATION OF THE MEDIUM

It was necessary to determine experimentally the time required to produce solutions with the desired dissolved oxygen content levels, by means of purging the solution with water saturated N_2 gas. This was done to simulate plant conditions and the dissolved oxygen level was kept below 1.0 ppm, thus suppressing the cathodic oxygen half-cell reaction. Purging was done with N_2 gas, which was saturated with water before entering the test solution at a rate of 1.0 l/min with a solution volume of 400 ml.

In the experiment purging was done for one hour, then it was ceased and the solution was exposed to the atmosphere for an additional 15 minutes, while the dissolved oxygen level was measured. A graphical representation is given in figure 4.3 while numerical data are tabulated in Appendix(A.1.3). From figure 4.3 it is evident that purging of one hour for the specified conditions would be satisfactory. After de-aeration, the solution could be exposed to the atmosphere for up to 10 minutes, before the dissolved oxygen content level would rise to undesirable high levels.

FIGURE 4.3 *Purging time required to reach desired dissolved oxygen level*

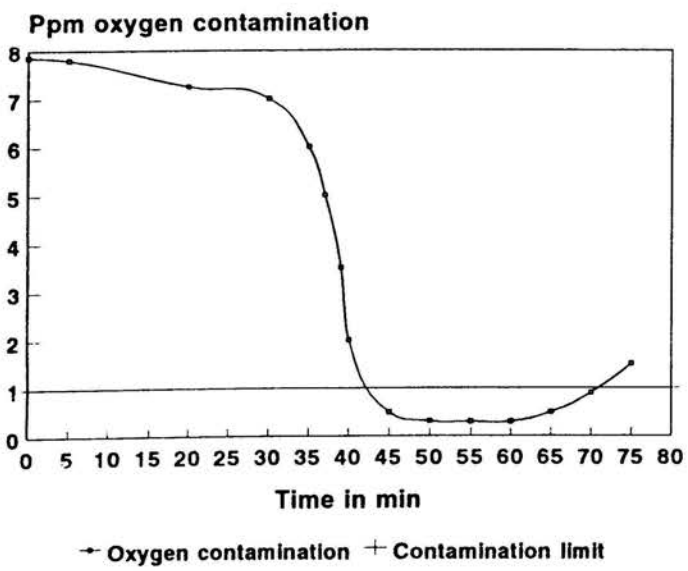

4.2 MAIN INVESTIGATION

The main investigation consisted of mass loss tests and electrochemical tests. By comparing the results of the different test methods the corrosion mechanism was determined.

4.2.1 MASS LOSS TESTS

Mass loss tests involved the determination of corrosion rates of mild steel in different de-aerated pure fatty acid solutions, tested at different temperatures and acid numbers. The media were de-aerated with water saturated N_2 gas to a dissolved oxygen content level of less than 1.0 ppm. Pure acid systems were investigated, while the media were stagnant. AISI 1020 mild steel samples, as shown in picture 1 no 3, were used in the tests. Exposure times were 72 hours unless otherwise stated.

Results obtained from mass loss experiments were noted as Δm. Using Eqn(37), raw data were converted to corrosion rates in μmpy. Results are represented on semi-logarithmic format.

From figures 4.4 to 4.14 it was identified that the corrosion rate increased with an increase in acid number. The corrosion rate increased initially with temperature and at certain elevated temperatures decreased with a further increase in temperature. At the relatively low temperatures corrosion products were soluble and no protective films could be identified on specimens. In the temperature regions where corrosion rates decreased with increasing temperatures corrosion products were less soluble and black protective corrosion product films formed on specimens. An increase in chain length of the organic acid molecule produced a decrease in the corrosion rates. These were general trends identified but there were some exceptions. See paragraphs 5.2.1.1 to 5.2.1.3.

4.2.1.1 Acetic acid

Numerical data for corrosion rates of mild steel in acetic acid solutions at different temperatures and acid numbers are tabulated in Appendix(A.1.4) and a graphical representation is given in figure 4.4.

FIGURE 4.4 *Corrosion rates of mild steel in acetic acid solutions (µmpy)*

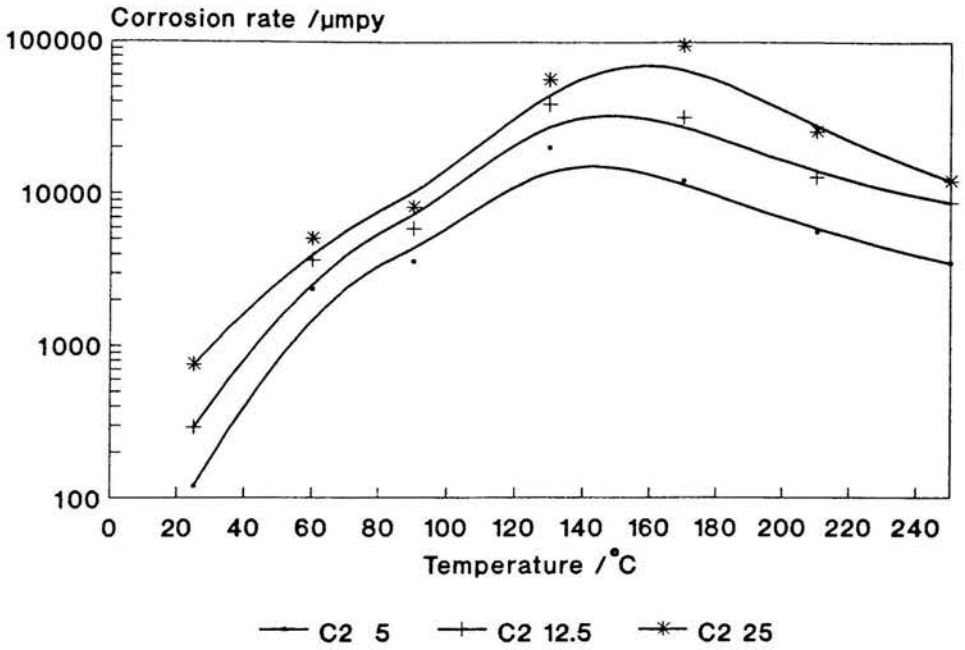

The results show a maximum corrosion rate in the region 140°C to 170°C at an acid number of 25 mg KOH/g solution. The corrosion characteristics of the other acid numbers followed the same tendencies, but reached a maximum corrosion rate in the region 130°C to 150°C.

4.2.1.2 Propionic acid

Numerical data for corrosion rates of mild steel in propionic acid solutions at different temperatures and acid numbers are tabulated in Appendix(A.1.5) and a graphical representation is given in figure 4.5.

FIGURE 4.5 *Corrosion rates of mild steel in propionic acid solutions (µmpy)*

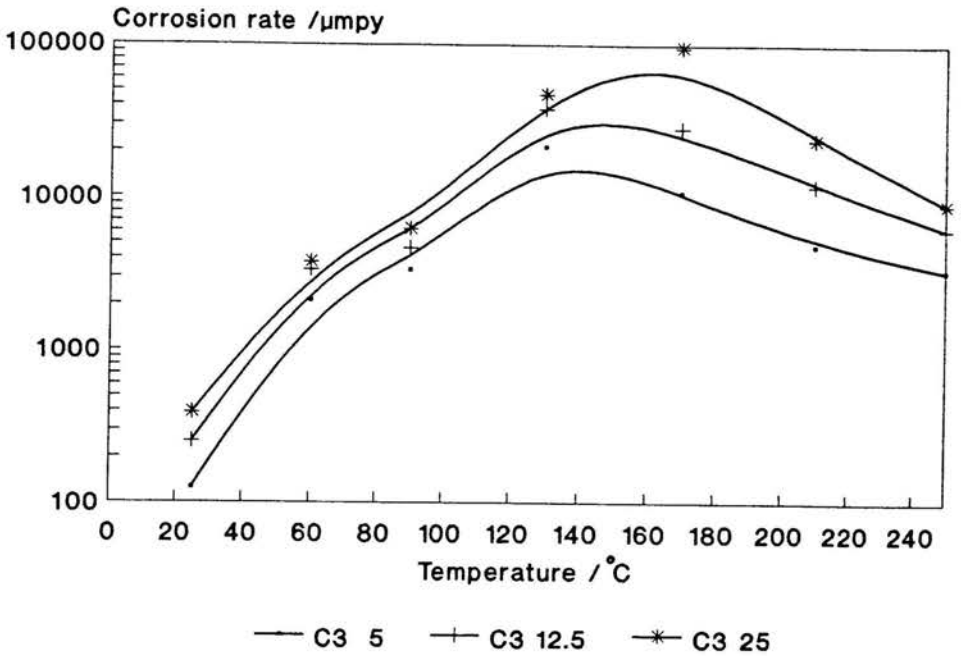

The results show a maximum corrosion rate in the region 140°C to 170°C at an acid number of 25 mg KOH/g solution. The corrosion characteristics of the other acid numbers followed the same tendencies, but reached a maximum corrosion rate in the region 130°C to 160°C.

4.2.1.3 Butyric acid

Numerical data for corrosion rates of mild steel in butyric acid solutions at different temperatures and acid numbers are tabulated in Appendix(A.1.6) and a graphical representation is given in figure 4.6.

FIGURE 4.6 *Corrosion rates of mild steel in butyric acid solutions (µmpy)*

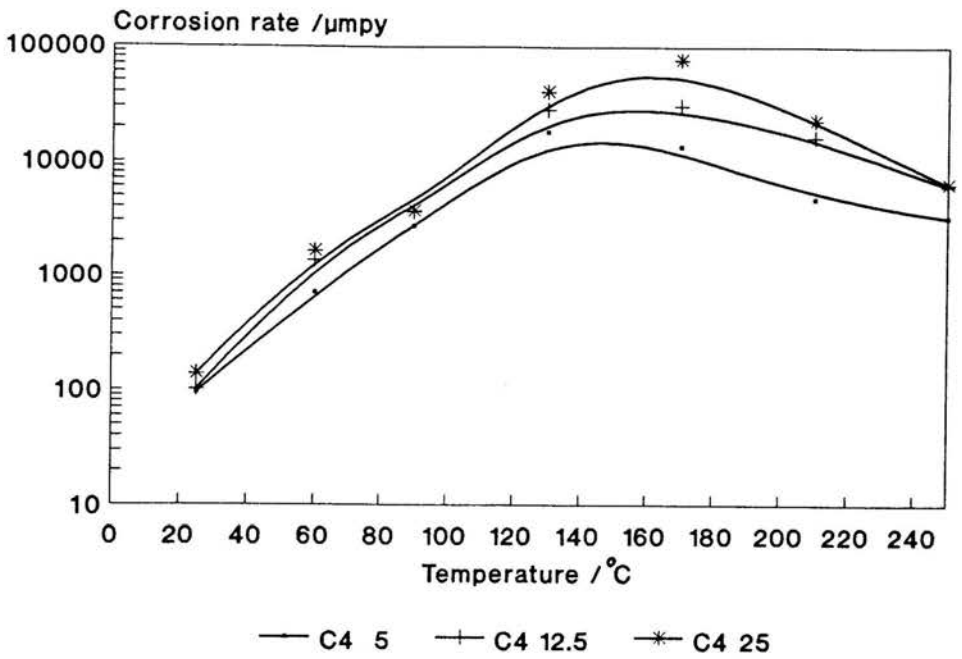

The results show a maximum corrosion rate in the region 140°C to 170°C at an acid number of 25 mg KOH/g solution. The corrosion characteristics of other acid numbers followed the same tendencies, but levelled more out towards the higher temperatures than acetic or propionic acid.

4.2.1.4 Valeric acid

Numerical data for corrosion rates of mild steel in valeric acid solutions at different temperatures and acid numbers are tabulated in Appendix(A.1.7) and a graphical representation is given in figure 4.7.

FIGURE 4.7 *Corrosion rates of mild steel in valeric acid solutions (µmpy)*

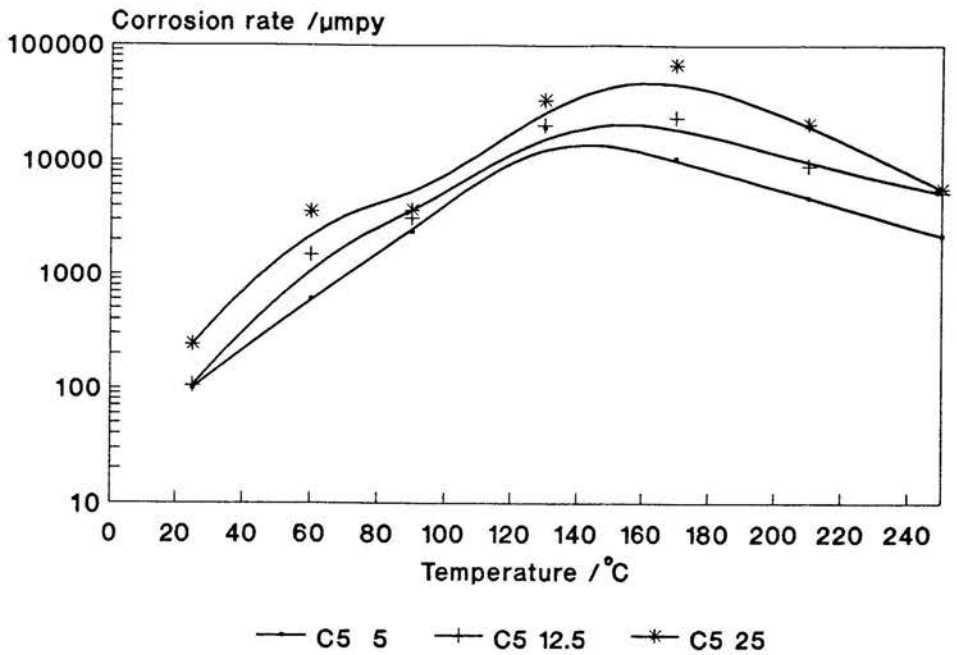

The results show a maximum corrosion rate in the region 130°C to 170°C at an acid number of 25 mg KOH/g solution. The corrosion characteristics of the other acid numbers followed the same tendencies, but reached a maximum corrosion rate in the region 120°C to 170°C.

4.2.1.5 Hexanoic acid

Numerical data for corrosion rates of mild steel in hexanoic acid solutions at different temperatures and acid numbers are tabulated in Appendix(A.1.8) and a graphical representation is given in figure 4.8.

FIGURE 4.8 *Corrosion rates of mild steel in hexanoic acid solutions (μmpy)*

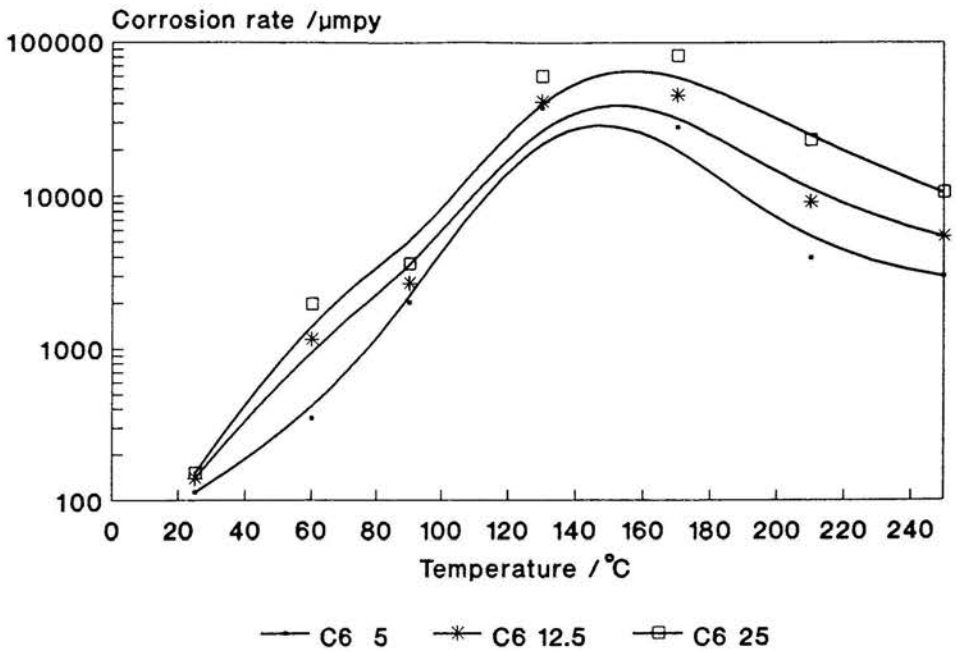

The results show a maximum corrosion rate in the region 150°C to 170°C at an acid number of 25 mg KOH/g solution. The corrosion characteristics of the other acid numbers followed the same tendencies, but reached a maximum corrosion rate in the region 130°C to 160°C.

4.2.1.6 Octanoic acid

Numerical data for corrosion rates of mild steel in octanoic acid solutions at different temperatures and acid numbers are tabulated in Appendix(A.1.9) and a graphical representation is given in figure 4.9.

FIGURE 4.9 *Corrosion rates of mild steel in octanoic acid solutions (µmpy)*

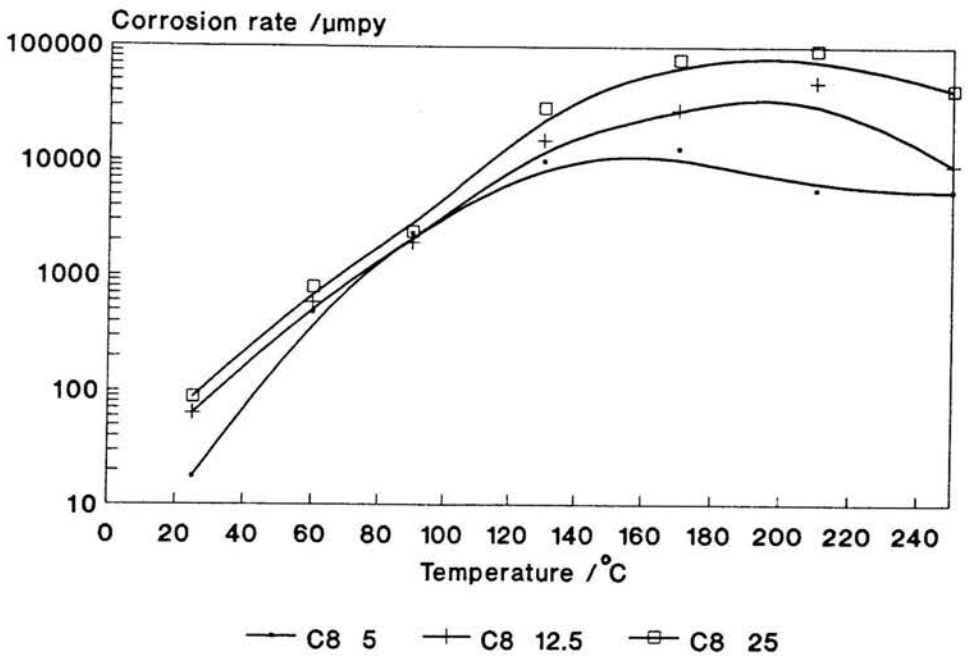

The results show a maximum corrosion rate in the region 180°C to 210°C at an acid number of 25 mg KOH/g solution. For an acid number of 12.5 mg KOH/g solution a maximum corrosion rate was reached in the region 170°C to 200°C while an acid number of 5 mg KOH/g solution reached a maximum in the region 130°C to 180°C.

4.2.1.7 Decanoic acid

Numerical data for corrosion rates of mild steel in decanoic acid solutions at different temperatures and acid numbers are tabulated in Appendix(A.1.10) and a graphical representation is given in figure 4.10.

FIGURE 4.10 *Corrosion rates of mild steel in decanoic acid solutions (µmpy)*

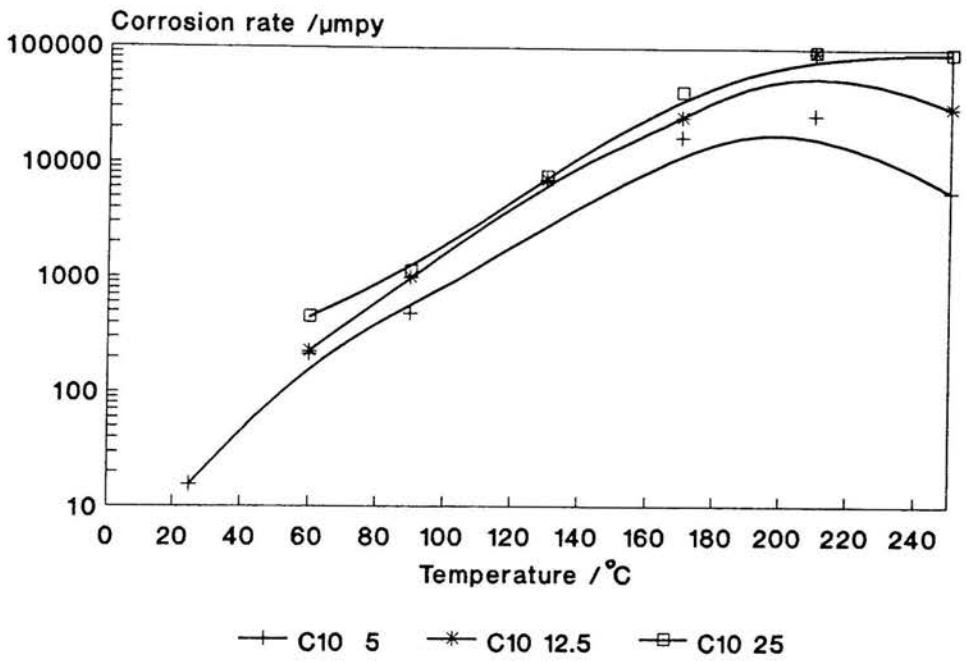

No corrosion rate peak was formed for decanoic acid at an acid number of 25 mg KOH/g solution in the investigated range. Maximum corrosion rates at ± 190°C and in the region 200°C to 230°C were identified for acid numbers 5 and 12.5 mg KOH/g solution respectively. Results obtained for acid numbers 5, 12.5 and 25 mg KOH/g solution were the same at 25°C, and this probably indicated that the solutions were most likely to be saturated with fatty acid at these "acid numbers".

4.2.1.8 Lauric acid

Numerical data for corrosion rates of mild steel in lauric acid solutions at different temperatures and acid numbers are tabulated in Appendix(A.1.11) and a graphical representation is given in figure 4.11.

FIGURE 4.11 *Corrosion rates of mild steel in lauric acid solutions (µmpy)*

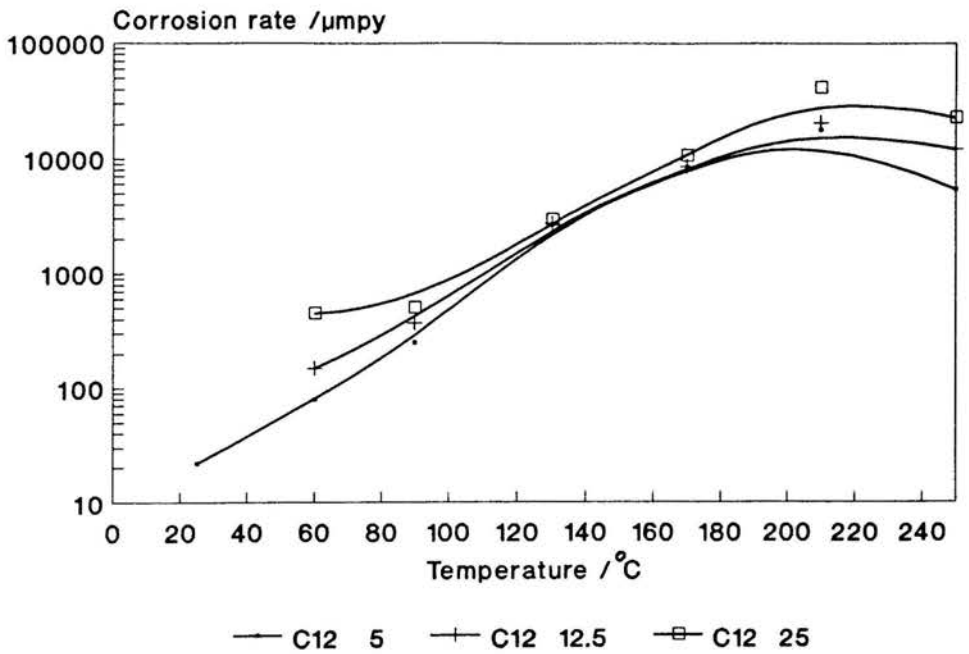

The results show maximum corrosion rates in the region between 210°C and 250°C at acid numbers 5 and 25 mg KOH/g solution. At an acid number of 12.5 mg KOH/g solution no maximum corrosion rate can be identified in the investigated range. Results obtained for acid numbers 5, 12.5 and 25 mg KOH/g solution were the same at 25°C, and this probably indicated that the solutions were most likely to be saturated with fatty acid at these "acid numbers".

4.2.1.9 Myristic acid

Numerical data for corrosion rates of mild steel in myristic acid solutions at different temperatures and acid numbers are tabulated in Appendix(A.1.12) and a graphical representation is given in figure 4.12.

FIGURE 4.12 *Corrosion rates of mild steel in myristic acid solutions (µmpy)*

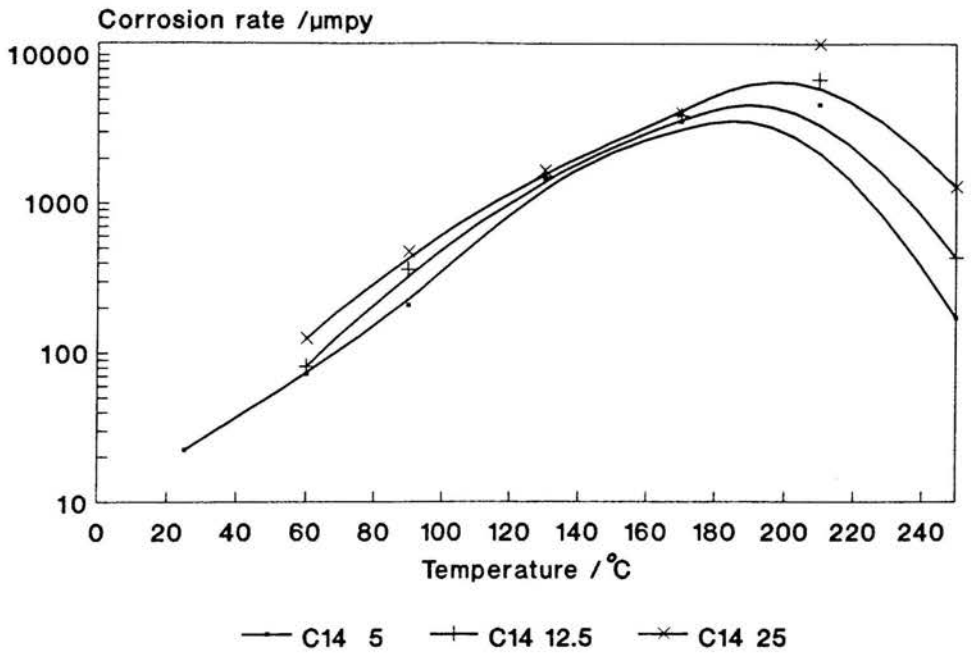

The results show maximum corrosion rates in the region 170°C to 210°C for all acid numbers investigated. Results obtained for acid numbers 5, 12.5 and 25 mg KOH/g solution were the same at 25°C, and this probably indicated that the solutions were most likely to be saturated with fatty acid at these "acid numbers".

4.2.1.10 Palmitic acid

Numerical data for corrosion rates of mild steel in palmitic acid solutions at different temperatures and acid numbers are tabulated in Appendix(A.1.13) and a graphical representation is given in figure 4.13.

FIGURE 4.13 *Corrosion rates of mild steel in palmitic acid solutions (μmpy)*

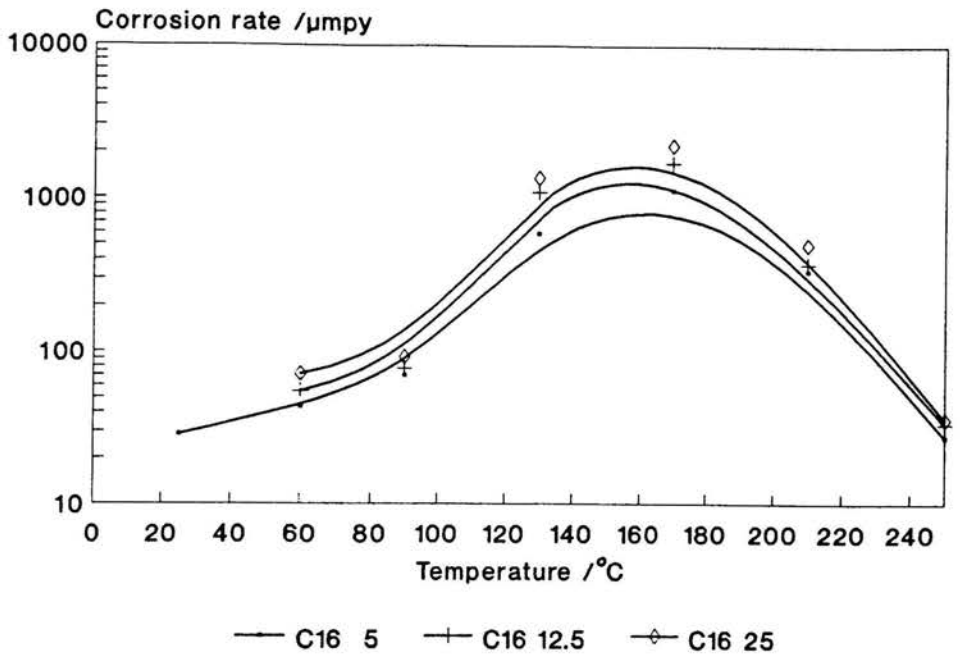

The results show maximum corrosion rates in the region 130° to 180°C for all acid numbers investigated. Results obtained for acid numbers 5, 12.5 and 25 mg KOH/g solution were the same at 25°C, and this probably indicated that the solutions were most likely to be saturated with fatty acid at these "acid numbers".

4.2.1.11 Stearic acid

Numerical data for corrosion rates of mild steel in stearic acid solutions at different temperatures and acid numbers are tabulated in Appendix(A.1.14) and a graphical representation is given in figure 4.14.

FIGURE 4.14 *Corrosion rates of mild steel in stearic acid solutions (μmpy)*

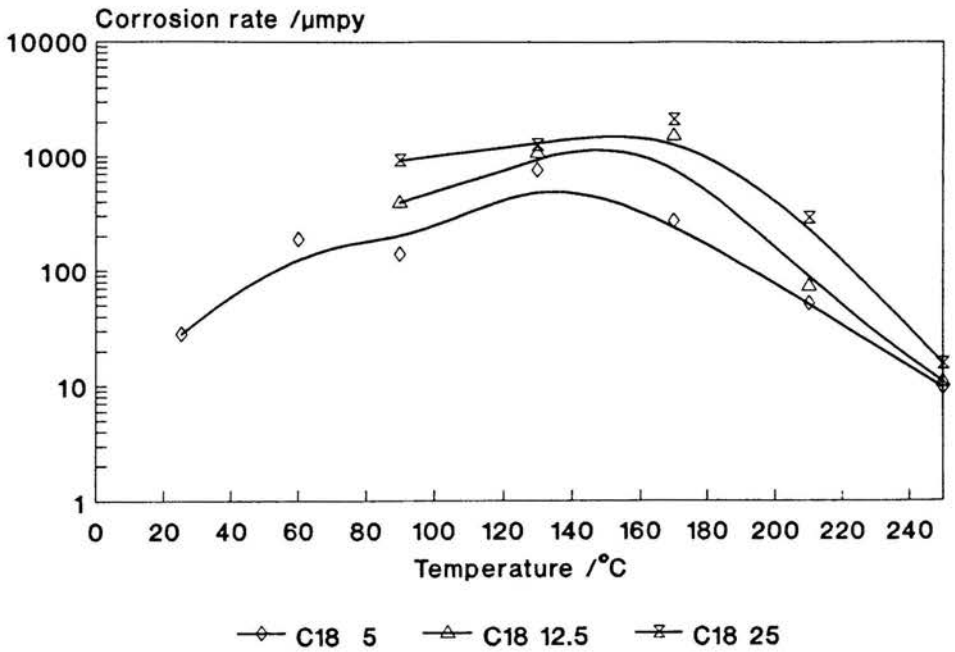

The results show maximum corrosion rates in the region 130°C to 170°C for all acid numbers investigated. Results obtained for acid numbers 5, 12.5 and 25 mg KOH/g solution were the same at 25°C and 60°C, and this probably indicated that the solutions were most likely to be saturated with fatty acid at these "acid numbers".

4.2.2 ELECTROCHEMICAL TESTS

Electrochemical tests were incorporated as part of the main investigation in order to compare the results with mass loss test results and to determine the corrosion mechanism.

Electrochemical apparatuses were standardised according to ASTM standards and results are graphically shown in Appendix(A.2.1)

Electrochemical tests consisting of polarisation resistance and potentiodynamical tests were conducted on AISI 1020 mild steel specimens (See picture 1 no 1). The media were kept stagnant at 25°C and de-aerated with water saturated N_2 gas to a dissolved oxygen level of less than 1.0 ppm. Systems investigated were acetic acid (AN = 5,12.5,25 mg KOH/g solution); propionic acid (AN = 25 mg KOH/g solution); butyric acid (AN = 25 mg KOH/g solution) and valeric acid (AN = 25 mg KOH/g solution).

Polarisation resistance tests were done while the system was unsteady and potentiodynamical tests were done when a steady state was reached.

4.2.2.1 POLARISATION RESISTANCE TESTS

A sample calculation is given for acetic acid at an acid number of 12.5 mg KOH/g solution after one hour of immersion.

Sample calculation

Data will be represented in the form (η ,i). Data used for the specific sample calculation were (-30,-44.6);(-20,-29.4);(-10,-15.5);(0,0);(10,15.3); (20,29.2) and (30,44.3). R_p was determined by the slope of the linear-polarisation curve. A correlation coefficient of 94.3% was obtained with linear regression assuming a linear model. R_p was determined as

1.639 $mV.cm^2/\mu A$, thus $1/R_p$ is equal to 0.61 $\mu A/mV.cm^2$. Other results are tabulated in table 4.2.2.1.

The data in table 4.2.2.1 are graphically represented in figure 4.15. According to figure 4.15 stability was reached after approximately 40 hours of exposure.

Table 4.2.2.1 *Polarisation resistance tests done on different systems*

Time	Systems tested			
	$C_2(12.5)$	$C_3(25)$	$C_4(25)$	$C_5(25)$
1	0.61	0.41	0.29	0.28
2	0.38	0.28	0.25	0.25
4	0.29	0.24	0.19	0.22
8	0.21	0.21	0.15	0.2
12	0.17	0.17	0.1	0.17
24	0.08	0.08	0.07	0.065
48	0.05	0.05	0.04	0.03
72	0.042	0.043	0.023	0.019

$1/R_p$ in [$\mu A/mV.cm^2$] and Time in [hours].

FIGURE 4.15 *Polarisation resistance test results obtained during the unsteady state of the corrosion process*

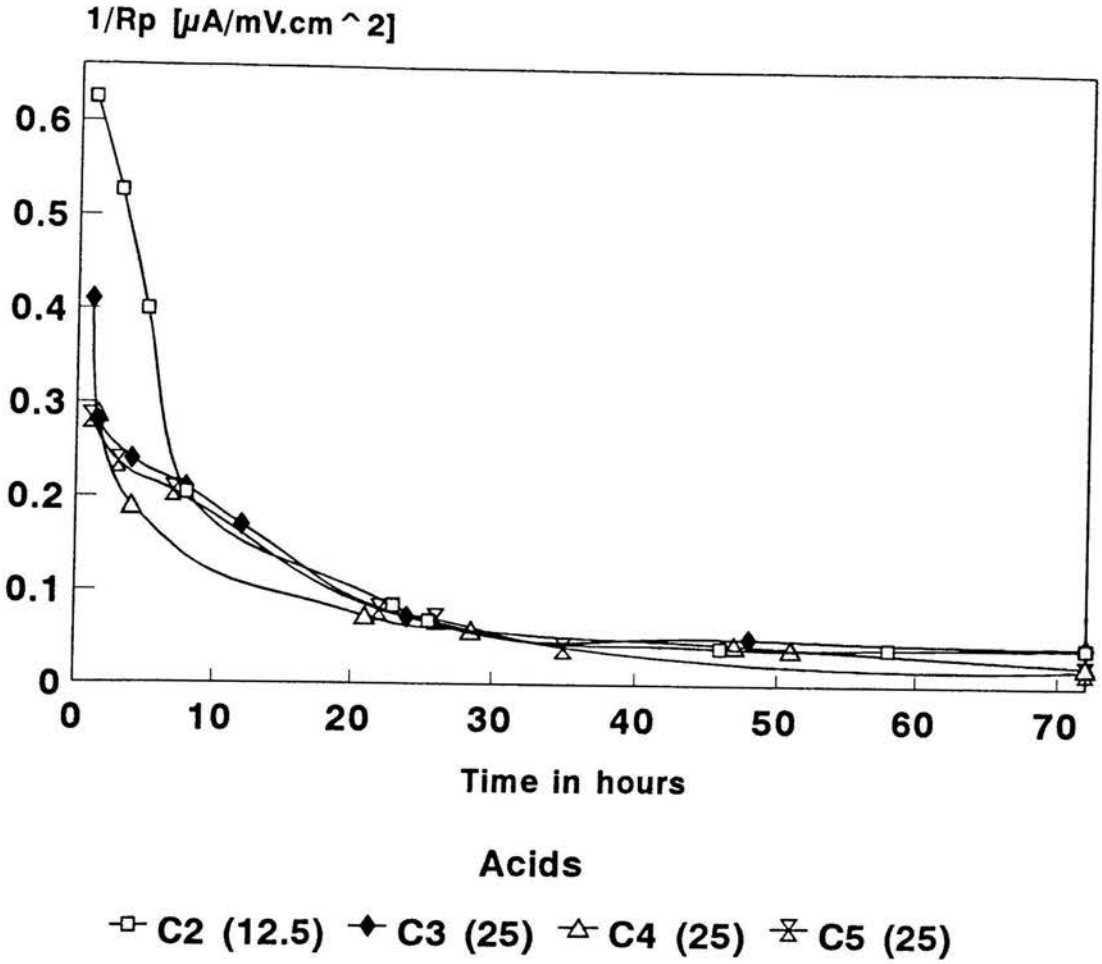

4.2.2.2 POTENTIODYNAMICAL TESTS

Anodic and cathodic characteristics were investigated during steady state conditions of the systems and results obtained are shown in figures 4.16 and 4.17. Data are tabulated in Appendices(A.2.2) to (A.2.7).

FIGURE 4.16 *Anodic and cathodic characteristics of mild steel in acetic acid systems*

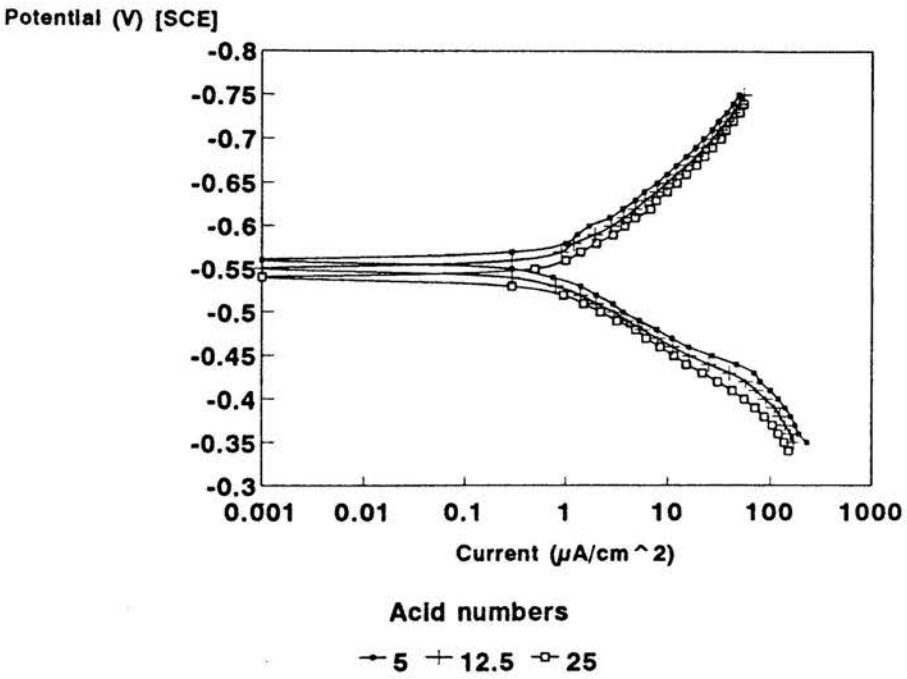

FIGURE 4.17 *Anodic and cathodic characteristics of mild steel in propionic, butyric and valeric acid systems*

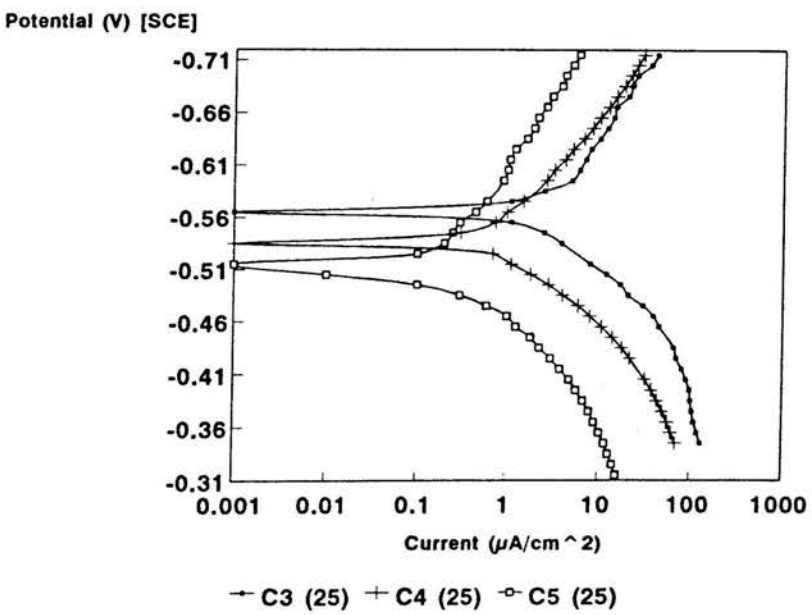

Sample calculations

Acetic acid with an acid number of 12.5 mg KOH/g solution, was chosen for the conduction of sample calculations after 72 h of immersion of the specimen in the test solution.

I_{CORR} was obtained with the aid of the Betacrunch program and it was converted to the corrosion rate as follows:

$$m = kI_{CORR}t$$

therefore

$$\frac{m}{A} = \frac{kIt}{A}$$

$$= ki_{CORR}t$$

Let x be an one-dimensional corrosion property, then

$$\frac{m}{Ax} = \frac{kit}{x}$$

$$\therefore \frac{x}{t} = \frac{kiAx}{m}$$

$$CR = \frac{x}{t} = \frac{ki}{\rho}$$

$\frac{x}{t}$ gives the corrosion rate, while the units are determined by the units of k, i and ρ. With k in kg/C, i in A/m^2 and ρ in kg/m^3 the units of the corrosion rate will be m/s, but can be converted to μmpy by the following[38]:

$$\therefore CR = \frac{ki_{CORR}.3600.24.365 \times 10^6}{\rho}$$

$$= \frac{3.1536 \times 10^7 \, ki_{CORR}}{\rho} \quad \frac{\mu m}{y}$$

and

$$k = \frac{atom\ mass}{nF}$$

$$\therefore CR = \frac{3.1536 \times 10^7 \, atom\ mass\, i_{CORR}}{\rho nF} \quad \frac{\mu m}{y}$$

For the system tested

Mole mass = 55.85 kg/kmole

F = 9.6519×10^7 C/kgeq

n = 2

ρ = 7860 kg/m^3

$$\therefore CR = \frac{3{,}1536 \times 10^7 . 55{,}85\, i_{CORR}}{7860 . 2 . 96519000} \qquad \frac{\mu m}{y}$$

$$\therefore CR = 1.16081 \times 10^3 \frac{I_{CORR}}{A_r} \qquad \frac{\mu m}{y} \qquad (39)$$

The Betacrunch program was used to calculate corrosion currents and Tafel-slopes. Results obtained for anodic and cathodic observation varied over a wide spectrum which indicated that side reactions played an important role in different potential regions. This limited simple applications of the program. Various analyses for the systems showed that the best results were obtained from cathodic observations in potential regions in which no side reactions could visually be detected. From figure 4.16 it can be seen that for the system C_2(12.5) side reactions initiated at potentials more negative than η = -130 mV. For the overpotential range from 0 to - 130 mV the data points chosen to be used in the Betacrunch program were (-5,0.1); (-10,0.3); (-40,2.2); (-70,6.2); (-100,15.2) and (-130,42.6) with E_{CORR} = -0.54 V. They rendered I_{CORR} = 15.92 μA. Tafel-slopes obtained from Betacrunch were not consistent and are not tabulated.

Substituting I_{CORR} in Eqn(39) a corrosion rate of 184.8 μmpy was obtained. Electrochemical evaluated corrosion rates for the systems investigated are tabulated in table 4.2.3 as electrochem N.

4.2.3 DETERMINING THE CORROSION MECHANISM

Determination of the corrosion mechanism, involved comparing mass loss test results with electrochemical test results. Results are tabulated in table 4.2.3. Mass loss corrosion rates are integrated rates for the period of

exposure and incorporate corrosion rates during the initial unsteady state. Electrochemically determined corrosion rates (see paragraph 4.2.2.2) are associated with steady state conditions. Valid comparisons require adjustments to the same base. A sample calculation of the adjustment for the system $C_2(12.5)$ will follow. The total area shown in figure 4.18 represent the mass loss corrosion rate, while the dotted area represents the electrochemical corrosion rate.

FIGURE 4.18 *Polarisation resistance tests done on $C_2(12.5)$*

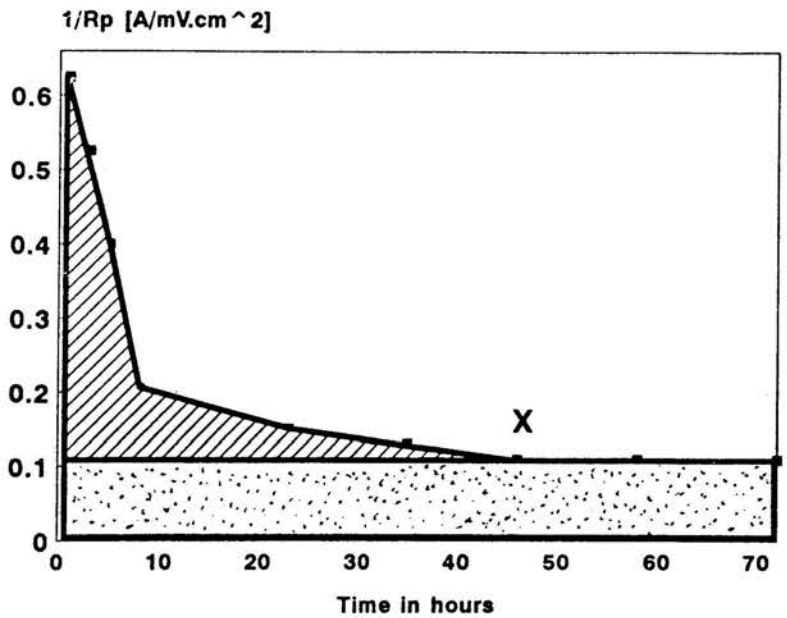

Adjustments to the same base require a correction factor. The correction factor is as follows:

$$ML)_c = \frac{\textit{total area}}{\textit{dotted area}}$$

$$= \textit{correction factor} \qquad (40)$$

For valid comparisons Eqn(41) is used, where

$$\textit{Electrochem A} = ML)_c \times \textit{Electrochem N} \qquad (41)$$

Raw results obtained from electrochemical tests were named electrochem N, while adjusted results were named electrochem A.

The mass loss test result obtained for $C_2(12.5)$ at 25°C was 290.2 μmpy, while the electrochemical result was 184.8 μmpy. Determination of the correction factor involved Eqn(40) in conjunction with figure 4.18. It was found that $ML)_c = 1.7679$ and with Eqn(41), the adjusted electrochemical result was obtained.

$$\textit{Electrochem A} = ML)_c \times \textit{Electrochem N}$$
$$= 1.7679 \times 184.8$$
$$= 326.7\ \mu mpy$$

$$\textit{\% Deviation} = \left[\frac{290.2 - 326.7}{290.2}\right] \times 100$$
$$= -12.5\%$$

% Deviation refers to the difference between mass loss results and Electrohem A results.

Results for other systems are tabulated in table 4.2.3.

Table 4.2.3 *Comparing electrochemical results with mass loss results*

	Corrosion rate in μmpy			
Acid	Mass loss	Electrochem N	Electrochem A	% Deviation
$C_2(12.5)$	290.2	184.8	326.7	-12.5
$C_3(25)$	387.6	197.2	339.6	12.4
$C_4(25)$	136.8	104.2	117.6	14.1
$C_5(25)$	242.3	88.5	214.2	11.6

Numbers between brackets refer to the acid numbers in mg KOH/g solution.

4.3 SUPPLEMENTARY INVESTIGATIONS

The following variables were investigated in the supplementary investigations: turbulence, impurities, corrosion monitoring, acid mixtures and a stabilised-Synthol-light-oil-water-phase.

4.3.1 TURBULENCE

Mass loss tests and electrochemical tests were conducted under turbulent conditions. The system tested was acetic acid at an acid number of 25 mg KOH/g solution at 25°C. The media were de-aerated with water saturated N_2 gas to a dissolved oxygen content level of less than 1.0 ppm. Cylindrical mild steel specimens (AISI 1020) were used, as shown in picture 1 no 2. Mass loss tests were done at 0, 500, 1500, 2000, 2500, 3000, 3250 and 4000 rpm (as indicated on the apparatus), while electrochemical tests were done at 0, 500, 2500 and 4000 rpm (as indicated on the apparatus). See paragraph 3.1.6.1. The turbulence range investigated, represented peripheral velocities up to 4.2 m/s, which corresponded to a Reynold's number of 8.4×10^6. Exposure times for mass loss tests and electrochemical tests were 144 hours.

4.3.1.1 MASS LOSS TESTS

Numerical data for mass loss turbulent tests are tabulated in Appendix(A.1.15). See figure 4.19 for a graphical representation. The results show that turbulence did not influence the corrosion rates in the region 0 to 1500 rpm (as indicated on the apparatus). In higher turbulence regions no results will be noted as the solution became contaminated with oxygen and rendered an increase in corrosion rate with turbulence followed by a decrease. The latter was due to a corrosion product film which formed on specimen surfaces.

The relationship between revolutions of the specimen, according to the gauge, and the peripheral velocity is given by the following:

$$1 \text{ rpm} = \frac{\pi D}{60}$$

$$= \frac{0.02\,\pi}{60}$$

$$= 1.047 \times 10^{-3} \ \frac{m}{s} \qquad (42)$$

With the specimen height 10.0 mm and diameter 20.0 mm the exposed area is 6.3×10^{-4} m^2

FIGURE 4.19 *Mass loss and electrochemical turbulence test results*

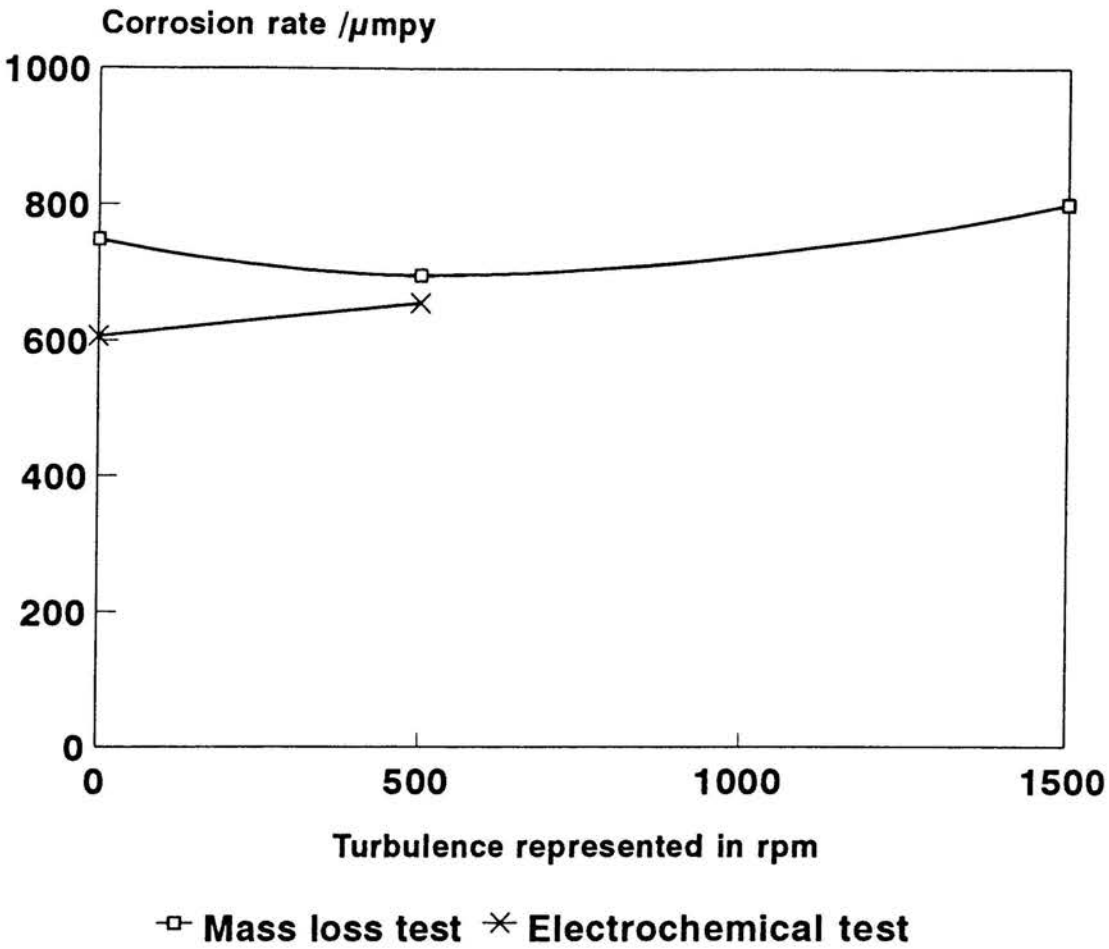

4.3.1.2 ELECTROCHEMICAL TESTS

Results from polarisation resistance tests are shown graphically in figure 4.20, while results from potentiodynamical tests are shown graphically in figure 4.21. Numerical data are tabulated in Appendices(A.2.8) and (A.2.9)

For a turbulence associated with 0 rpm and 500 rpm (as indicated on the apparatus), $1/R_p$ showed a decrease and then became steady, after 80 hours of immersion.

FIGURE 4.20 *Polarisation resistance tests under turbulent conditions*

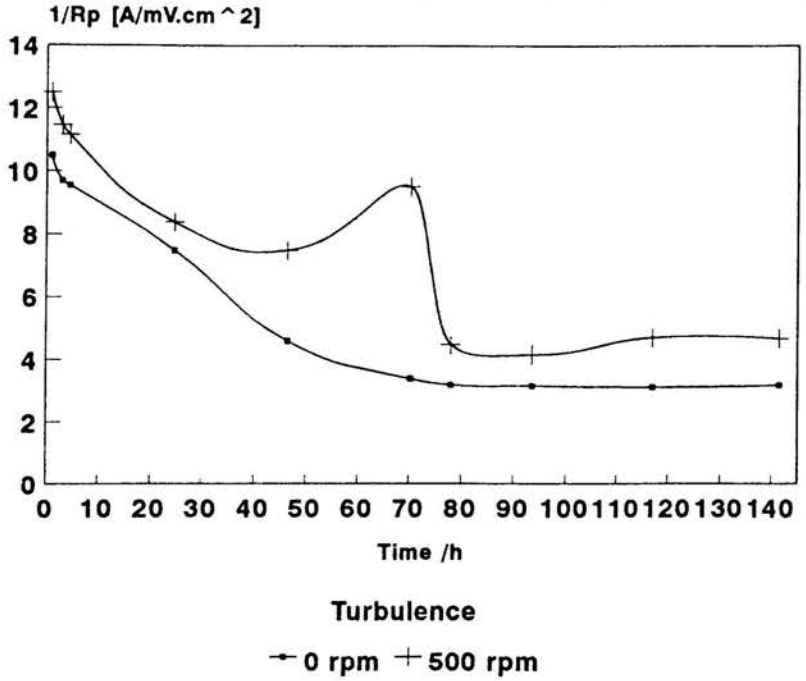

FIGURE 4.21 *Anodic and cathodic characteristics of mild steel in an acetic acid system under turbulent conditions*

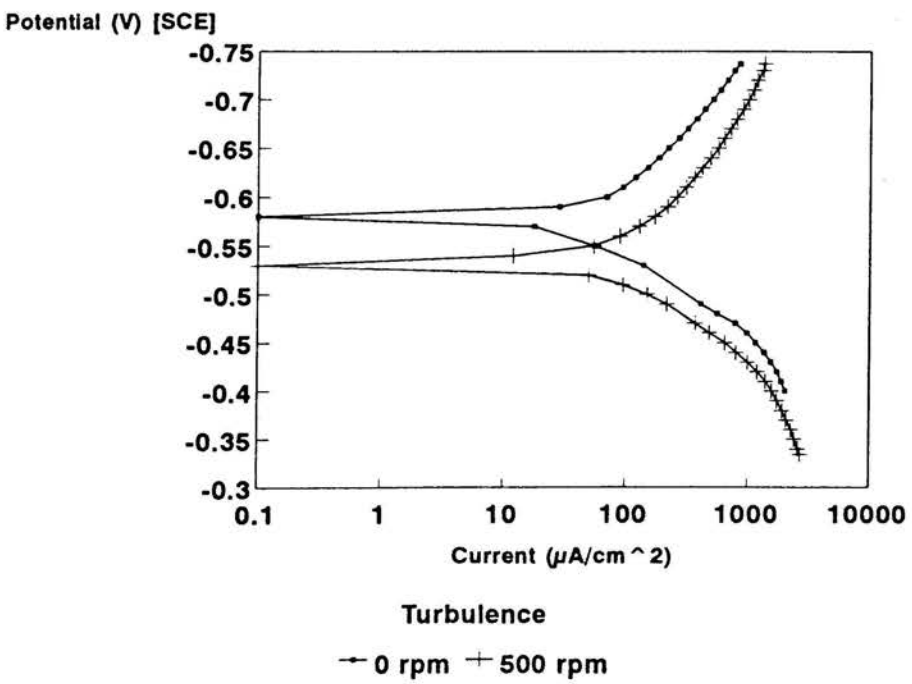

The procedures used in paragraphs 4.2.2.2 and 4.2.3 were followed to produce corrosion rates, correction factors and adjusted electrochemical results. Numerical data are tabulated in table 4.3.1.2. A graphical representation of the corrosion rates is given in figure 4.19. The corrosion rates were not influenced by turbulence. See figure 4.19. Mass loss and electrochemical results correlated well.

Table 4.3.1.2 *Corrosion rates obtained with the aid of electrochemical tests under turbulent conditions*

Turbulence in rpm	0	500
Peripheral velocity m/s	0.0	0.5
Reynold's number $x10^{-6}$	0.0	1.1
i_{CORR} in $\mu A/cm^2$	60.7	54.0
Electrochem N	737.9	656.5
Correction factor	1.15	1.23
Electrochem A	848.6	807.5
Mass loss results	748.9	695.4
% Deviation	-13.3	-16.1

4.3.2 IMPURITIES

Impurities investigated were 20 ppm Cl^-, 1000 ppm S^{2-} and 7.86 ppm dissolved oxygen, respectively added to acetic acid with an acid number of 25 mg KOH/g solution. The media were de-aerated with water saturated N_2 gas to a dissolved oxygen content level of less than 1.0 ppm, except when oxygen contamination was investigated. Exposure times were 6 hours.

Mass loss results were obtained with the aid of Eqn(37). Numerical data are

tabulated in the Appendix(A.1.16), with a graphical representation given in figure 4.22.

From figure 4.22 it was seen that the addition of chloride and oxygen to the acid solution resulted in small increases in corrosion rates, but sulphur rendered lower corrosion rates.

FIGURE 4.22 *Mass loss results for acetic acid, with the addition of impurities*

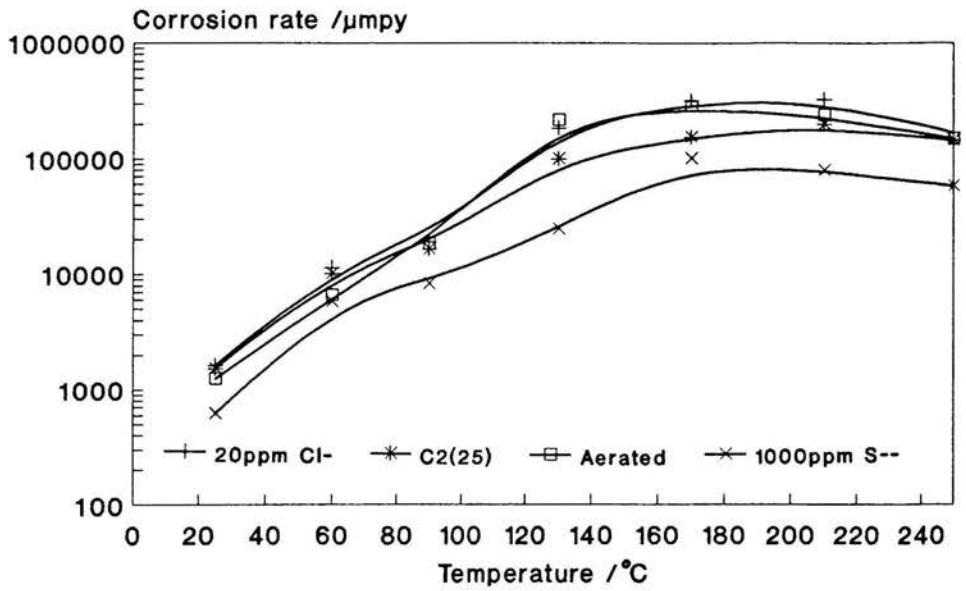

4.3.3 CORROSION MONITORING

The system tested was acetic acid with an acid number of 25 mg KOH/g solution at 25°C. Media were de-aerated with water saturated N_2 gas to a dissolved oxygen content level of less than 1.0 ppm. Stagnant solution conditions prevailed, while exposure times were 144 hours.

Corrosion monitoring was conducted with the aid of a Corrator and a Corrosometer to investigate the applicability of the apparatuses to the system. Data obtained with the Corrosometer are shown in figure B.1 in Appendix(B.1). Figure 4.23 shows the corrosion rates obtained with different test methods.

The Corrator produced a corrosion rate of 569.6 μmpy for the tested system, which was directly read off from the display on the instrument.

Calculation for the Corrosometer

The equation to determine the corrosion rate is :

$$CR = \frac{\Delta \text{reading}}{\Delta \text{time[days]}} \; 0.365 \text{ s}$$

with $s = 2$ (the probe span)

thus $$CR = \frac{(188.0 - 54.3)}{(6.02 - 0.0)} \; (0.365) \; (2)$$

$$= 16.21 \text{ mpy}$$

$$= 412.6 \; \mu\text{mpy}$$

FIGURE 4.23 *Comparing the different test methods*

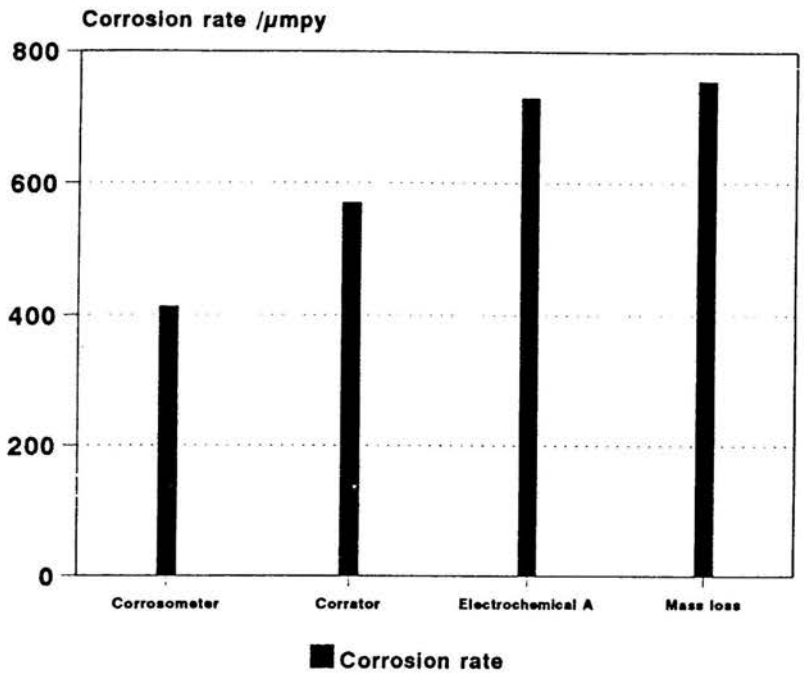

Figure 4.23 shows that the Corrator result approached the result obtained with mass loss better than the Corrosometer result.

4.3.4 ACID MIXTURES

Equal mole amounts of acetic acid and decanoic acid were mixed to produce an acid number of 25 mg KOH/g solution for the mixture. The media were de-aerated with water saturated N_2 gas to a dissolved oxygen content level of less than 1.0 ppm. The media were stagnant and exposure times were 6 hours.

Numerical data are tabulated in Appendix(A.1.17) and graphical representations are given in figure 4.24.

FIGURE 4.24 *Corrosion rates obtained for an acetic/decanoic acid mixture*

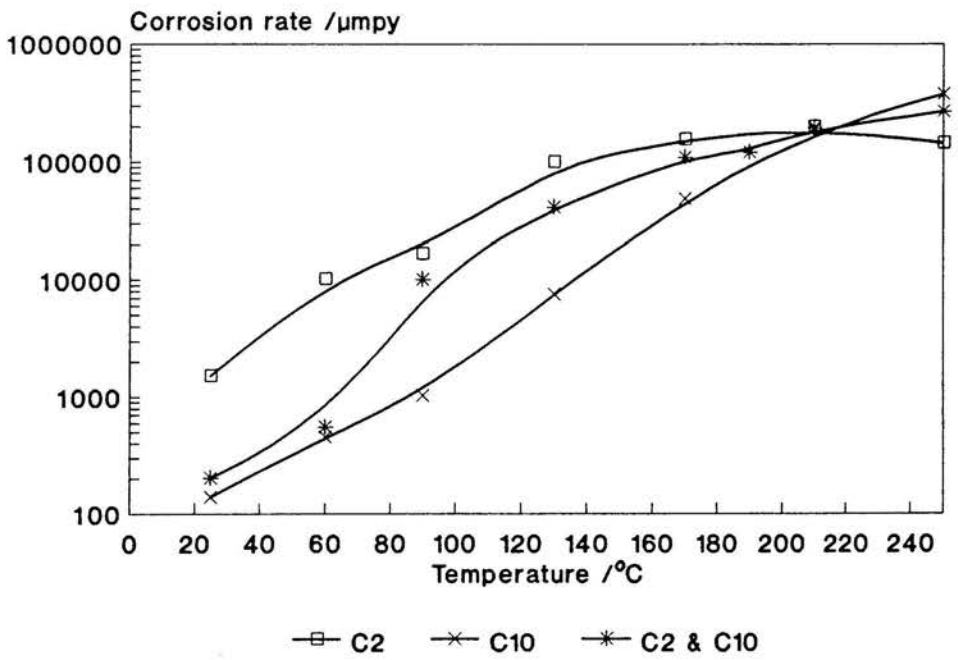

As seen in figure 4.24, mixing of the acids showed no synergistical effects but approximately average corrosion rates between the corrosion rates for the individual acids were obtained.

4.3.5 STABILISED-SYNTHOL-LIGHT-OIL-WATER-PHASE INVESTIGATION

A stream from the SASOL plant was investigated to compare it's corrosion rate with the corrosion rates of the tested systems. The media were de-aerated with water saturated N_2 gas to a dissolved oxygen content level of less than 1.0 ppm. The media were stagnant, with exposure times of 6 hours.

The stream received from SASOL had an acid number of 9.39 mg KOH/g solution (system A). With an addition of acetic acid to system A, system B was obtained which had an acid number of 25 mg KOH/g solution.

Numerical data are tabulated in Appendix(A.1.18) while a graphical representation is given in figure 4.25.

FIGURE 4.25 *Corrosion characteristics of mild steel in a stable-Synthol-light-oil-water-phase stream*

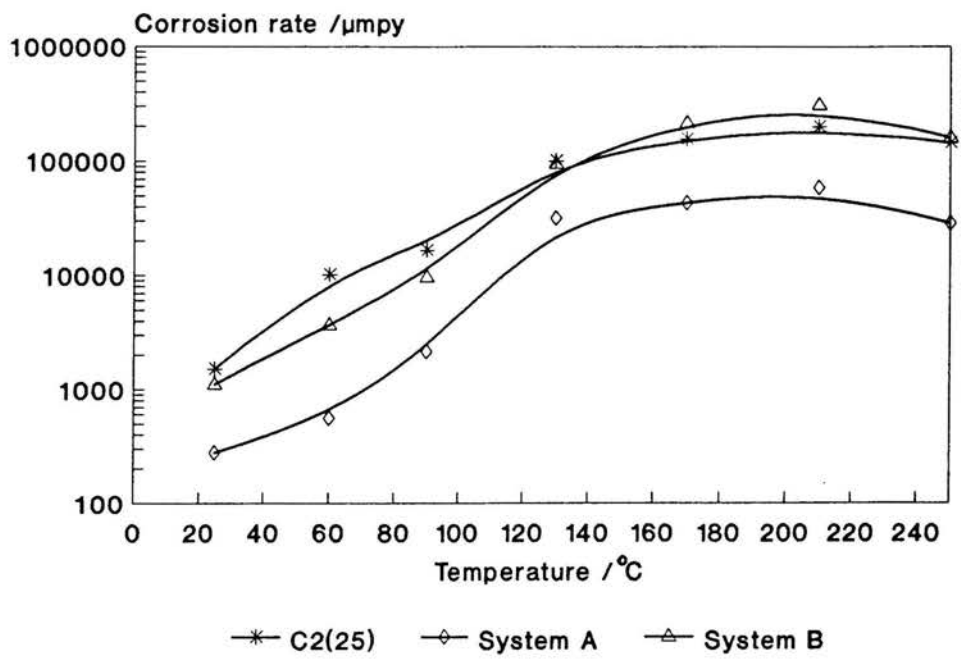

Systems B correlated to a certain extent with $C_2(25)$. Systems A and B showed similar tendencies.

5 DISCUSSION AND CONCLUSIONS

5.1 ACID NUMBER DETERMINATION

Figures 4.1 and 4.2 show a linear relationship between concentration and acid number. In the case where concentration is expressed as mole percentage the correlation is independent of the fatty acid type. This is in accordance with theory because acid number represents all available acid hydrogen ions, whether they are ionised or not[38]. For equal mole concentrations the available hydrogen ions of two fatty acids will be the same and will be independent of the fatty acid type.

5.2 MAIN INVESTIGATION

Mass loss results are tabulated in Appendices(A.1.4) to (A.1.14) and graphically represented in figures 4.4 to 4.14. Situations where solutions became saturated at acid numbers lower than 25 mg KOH/g solution can be identified in the tables. For example, in the case of decanoic acid, corrosion rates for acid numbers 5, 12.5 and 25 mg KOH/g solution are the same at 25°C. See table A.1.10. This indicates that the solutions were most likely saturated with fatty acid at these "acid numbers". In such cases the results for the higher "acid numbers" were not considered for the graphical representations.

In section 4.2.3 it was shown that an electrochemical corrosion mechanism prevailed at 25°C. Deviations between mass loss determined corrosion rates and electrochemically determined corrosion rates varied between -12.5% and 14.1%. Deviations of these orders are acceptable in corrosion tests[36]. Although the mechanism at higher temperatures was not investigated, it is likely that an electrochemical mechanism was applicable for all the systems investigated.

5.2.1 CORROSION RATE AS A FUNCTION OF TEMPERATURE

Corrosion rate initially increased with temperature until a maximum rate was obtained. With further increases in temperature corrosion rates decreased. See figures 4.4 to 4.14.

5.2.1.1 ZONE OF INCREASING CORROSION RATE WITH TEMPERATURE

According to the polarisation diagrams in figures 4.16 and 4.17 the systems are activation controlled at 25°C. Considering the prevailing conditions the most likely reactions are the following:

i. The cathodic reaction is believed to be the hydrogen evolution reaction, due to a dissolved oxygen content of less than 1.0 ppm and solvated hydrogen ions which are present from the acids.

$$2H^+ + 2e^- \rightarrow H_2$$

ii. The anodic reaction is

$$Fe \rightarrow Fe^{2+} + 2e^-$$

An increase in temperature causes i_o to increase and the Tafel-slope to decrease, which will then lead to an increase in the corrosion rate. See figure 2.3. This relationship is also reflected in the Arrhenuis expression

$$CR = A \exp\left(\frac{-E}{RT}\right)$$

where A is a preexponential factor, E is the activation energy, R is the gas constant and T is the absolute temperature. The relationship is common for corrosion under acidic conditions where the systems are activation controlled. With reference to the systems under investigation the corrosion rate will thus increase with an increase in temperature. See figures 4.4 to 4.14.

5.2.1.2 ZONE OF DECREASING CORROSION RATE WITH TEMPERATURE

The decrease in corrosion rate with temperature coincide with an appearance of a black corrosion product film on the specimen surface. See tables A.1.4 to A.1.14. At these temperatures the corrosion product film renders the system passivation controlled. The results indicate that the effectiveness of films increased with temperature. See figures 4.4 to 4.14. This is in contradiction to normal corrosion rate-temperature relationships for passivation controlled systems.

Potter and Mann described the formation of Fe_3O_4 films with various microstructures on mild steel in deoxygenated water at temperatures higher than 200°C[12]. In neutral and alkaline solutions Potter and Mann found that a protective duplex film grows on the specimen surface according to a logarithmic time law. In acidic solutions under the same conditions the films are protective and they grow rapidly according to linear kinetics, and they have a characteristic multi-laminated microstructure[70]. Bengough and Wormwell[71] showed that the efficiency of a passivation film under stagnant conditions depend on the pressure of the test solution. As the pressure increases the efficiency of the multi-laminated corrosion product film also increases. Normal corrosion rate-temperature relationships for passivation controlled systems do not normally incorporate the effects of pressure. High temperature experiments were done in autoclaves where pressure effects played a significant role. An increase in temperature caused the partial pressures to increase, which then caused the total pressure inside the autoclave to increase. This increase in total pressure caused the effectiveness of the corrosion product films to increase with temperature.

5.2.2 CORROSION RATE AS A FUNCTION OF ACID NUMBER

Corrosion rates increased with acid number over the whole range of investigated temperatures for all the investigated acids. This occurred irrespective of the control mechanisms of the acids. See figures 4.4 to 4.14.

5.2.2.1 ABSENCE OF CORROSION PRODUCT FILMS

Corrosion product films were absent in the lower region of the investigated temperature range for the tested acids. These regions were different for various acids.

According to figures 4.16 and 4.17 the systems are activation controlled at 25°C. By increasing the acid number, the solvated hydrogen ions present will increase[36], causing the cathodic reaction to shift as indicated in figure 5.1[3]. This explains the behaviour observed in the experiments because ϕ_{CORR} increased with an increase in acid number which caused the corrosion rate to increase. See figure 5.1.

FIGURE 5.1 *Corrosion characteristics in the absence of corrosion product films with an increase in acid number*[3]

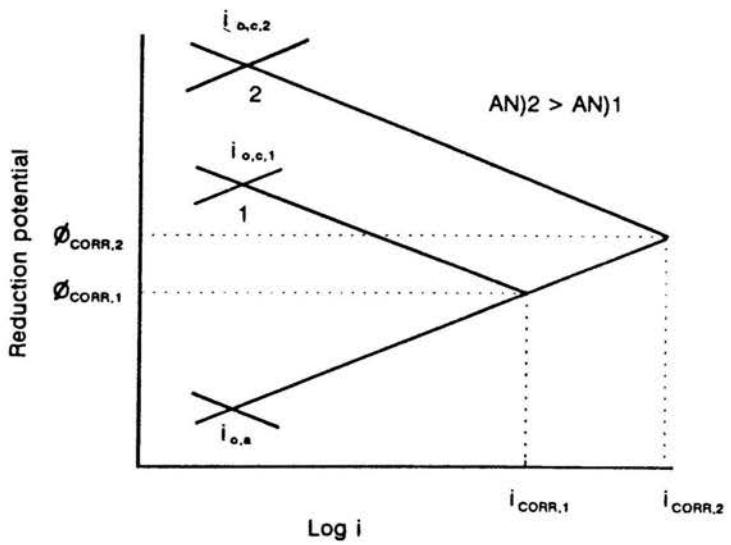

5.2.2.2 PRESENCE OF CORROSION PRODUCT FILMS

Corrosion product films were present in the upper regions of the investigated temperature range for the investigated acids. Where corrosion product films were present it is believed that the anodic reaction is passivation controlled. The effectiveness of a passive film is mostly a function of pH. Consider passivation by the formation of M_2O_3 as the passive film. A typical halfcell reaction is

$$2M^{2+} + 3H_2O \rightleftarrows M_2O_3 + 6H^+ + 2e^-$$

The reaction shows that an increase in acid concentration will give an increase in the solubility of the passive film which will lead to increased corrosion rates. The mechanism is illustrated in figure 5.2.

FIGURE 5.2 *Corrosion characteristics in the presence of corrosion product films with an increase in acid number*[3]

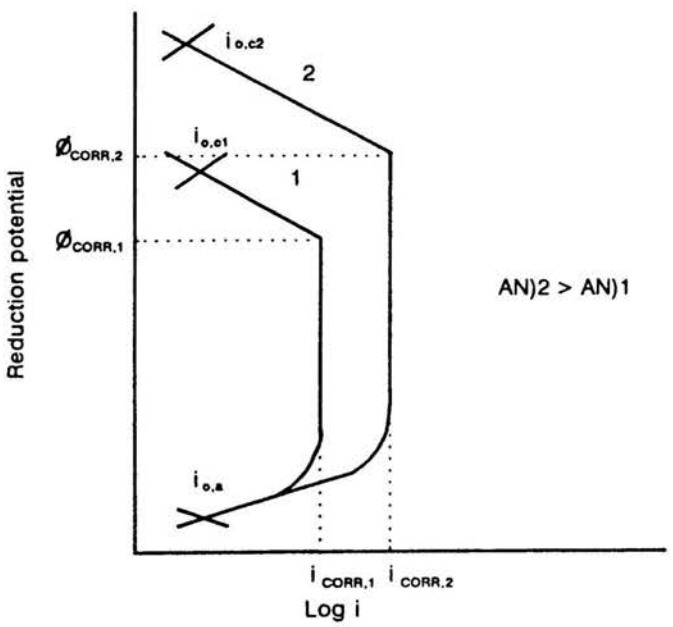

It can be concluded from paragraphs 5.2.2.1 and 5.2.2.2 that an increase in acid number causes an increase in the corrosion rate irrespective of the control mechanism.

5.2.3 CORROSION RATE AS A FUNCTION OF THE TYPE OF FATTY ACID

All the acids investigated showed similar corrosion rate-temperature characteristics. See figures 4.4 to 4.14. The initial increases in corrosion rate with temperature were followed by temperature regions in which the corrosion rates decreased. As shown in figure 5.3 the temperature at which the maximum corrosion rates occurred are functions of the fatty acid type.

FIGURE 5.3 *Temperature of the maximum corrosion rate as a function of the fatty acid type*

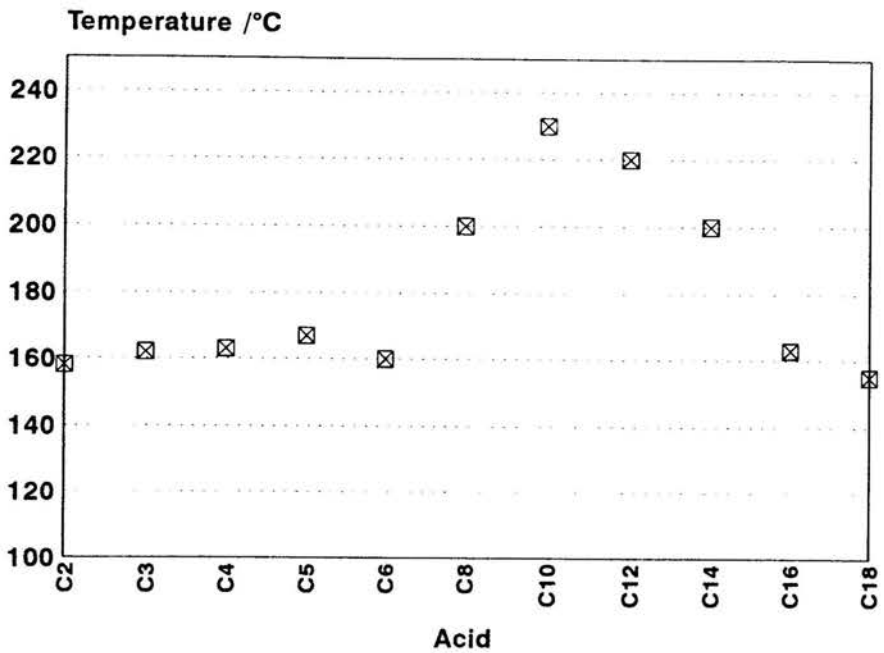

The corrosion rate as a function of the fatty acid type will be discussed by considering temperatures 90°C and 250°C. At 90°C corrosion product films were absent while they were present at 250°C.

5.2.3.1 ABSENCE OF CORROSION PRODUCT FILMS

The general tendency, except for the case of C_{18}, was that the corrosion rate decreased with an increase in chain length irrespective of the investigated acid number. Corrosion rates at 90°C are given in figure 5.4.

FIGURE 5.4 *Corrosion rates at 90°C for investigated acids*

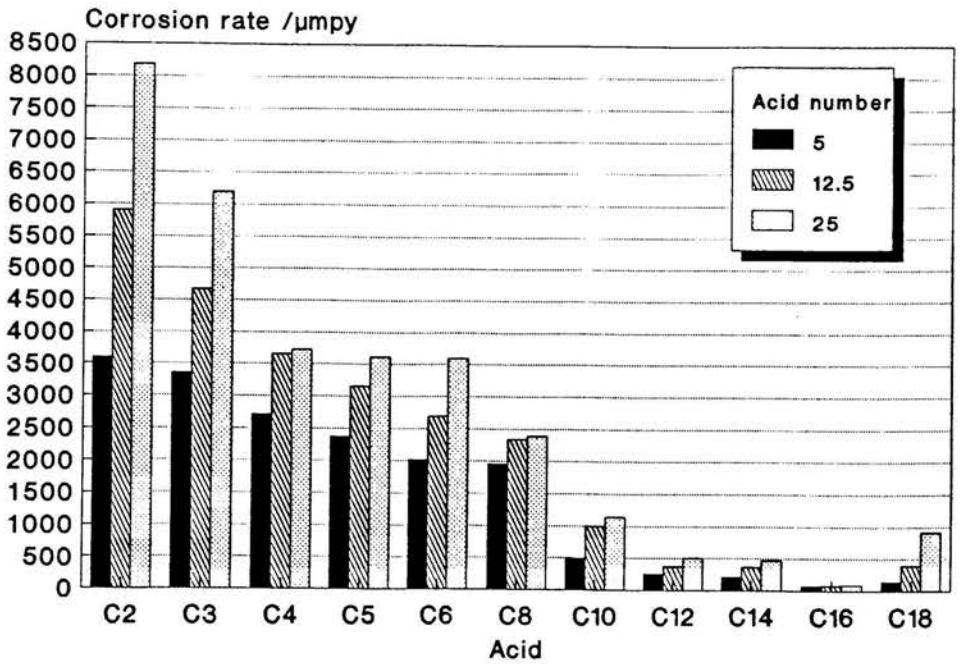

The ionisation ability of a fatty acid decreases as the chain length increases[72]. For the same acid number the pH of a short chain fatty acid will be lower than the pH of a long chain fatty acid. According to the corrosion mechanism illustrated in figure 5.1, corrosivity should decrease with chain length. The increase in corrosivity between C_{16} and C_{18} can not be explained.

5.2.3.2 PRESENCE OF CORROSION PRODUCT FILMS

Figure 5.5 gives a correlation between corrosion rate and type of fatty acid at 250°C for different acid numbers. At this relatively high temperature the relation is more complex than at 90°C. Maximum corrosion rates are obtained with decanoic acid at 250°C for different acid numbers. This is associated with the relatively high temperatures at which the corrosion rate of decanoic acid reaches a maximum. See figure 5.3.

FIGURE 5.5 *Corrosion rates at 250°C for investigated acids*

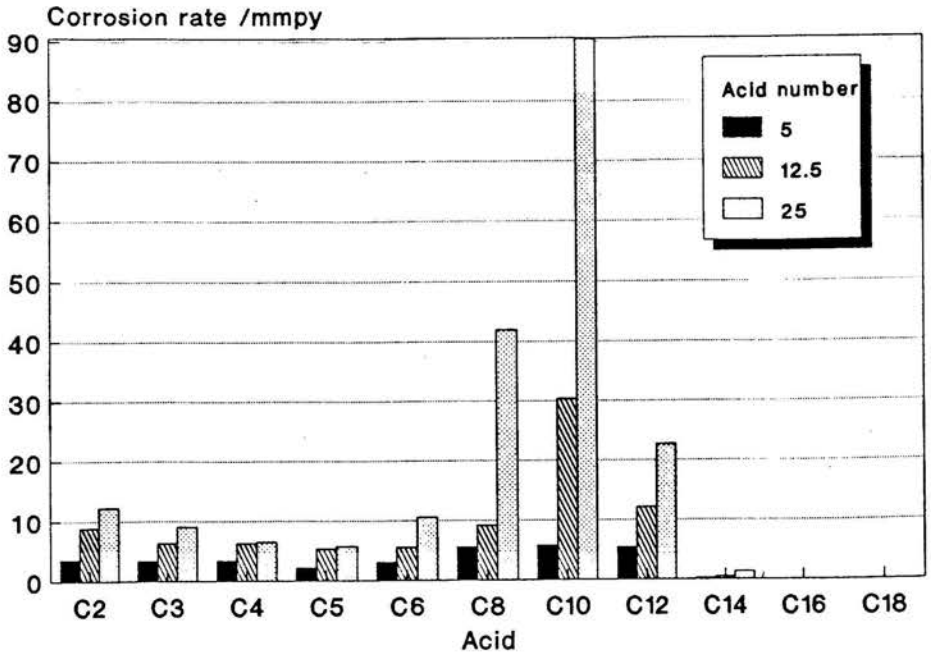

This result is of great importance from a processing point of view because temperatures of 250°C are often encountered in hydrocarbon processings. The presence of C_8, C_{12} and especially C_{10} under these conditions may cause serious corrosion problems.

5.2.4 CORROSION RATE AS A FUNCTION OF EXPOSURE TIME

$C_2(25)$ was tested at different temperatures with different exposure times. See figure 5.6. For exposures of 6 hours the corrosion rates increased with temperature and levelled out from 170°C to 250°C. For exposures of 72 hours the corrosion rates increased with temperature until a maximum corrosion rate was obtained at ± 170°C and then decreased. Exposures of 6 hours produced higher corrosion rates than exposures of 72 hours, irrespective of the control mechanism of the acid.

FIGURE 5.6 *The time dependency of corrosion product film growth in $C_2(25)$*

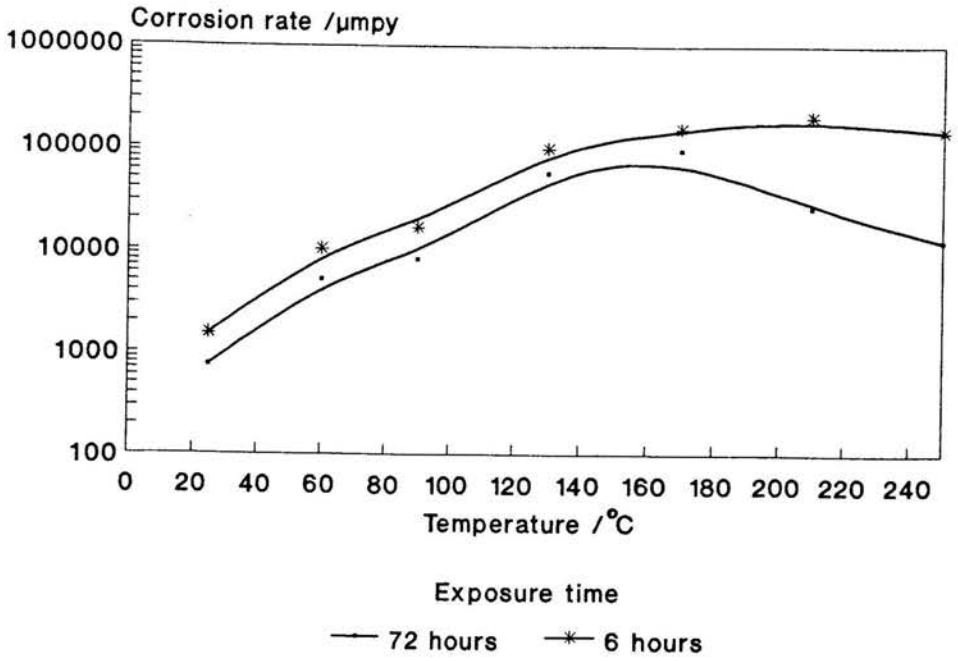

According to the polarisation resistance diagram in figure 4.18 at 25°C a higher corrosion rate will be obtained for an exposure time of 6 hours in comparison to an exposure time of 72 hours. Although the graph is given for $C_2(12.5)$ at 25°C, the same tendency is expected for $C_2(25)$ at 25°C. It can also be assumed that the same tendencies will be relevant at higher temperatures where the system is still under activation control.

In the case of high temperatures but where systems are under passivation control the differences in corrosion rates obtained for different exposure periods were even more pronounced. This indicate that the passive films that formed became more effective with time. This correlates well with results obtained by Potter and Mann[12].

5.3 SUPPLEMENTARY INVESTIGATIONS

In the supplementary investigations turbulence, impurities, corrosion monitoring, acid mixtures and a stable-Synthol-light-oil-water-phase were investigated.

5.3.1 TURBULENCE

According to polarisation diagrams in figures 4.21 the systems under investigation were activation controlled. The turbulence region associated with 0 to 1500 rpm showed that turbulence played no role in the corrosion process. For corrosion processes which are controlled by activation polarisation, agitation and velocity has no effect on the corrosion rate[2]. Higher turbulent conditions were also investigated, but produced non relevant information due to oxygen contamination of the solution. It was found that the design of the holder (picture 8) was inadequate to prevent a vortex-effect from taking place in the higher turbulent regions. This led to oxygen contamination of the solution although a positive N_2 pressure existed inside the holder. Oxygen contamination led to an increase in corrosion rate with turbulence followed by a decrease when a passivation layer formed on the specimen surface. None of these data will be presented in this paper.

Mass loss tests and electrochemical tests were conducted and correlated well.

5.3.2 IMPURITIES

The effect impurities have on corrosion rates of mild steel are represented graphically in figure 4.22.

5.3.2.1 CHLORIDE

Addition of 20 ppm Cl^- led to increases in corrosion rates at investigated temperatures. In de-aerated acidic solutions contaminated with chloride, films that form are non-protective and grow rapidly according to linear kinetics, and have a characteristic porous, laminated microstructure[70]. The corrosion mechanism is proposed to involve the stabilisation of porosity across the oxide layer by the presence of Cl^- ions, allowing unimpeded access of the oxidant to the reaction side, the oxide-water interface. It is proposed that Cl^- ions introduce porosity by adsorbing onto the oxide surface, reducing the oxide-solution interface energy, so that the solution now wets the oxide boundaries and prevents complete intergranular cohesion of the corrosion product film[73]. The corrosion mechanism when film formation is absent is proposed to involve the adsorption of Cl^- ions on the metal surface, thus reducing the interface energy and promoting corrosion.

Specimens also showed pitting corrosion. The mechanism by which chlorides promote pitting and other localised corrosion types has been studied in detail[3].

5.3.2.2 OXYGEN

The addition of 7.86 ppm of dissolved oxygen was achieved by purging the solution with medically clean air for one hour. This led to small increases in the corrosion rates at investigated temperatures, irrespective of the control mechanism that prevailed in the absence of protective films. This can be ascribed to the fact that the addition of oxygen will lead to additional

cathodic reaction possibilities, thus causing higher corrosion rates [3,19]. The results also indicated that passive films formed in the presence of oxygen are less effective.

5.3.2.3 SULPHUR

The addition of 1000 ppm S^{2-} to the test solution, led to a decrease in the corrosion rate. An effective solid corrosion product film formed on the surface of specimens, which reduced the corrosion rate of mild steel for the investigated systems. Gutzeit stated that iron sulphide corrosion products form efficient corrosion inhibiting films which have a low solubility and precipitate rapidly in de-aerated water solutions[74]. The sulphination reaction which causes the corrosion rate to increase, takes place at temperatures higher than 250°C, which was outside the investigated temperature range[72].

5.3.3 CORROSION MONITORING

Results are graphically represented in figure 4.23. Corrator results compared more favourably to mass loss than Corrosometer results.

The poor performance of the Corrosometer can be attributed to the probe span that was used. A low probe span of 2 leads to an upward and downward movement within the limits of the instrument's resolution, i.e. noise. Noise makes it more difficult to distinguish the linear portion of the curve resulting in an inaccurate estimation of the corrosion rate.

5.3.4 ACID MIXTURES

The corrosion characteristics of the equimolar mixture are shown in figure 4.24.

The system was chosen because the individual corrosion rates of the acids

differed substantially. The equimolar mixture of acetic acid and decanoic acid produced an acid number of 25 mg KOH/g solution and showed no synergistic effect. See figure 4.24. The acid mixture produced an approximate average corrosion rate of the two individual corrosion rates.

5.3.5 STABILISED-SYNTHOL-LIGHT-OIL-WATER-PHASE INVESTIGATION

The corrosion characteristics obtained from the process water phase are shown in figure 4.25.

The acid number of the stream received was 9.39 mg KOH/g solution (system A). Additions of acetic acid were made to the system to produce a test solution with an acid number of 25 mg KOH/g solution (system B). System A and system B showed similar tendencies. System B correlated well with $C_2(25)$. It can thus be concluded that the corrosion characteristics of the process stream can be simulated by acetic acid systems with the same acid number.

6 REFERENCES

1 Green, N.D., and Gandhi, R.H., *Mat. Perf.*, 34, July (1982)

2 Skinner, W., 'n Elektrochemiese ondersoek na die invloed van turbulensie op korrosiekarakterisiek met die klem op inhibitor sisteme., Doctoral dissertation, University of Pretoria, Pretoria, (1984).

3 Shreir, L.L., Corrosion., Newness-Butterworths London., Second Edition, (1976)

4 Ailor, W.H., Handbook on Corrosion Testing and Evaluation., John Wiley., New York, (1971)

5 Bockris J O'M, Conway B E, Yeager E and White R E, Comprehensive Treatise of Electrochemistry, Vol 4 : Electrochemical Materials Science, Plenum Press, New York, 1981

6 Nguyen, T.H. and Foley, R.T., *J.Electrochem. Soc.*, **126**, 1855, (1979)

7 Heusler, K.E., The influence of electrolyte composition on the formation and dissolution of passivating films., *Corrosion Science.*, Vol.29., (1989)

8 Foroulis, Z.A., High Temperature Degradation of Structural Materials in Environments Encountered in the Petroleum and Petrochemical Industries: Some Mechanistic Observations, *Anti-Corrosion*, **11**, 4-9, (1985)

9 Pourbaix, M., *Corrosion*, **26**, 431, (1970)

10 Welty, J.R., Wicks, C.E., Wilson, R.E., Fundamentals of momentum, heat and mass transfer., John Wiley & Sons New York, Third Edition, (1976)

11 Lautzenkeiser, C.E., Nondestuctive Test Methods for Corrosion Detection, *Materials Protection*, **2** No.8, 72, Aug (1963)

12 Potter, E.C., and Mann, G.M.W., The fast linear growth of magnetite on mild steel in high temperature aqueous conditions, *Br.Corr.J*, **1**, 26, (1965)

13 Evans, U.R., An Introduction to Metallic Corrosion, Edward Arnold, London, (1975)

14 Castle, J.E. and Masterton, H.G., *Corrosion. Sct.*, **6**, 93, (1966)

15 Robertson, J., The mechanism of high temperature aqueous corrosion of steel., *Corrosion Science.*, Vol.29., (1989)

16 Fontana, M.G., Stachle, R.W., Advances in Corrosion Science and Technology., Volume 6, Plenum Press, New York, (1976)

17 Effertz, P.H., Proc. 5th Int.Congress of Metallic Corrosion., *National Association of Corrosion Engineers*, Houston U.S.A, (1972)

18 Tomlinson, L., *Corrosion*, **37**, 591, (1981)

19 Fontana, M.G., and Green, N.D., Corrosion Engineering, McGraw-Hill, New York, (1978)

20 Fontana, M.G., and Stachle, R.W., Advances in Corrosion Science and Technology, Vol. 6, Plenum Press, New York, (1976)

21 Coulson, J.M., and Richardson, J.F., Chemical Engineering, Vol. 6, Design, Pergamon Press, New York, (1983)

22 Ellison, B.T., and Schmeal, W.R., *J. Electrochem. Soc.*, 524, April

(1978)

23 Levich, V.G., Physiochemical Hydrodynamics, Prentice-Hall, Inc., (1962)

24 Ross, T.K., Wood, G.C. and Mahmud, I., *J.Electrochem.Soc.*, **113**, 334, (1966)

25 Süry, P. and Hiltbrunner,K., *Sulzer Technical Review*, **4**, 172, (1978)

26 Coulson, J.M., Richardson, J.F. and Sinnott, R.K., Chemical Engineering Volume 6 Design, Pergamon Press Oxford, (1983)

27 Bianchi G, *Corrosion*, **34**, 396, 1978

28 Loss, C. and Heitz, E., *Werkst. Korros.*, **24**, 38, (1973)

29 Syrett, B.C., *Corrosion*, **32**, 242, (1976)

30 Foroulis, Z.A., *Corrosion*, **35**, 340, (1979)

31 Evans.,U.R., The corrosion and oxidation of metals., Arnold, London, (1961)

32 Burger, B.V., et.al., Inleiding tot die Organiese Chemie. McGraw-Hill, (1985)

33 Allinger, N.L., Cava. M.P., et.al., Organic Chemistry., Worth Publishers Incorporated., Second Edition., (1976)

34 Heitz,E., Corrosion of Metals in Organic Solvents, *Advances in Science and technology.*, Vol 4., Plenum Press, (1974)

35 Mantell, G.E., Engineering Materials Handbook., McGraw-Hill New York.,(1958)

36 Champion, F.A., Corrosion Testing Procedures, Chapman and Hall, 2nd edition, (1964)

37 ASTM G31 Standard Recommended Practice for Laboratory Immersion Corrosion Testing of Metals, ASTM G1-78 Standard Practice for Preparing, Cleaning and Evaluating Corrosion Test Specimens, ASTM G5-78 Standard Recommended Practice for Standard Reference Methods for Making Potentiostatic or Potentiodynamic Anodic Polarisation Measurements.

38 Perry, R.H., Green, D.W. and Maloney, J.O., Perry's Chemical Engineers' Handbook., McGraw-Hill New York, Sixth Edition, (1984)

39 Sathyaharayana, S., *Electroanal. Chem. and Interfacial Electrohem.*, **50**, 411, (1974)

40 Evans, U.R., and Hoar, T.P., *Proc. Roy. Soc.*, **137**, 343, (1932)

41 Hickling, A., *Trans. Faraday Soc.*, **38**, 27, (1942)

42 Indig, M.D. and Groot,C., *Corrosion*, **25**, 455, (1969)

43 Damson, G.D., *Ind. Eng. Chem.*, **33**, 67, (1941)

44 Rothwell, G.P., Pipes and Pipelines International, 16, Feb (1979)

45 Stern, M., *J. Electrochem. Soc.*, **105**, 638, (1958); ibid., **107**, 728, (1960); ibid., *Corrosion*, **14**, 329, (1958)

46 Mansfeld, F., *J. Electrochem. Soc.*, **120**, 515, (1973)

47 Stern, M. and Weisert, D., *Proc. ASTM*, **59**, 1280, 1959

48 Barnartt S and Donaldson M, *Corrosion*, **39**, 33, 1983

49 Barnett S, *Electrochem. Acta*, **15**, 1313, (1970)

50 Jankowski, J. and Juchniewicz R., *Corrosion Science*, **20**, 841, (1980)

51 McLaughlin, B.D., *Corrosion*, **37**, 723, (1981)

52 Mansfeld, F., *Corrosion*, **29**, 387, (1973)

53 Gerchakov, S.M., Udey, L.R., and Mansfeld, F., *Corrosion*, **37**, 696, (1981)

54 Cleland, J.H., and Edeleanu, C., *Br. Corr. J.*, **18**, 15, (1983)

55 Dillon, C.P., Plant Corrosion Tests, *Handbook on Corrosion Testing and Evaluation.*, Wiley, (1971)

56 Abramchuk, J., Basic inspection method, *Materials Protection*, **1** No.3, 60, March (1962).

57 Minton, W.C., Wall Thickness Measurement, *Materials Protection.*, **1** No.10, 17, Jan (1971)

58 Wingate, R.H., Monitoring corrosion., Materials Protection, 1 No. 7, 64 July 1962

59 Mansfeld F and Kendig M, *Corrosion.*, **37**, 545, (1981)

60 Fincher, D.F. and Nestle, A.C., New Developments in Monitoring

Corrosion Control, *Materials Protection*, **12** No.7, 17, July (1973)

61 Minton, W.C., Wall Thickness Measurement, *Materials Protection*, **1** No. 10, 27, Jan (1971)

62 Britton, C.F., Corrosion Monitoring and Chemical Plant, Corrosion Volume 2 Corrosion control., Newness-Butterworths London, 1976, 2nd edition.

63 McGregor A., On-Stream Radiography is Worth the Money, Materials Protection, **10**, 26, Oct (1965)

64 Stephanopoulos, G., Chemical Process Control : An Introduction to Theory and Practice., Pretice-Hall International Editions., (1984)

65 Feitler, H., *Mat. Prot. and Perf.*, **9**, 37, (1970)

66 Mansfeld, F., *Corrosion*, **32**, 143, (1976)

67 Syrett, B.C. and Acharya, A., American society for testing and materials, Materials and Devices and ASTM Committee G-1 on Corrosion of Metals. *American society for testing and materials Philadelphia*, (1979)

68 ASTM D974 Standard Test Method for Neutralization Number by Colour-Indicator Titration.

69 ASTM D2778 Standard Extraction of Organic Matter from Water.

70 Potter, E.C and Mann, G.M.W, Proc. Second Int., Congr. on Metallic Corrosion, (1963), New York, (1964), (Houston: Nat. Ass. Corr. Engrs)

71 Bengough., G.D., and Wormmwell, F., in Evans, U.R., Metallic Corrosion

Protection., Passivity and Protection., Arnold, London, Second Edition, (1946)

72 American society for Metals Handbook committee., *Metals Handbook Volume 13 Corrosion.*, Ninth Edition, American society for Metals, Metals Park, (1987)

73 Robertson, J., and Forrest, J.E., Corrosion of carbon steels in high temperature acid chloride solutions., Vol.32.,(1991)

74 Gutzeit.,J., Corrosion of Steel by sulfides and cyanides in Refinary Condensate Water., Mater.Prot., Vol 7 (No.12), (1968)

7 APPENDICES

A.1 RESULTS FROM PRELIMINARY INVESTIGATIONS AND MASS LOSS RESULTS FROM MAIN INVESTIGATIONS.

A.1.1 ACID NUMBER AS A FUNCTION OF MASS % AT 25°C

Table A.1.1 *Results of acid number determination for water soluble acids, based on mass %*

Acid numbers for	% Mass concentration of acids							
	0.5	1.0	1.5	2.0	2.5	3.0	3.5	4.0
C_2	4.2	8.9	13.3	17.5	22.0			
C_3	3.5	7.0	10.5	14.2	17.8	21.3	25.2	
C_4	3.3	6.4	9.5	12.8	16.0	19.5	22.4	
C_5	2.8	5.4	8.3	11.1	14.1	16.8	19.7	22.5

A.1.2 ACID NUMBER AS A FUNCTION OF MOLE % AT 25°C

Table A.1.2 *Results of acid number determination for water soluble acids, based on mole %*

Acid numbers for	% Mole concentration of acids					
	0.0	0.1	0.2	0.3	0.4	0.5
C_2	0	5.2	10.3	15.5	20.7	25.8
C_3	0	5.3	10.2	15.7	20.6	26.0
C_4	0	5.2	10.2	15.4	20.8	25.5
C_5	0	5.1	10.2	15.6	20.5	25.9

A.1.3 DE-AERATION OF THE MEDIUM

Table A.1.3 *Time required to reduce dissolved oxygen level of the medium to 1.0 ppm. Purging was stopped after 60 minutes*

Time in minutes	Dissolved oxygen level in ppm
0	7.86
5	7.80
20	7.25
30	7.00
35	6.00
37	5.00
39	3.50
40	2.00
45	0.50
50	0.31
55	0.30
60	0.30
65	0.50
70	0.90
75	1.50

A.1.4 ACETIC ACID

Table A.1.4 *Corrosion rates in µmpy obtained from mass loss tests for acetic acid*

Temp. in °C	Acid numbers			
	0	5	12.5	25
25	2.0	119.4	290.2	754.5
60	65.5	2371.2	3699.0	5128.5
90	112.0	3592.9	5898.8	8172.6
130	156.0	19982.0	38892.0	56644.6
170	200.0	12171.0*	31700.0*	96682.0
210	0.0*	5658.0*	12860.0*	25642.6*
250	0.0*	3513.0*	8783.0*	12173.3*

* Corrosion product film present on specimen surface

A.1.5 PROPIONIC ACID

Table A.1.5 *Corrosion rates in µmpy obtained from mass loss tests for propionic acid*

Temp. in °C	Acid numbers			
	0	5	12.5	25
25	2.0	125.3	251.8	387.6
60	65.5	2113.3	3338.6	3762.8
90	112.0	3350.5	4674.5	6202.7
130	156.0	21474.8	37834.4	47287.8
170	200.0	10748.0*	28253.3*	94736.6
210	0.0*	4853.2*	11989.4*	24104.3*
250	0.0*	3335.7*	6218.7*	9062.1*

* Corrosion product film present on specimen surface

A.1.6 BUTYRIC ACID

Table A.1.6 *Corrosion rates in µmpy obtained from mass loss tests for butyric acid*

Temp. in °C	Acid numbers			
	0	5	12.5	25
25	2.0	94.0	100.0	136.8
60	65.5	704.2	1366.0	1641.4
90	112.0	2710.9	3649.9	3724.9
130	156.0	18199.1	28417.1	40971.7
170	200.0	13571*	30758.0	77344.0
210	0.0*	4757*	16356*	22822.0*
250	0.0*	3275.8*	6186.0*	6463.8*

* Corrosion product film present on specimen surface

A.1.7 VALERIC ACID

Table A.1.7 *Corrosion rates in µmpy obtained from mass loss tests for valeric acid*

Temp. in °C	Acid numbers			
	0	5	12.5	25
25	2.0	100.0	104.5	242.3
60	65.5	610.6	1490.5	3578.8
90	112.0	2362.5	3155.7	3640.1
130	156.0	19398.8	20364.9	33526.6
170	200.0	10429.0*	23790.1	67883.1
210	0.0*	4742.4*	9024.2*	21050.9*
250	0.0*	2187.8*	5258.4*	5653.6*

* Corrosion product film present on specimen surface

A.1.8 HEXANOIC ACID

Table A.1.8 *Corrosion rates in µmpy obtained from mass loss tests for hexanoic acid*

Temp. in °C	Acid numbers			
	0	5	12.5	25
25	2.0	112.2	139.3	150.9
60	65.5	347.5	1155.9	1960.3
90	112.0	2009.9	2687.6	3594.7
130	156.0	37335.6	41438	60332.6
170	200.0	28123*	45259.8	81516.7
210	0.0*	3947.8*	9202.9*	23086.1*
250	0.0*	3001.5*	5442.2*	10513.2*

* Corrosion product film present on specimen surface

A.1.9 OCTANOIC ACID

Table A.1.9 *Corrosion rates in µmpy obtained from mass loss tests for octanoic acid*

Temp. in °C	Acid numbers			
	0	5	12.5	25
25	2.0	17.4	63.4	87.6
60	65.5	481.6	584.3	785.7
90	112.0	1951.5	2336.4	2391.3
130	156.0	9991	15143.4	28923
170	200.0	12906.7	27593.7	76813.5
210	0.0*	5637.7*	48550.9	92972.2
250	0.0*	5479.9*	9160.7*	41966.8*

* Corrosion product film present on specimen surface

A.1.10 DECANOIC ACID

Table A.1.10 *Corrosion rates in µmpy obtained from mass loss tests for decanoic acid*

Temp. in °C	Acid numbers			
	0	5	12.5	25
25	2.0	15.5	(15.5)	(15.5)
60	65.5	215.3	226.7	450.9
90	112.0	487.6	998.3	1137.6
130	156.0	564.3	7168.1	7572.4
170	200.0	16751.8	25119.8	41457.7
210	0.0*	26346.6	83333.7	94102.9
250	0.0*	5651.1*	30326*	90384.1

* Corrosion product film present on specimen surface

A.1.11 LAURIC ACID

Table A.1.11 *Corrosion rates in µmpy obtained from mass loss tests for lauric acid*

Temp. in °C	Acid numbers			
	0	5	12.5	25
25	2.0	21.6	(21.6)	(21.6)
60	65.5	79.3	147.3	446.2
90	112.0	248.8	369.2	503.0
130	156.0	2652.9	2716.7	2954.5
170	200.0	8439.2	8533.0	10567.7
210	0.0*	17617.4	20353.0	41420.0
250	0.0*	5348.5*	12126*	22728*

* Corrosion product film present on specimen surface

A.1.12 MYRISTIC ACID

Table A.1.12 *Corrosion rates in µmpy obtained from mass loss tests for myristic acid*

Temp. in °C	Acid numbers			
	0	5	12.5	25
25	2.0	21.5	(21.5)	(21.5)
60	65.5	72.5	80.9	124.7
90	112.0	208.0	360.3	469.0
130	156.0	1460.0	1505.5	1657.1
170	200.0	3566.3	3951.8	4059.4
210	0.0*	4640.9	6888.6	11931.3
250	0.0*	172.3*	434.1*	1286.0*

* Corrosion product film present on specimen surface

A.1.13 PALMITIC ACID

Table A.1.13 *Corrosion rates in µmpy obtained from mass loss tests for palmitic acid*

Temp. in °C	Acid numbers			
	0	5	12.5	25
25	2.0	28.6	(28.6)	(28.6)
60	65.5	42.6	43.6	71.6
90	112.0	69.7	77.4	92.9
130	156.0	585.9	1094.8	1347.7
170	200.0	1130.7	1700.6	2216.8
210	0.0*	337.1*	376.1*	503.0*
250	0.0*	27.4*	33.6*	35.0*

* Corrosion product film present on specimen surface

A.1.14 STEARIC ACID

Table A.1.14 *Corrosion rates in µmpy obtained from mass loss tests for stearic acid*

Temp. in °C	Acid numbers			
	0	5	12.5	25
25	2.0	28.0	(28.0)	(28.0)
60	65.5	191.2	(191.2)	(191.2)
90	112.0	139.3	395.1	920.9
130	156.0	760.7	1075.5	1247.1
170	200.0	271.5	1514.5	2085.6
210	0.0*	51.9*	74.3*	292.1*
250	0.0*	9.6*	10.9*	15.5*

* Corrosion product film present on specimen surface

A.1.15 CORROSION RATE OF MASS LOSS TESTS IN TURBULENT CONDITIONS

Table A.1.15 *Corrosion rates obtained with the aid of mass loss tests under turbulent conditions for acetic acid at an acid number of 25 mg KOH/g solution*

Turbulence in rpm.	Peripheral velocity in m/s.	Reynold's number $x10^{-6}$	Corrosion rate in μmpy.
0	0.0	0.0	748.9
500	0.5	1.1	695.4
1500	1.6	3.1	800.7

A.1.16 IMPURITIES

Table A.1.16 *Mass loss results of mild steel in µmpy, in contaminated acetic acid solutions at an acid number of 25 mg KOH/g solution. Exposure time = 6 hours*

Contaminant	Temperatures in °C						
	25	60	90	130	170	210	250
Aeration	1830	12408	22364	215449	284146	238921	148817
20 ppm Cl^- &	1616	11437	19017	183306	317624	329405	168887
1000 ppm S^{2-}	618	5751	8230	24609	100388	79400	58203
C2(25)	1516	10194	16580	99359	154507	199585	143865

& Localised corrosion and pit corrosion occurred

A.1.17 ACID MIXTURES

Table A.1.17 *Corrosion rate of acetic acid mixed with decanoic acid to produce an acid number of 25 mg KOH/g solution. Exposure time = 6 hours*

Temperature in °C	Corrosion rate in μmpy.		
	C_2	C_{10}	C_2 mixed with C_{10}
25	1516	(39)	307
60	10194	748	5557
90	16580	3021	7000
130	99359	10554	41511
170	154507	48457	109333
210	199585	189493	194317
250	143865	374760	265225

A.1.18 CORROSION RATES FROM STABILISED-SYNTHOL-LIGHT-OIL-WATER PHASE

Table A.1.18 *Mass loss results obtained from a process stream brought in contact with water. Exposure time = 6 hours*

Temperature in °C	Corrosion rate in μmpy.		
	System A	System B	C2(25)
25	278	1114	1516
60	556	3714	10194
90	2134	9564	16580
130	31771	95477	99359
170	43020	214613	154507
210	58575	309151	199585
250	28440	159683	143865

A.2 ELECTROCHEMICAL TEST RESULTS

A.2.1 STANDARDISATION OF THE POTENTIOSTAT

Figure A.2.1 *Standardisation of the potentiostat according to ASTM G5 - 82 at a temperature of 304.5 K. Lines represent the ASTM boundaries*

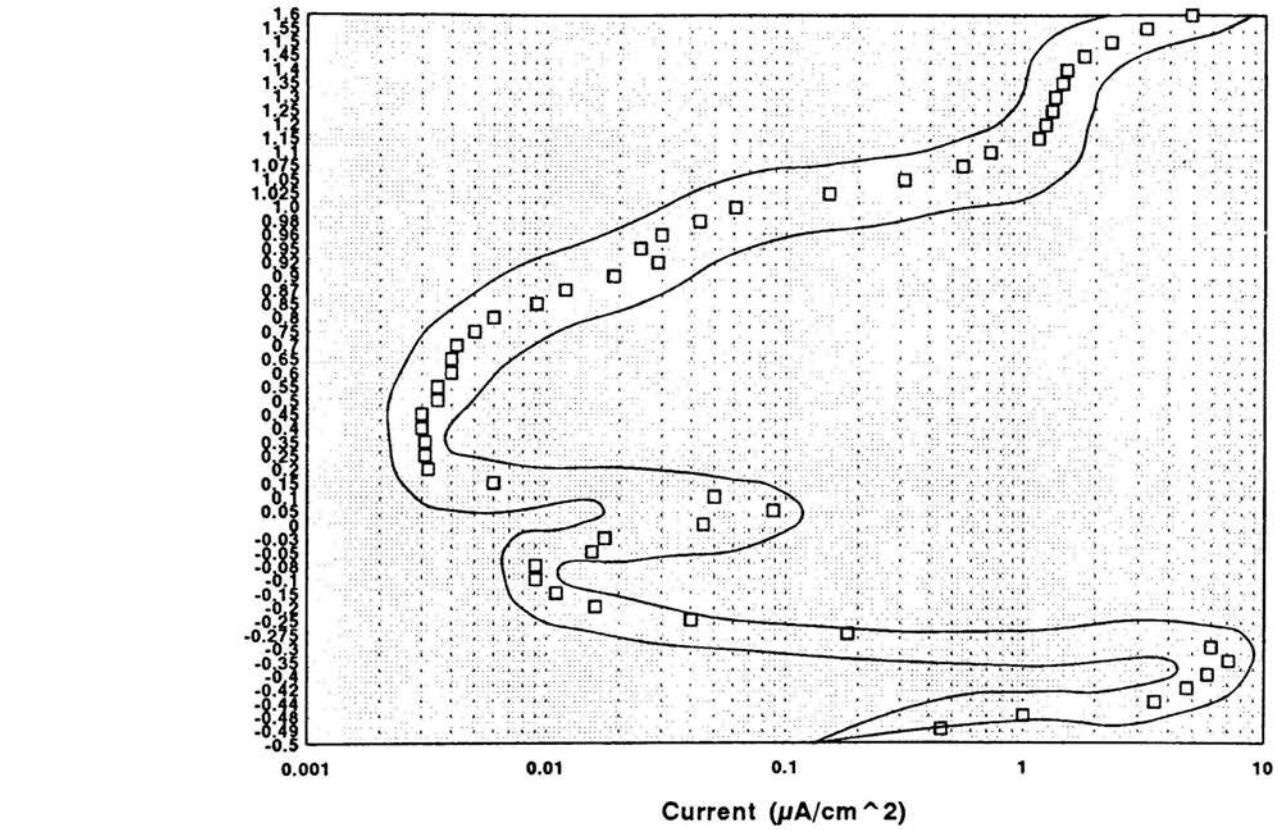

A.2.2 ACETIC ACID AT AN ACID NUMBER OF 25 mg KOH/g solution

TABLE A.2.2 *Acetic acid at an acid number of 25 mg KOH/g solution, a temperature of 298 K and under stagnant conditions.*
Ecorr = -0.557 V

App.Volt.(V)	Current (mA)	App.Volt.(V)	Current (mA)
-0.76	-161.0	-0.51	11.9
-0.75	-150.0	-0.50	17.9
-0.74	-132.0	-0.49	27.0
-0.73	-119.0	-0.48	40.0
-0.72	-103.0	-0.47	58.0
-0.71	-90.0	-0.46	79.0
-0.70	-78.0	-0.45	105.0
-0.69	-65.0	-0.44	135.0
-0.68	-55.0	-0.43	165.0
-0.67	-46.0	-0.42	195.0
-0.66	-37.5	-0.41	228.0
-0.65	-30.4	-0.40	260.0
-0.64	-24.0	-0.39	290.0
-0.63	-19.3	-0.38	320.0
-0.62	-15.0	-0.37	355.0
-0.61	-11.6	-0.36	382.0
-0.60	-8.9	-0.35	392.0
-0.59	-6.5		
-0.58	-4.7		
-0.57	-3.0		
-0.56	-1.5		
-0.55	0.3		
-0.54	1.8		
-0.53	3.9		
-0.52	7.0		

A.2.3 ACETIC ACID AT AN ACID NUMBER OF 12.5 mg KOH/g solution

TABLE A.2.3 *Acetic acid at an acid number of 12.5 mg KOH/g solution, a temperature of 298 K and under stagnant conditions.*
Ecorr = -0.552 V

App.Volt.(V)	Current (mA)	App.Volt.(V)	Current (mA)
-0.76	-58.0	-0.51	2.0
-0.75	-55.0	-0.50	3.0
-0.74	-49.0	-0.49	4.0
-0.73	-43.0	-0.48	5.7
-0.72	-37.0	-0.47	8.0
-0.71	-31.5	-0.46	11.2
-0.70	-26.8	-0.45	16.1
-0.69	-22.0	-0.44	25.0
-0.68	-18.5	-0.43	40.0
-0.67	-15.0	-0.42	58.0
-0.66	-12.0	-0.41	73.0
-0.65	-9.7	-0.40	90.0
-0.64	-7.8	-0.39	110.0
-0.63	-6.0	-0.38	125.0
-0.62	-4.8	-0.37	140.0
-0.61	-3.7	-0.36	158.0
-0.60	-2.8	-0.35	170.0
-0.59	-1.9		
-0.58	-1.2		
-0.57	-0.9		
-0.56	-0.3		
-0.55	0.1		
-0.54	0.3		
-0.53	0.8		
-0.52	1.4		

A.2.4 ACETIC ACID AT AN ACID NUMBER OF 5 mg KOH/g solution

TABLE A.2.4 *Acetic acid at an acid number of 5 mg KOH/g solution, a temperature of 298 K and under stagnant conditions. Ecorr = -0.572 V*

App.Volt.(V)	Current (mA)	App.Volt.(V)	Current (mA)
-0.775	-27.0	-0.525	2.5
-0.765	-24.3	-0.515	3.5
-0.755	-21.5	-0.505	4.7
-0.745	-19.0	-0.495	6.1
-0.735	-17.0	-0.485	8.1
-0.725	-14.5	-0.475	11.7
-0.715	-12.8	-0.465	18.0
-0.705	-11.0	-0.455	24.3
-0.695	-9.0	-0.445	30.7
-0.685	-7.7	-0.435	37.0
-0.675	-	-0.425	43.0
-0.665	-5.1	-0.415	48.5
-0.655	-4.1	-0.405	54.0
-0.645	-3.3	-0.395	59.5
-0.635	-2.8	-0.385	64.0
-0.625	-2.0	-0.375	70.0
-0.615	-1.8		
-0.605	-1.2		
-0.595	-0.9		
-0.585	-0.5		
-0.575	-0.1		
-0.565	0.1		
-0.555	0.6		
-0.545	1.0		
-0.535	1.8		

A.2.5 PROPIONIC ACID AT AN ACID NUMBER OF 25 mg KOH/g solution

TABLE A.2.5 *Propionic acid at an acid number of 25 mg KOH/g solution, a temperature of 298 K and under stagnant conditions.*
Ecorr = -0.56 V

App.Volt.(V)	Current (mA)	App.Volt.(V)	Current (mA)
-0.765	-40.0	-0.515	9.7
-0.755	-38.4	-0.505	-
-0.745	-35.2	-0.495	14.7
-0.735	-32.6	-0.485	17.3
-0.725	-30.4	-0.475	20.2
-0.715	-28.1	-0.465	-
-0.705	-25.4	-0.455	25.6
-0.695	-23.0	-0.445	28.8
-0.685	-21.4	-0.435	32.6
-0.675	-19.2	-0.425	35.5
-0.665	-19.9	-0.415	39.0
-0.655	-	-0.405	42.2
-0.645	-13.8	-0.395	46.1
-0.635	-12.1	-0.385	49.6
-0.625	-	-0.375	53.8
-0.615	-8.9	-0.365	57.6
-0.605	-7.4		
-0.595	-		
-0.585	-4.2		
-0.575	-2.4		
-0.565	-0.5		
-0.555	0.5		
-0.545	3.3		
-0.535	5.3		
-0.525	7.4		

A.2.6 BUTYRIC ACID AT AN ACID NUMBER OF 25 mg KOH/g solution

TABLE A.2.6 *Butyric acid at an acid number of 25 mg KOH/g solution, a temperature of 298 K and under stagnant conditions. Ecorr = -0.54 V*

App.Volt.(V)	Current (mA)	App.Volt.(V)	Current (mA)
-0.74	-55.0	-0.49	3.2
-0.73	-50.0	-0.48	4.9
-0.72	-43.0	-0.47	6.2
-0.71	-36.0	-0.46	8.4
-0.70	-32.0	-0.45	11.5
-0.69	-27.0	-0.44	15.2
-0.68	-22.5	-0.43	21.6
-0.67	-18.8	-0.42	30.4
-0.66	-15.0	-0.41	42.6
-0.65	-12.2	-0.40	56.0
-0.64	-9.8	-0.39	71.0
-0.63	-7.7	-0.38	88.0
-0.62	-6.0	-0.37	105.0
-0.61	-4.8	-0.36	120.0
-0.60	-3.8		
-0.59	-2.9		
-0.58	-2.0		
-0.57	-1.4		
-0.56	-1.0		
-0.55	-0.5		
-0.54	0.0		
-0.53	0.3		
-0.52	0.9		
-0.51	1.5		
-0.50	2.2		

A.2.7 VALERIC ACID AT AN ACID NUMBER OF 25 mg KOH/g solution

TABLE A.2.7 *Valeric acid at an acid number of 25 mg KOH/g solution, a temperature of 298 K and under stagnant conditions. Ecorr = -0.515 V*

App.Volt.(V)	Current (mA)	App.Volt.(V)	Current (mA)
-0.715	-5.8	-0.465	1.0
-0.705	-5.0	-0.455	1.2
-0.695	-4.1	-0.445	1.8
-0.685	-3.8	-0.435	2.2
-0.675	-3.0	-0.425	3.0
-0.665	-2.6	-0.415	3.8
-0.655	-2.1	-0.405	4.8
-0.645	-1.9	-0.395	5.7
-0.635	-1.6	-0.385	6.8
-0.625	-1.2	-0.375	7.9
-0.615	-1.1	-0.365	9.0
-0.605	-1.0	-0.355	10.3
-0.595	-0.9	-0.345	11.8
-0.585	-	-0.335	13.0
-0.575	-0.6	-0.325	14.5
-0.565	-0.4	-0.315	15.9
-0.555	-0.3		
-0.545	-0.3		
-0.535	-0.2		
-0.525	-0.1		
-0.515	0.0		
-0.505	0.01		
-0.495	0.1		
-0.485	0.3		
-0.475	0.6		

A.2.8 ACETIC ACID (AN OF 25 mg KOH/g solution) AT 0 RPM

TABLE A.2.8 *Acetic acid at an acid number of 25 mg KOH/g solution, a temperature of 298 K, with a turbulence of 0 rpm. Ecorr = -0.565 V*

App.Volt.(V)	Current (mA)	App.Volt.(V)	Current (mA)
-0.77	-1085.0	-0.52	77.0
-0.76	-1025.0	-0.51	96.0
-0.75	-930.0	-0.50	114.0
-0.74	-840.0	-0.49	140.0
-0.73	-760.0	-0.48	-
-0.72	-670.0	-0.47	200.0
-0.71	-585.0	-0.46	262.0
-0.70	-510.0	-0.45	410.0
-0.69	-438.0	-0.44	560.0
-0.68	-374.0	-0.43	790.0
-0.67	-317.0	-0.42	980.0
-0.66	-267.0	-0.41	1160.0
-0.65	-220.0	-0.40	1360.0
-0.64	-185.0	-0.39	1550.0
-0.63	-151.0	-0.38	1750.0
-0.62	-120.0	-0.37	1900.0
-0.61	-95.0	-0.36	2050.0
-0.60	-70.0		
-0.58	-29.0		
-0.56	4.0		
-0.54	18.0		

A.2.9 ACETIC ACID (AN OF 25 mg KOH/g solution) AT 500 RPM

TABLE A.2.9 *Acetic acid at an acid number of 25 mg KOH/g solution, a temperature of 298 K. Ecorr = -0.537 V*

App.Volt.(V)	Current (mA)	App.Volt.(V)	Current (mA)
-0.74	-1340.0	-0.49	21.0
-0.73	-1300.0	-0.48	-
-0.72	-1180.0	-0.47	370.0
-0.71	-1095.0	-0.46	485.0
-0.70	-1000.0	-0.45	650.0
-0.69	-900.0	-0.44	800.0
-0.68	-800.0	-0.43	1000.0
-0.67	-715.0	-0.42	1200.0
-0.66	-630.0	-0.41	1400.0
-0.65	-565.0	-0.40	1580.0
-0.64	-490.0	-0.39	1750.0
-0.63	-420.0	-0.38	1930.0
-0.62	-362.0	-0.37	2100.0
-0.61	-310.0	-0.36	2300.0
-0.60	-260.0	-0.35	2450.0
-0.59	-218.0	-0.34	2610.0
-0.58	-172.0	-0.33	2725.0
-0.57	-130.0		
-0.56	-90.0		
-0.55	-55.0		
-0.54	-12.0		
-0.53	9.0		
-0.52	50.0		
-0.51	95.0		
-0.5	150.0		

B.1 CORROSION MONITORING

Figure B.1 *Data obtained from the Corrosometer presented in graphical form*